DOCTOR OF PHILOSOPHY

Flexible tactile digital feedback for clinical applications

Yusuf Bulale

2014

Aston University

FLEXIBLE TACTILE DIGIT FEEDBACK FOR CLINICAL APPLICATIONS

YUSUF ISMAIL BULALE

Doctor of Philosophy of Engineering and Applied Science

ASTON UNIVERSITY

FLEXIBLE TACTILE DIGIT FEEDBACK FOR CLINICAL APPLICATIONS

Yusuf Ismail Bulale

Doctor of Philosophy

November 2013

Thesis Summary

Trauma and damage to the delicate structures of the inner ear frequently occurs during insertion of electrode array into the cochlea. This is strongly related to the excessive manual insertion force of the surgeon without any tool/tissue interaction feedback. The research is examined tool-tissue interaction of large prototype scale (12.5:1) digit embedded with distributive tactile sensor based upon cochlear electrode and large prototype scale (4.5:1) cochlea phantom for simulating the human cochlear which could lead to small scale digit requirements. This flexible digit classified the tactile information from the digit-phantom interaction such as contact status, tip penetration, obstacles, relative shape and location, contact orientation and multiple contacts. The digit, distributive tactile sensors embedded with silicon-substrate is inserted into the cochlea phantom to measure any digit/phantom interaction and position of the digit in order to minimize tissue and trauma damage during the electrode cochlear insertion. The digit is pre-curved in cochlea shape so that the digit better conforms to the shape of the scala tympani to lightly hug the modiolar wall of a scala.

The digit have provided information on the characteristics of touch, digit-phantom interaction during the digit insertion. The tests demonstrated that even devices of such a relative simple design with low cost have potential to improve cochlear implants surgery and other lumen mapping applications by providing tactile feedback information by controlling the insertion through sensing and control of the tip of the implant during the insertion. In that approach, the surgeon could minimize the tissue damage and potential damage to the delicate structures within the cochlear caused by current manual electrode insertion of the cochlear implantation. This approach also can be applied diagnosis and path navigation procedures. The digit is a large scale stage and could be miniaturized in future to include more realistic surgical procedures.

Keywords: Cochlear implantation, minimally invasive surgery, minimally access surgery, Flexible digit, tool/tissue interaction, distributive tactile system, cochlear electrode insertion, tactile information.

ACKNOWLEDGEMENTS

List of Abbreviations

AFM: atomic force microscopes

AOS: advance off stylet

CI: cochlear implant

DAQ: Data Acquisition

DB: decibels

DB HL: Hearing Loss Decibels

DOF: degrees of freedom

EA: Electrode array

FDA: Food and Drug Administration

MAS: minimum access surgery

MEMS:Micro-Electro-Mechanical Systems

MIS: Minimally invasive surgery

MLP: multilayer perceptron

NI: National instrument

PVA: Poly Vinyl Alcohol

RNID: Royal National Institute for Deaf People

RTV: room-temperature vulcanizing

SMA: Shape memory alloy

ST: scala tympani

Contents

List of Figures

List of Tables

1   Chapter 1 INTRODUCTION

This thesis demonstrates the potential for the application of distributed tactile sensing methods to provide information about tool-tissue interaction during minimally invasive surgical procedures. Minimally invasive surgery is better for the patient because it has quicker healing time, small incision, and less pain and trauma than with conventional surgery. However, this technique has more challenges for the surgeon including reduced dexterity and perception, reduced accessibility, limited vision information and lack of sensation information.

Providing more information about the tool-tissue interaction during a surgical procedure can have a positive impact on the surgical outcome of a surgical procedure. The thesis presents an instrumented flexible digit prototype for the application of cochlear implantation surgery.

1.1   AIM AND OBJECTIVES OF THE THESIS

The aim of this research is to develop a flexible digit to aid palpation and navigation in lumen for clinical applications. More specifically, a tactile electrode digit that can provide tool/tissue feedback to reduce tissue damage and trauma to the delicate structure of the cochlea during electrode insertion of the current cochlear implant surgery techniques is focused on in this study. Future improvement of the cochlear electrode implant insertion needs to minimise the exerted force which causes tissue damage and trauma. The research hypothesises that a reduction in the tool/tissue interaction forces with the walls of the cochlear will result in a significant decrease in the risk of trauma to the delicate structures of the cochlear. Tactile

feedback of tool/tissue interaction information to the surgeon will enhance surgeons operation in cochlear electrode insertion and many other palpation and navigation procedures and that is the main contribution of this thesis.

Principal objectives are

- To design and build a cost effective novel flexible tactile digit to reduce intracochlear damage associated with surgical electrode array insertion

- To investigate the challenges of cochlear implant surgery procedures

- To build a distributive tactile digit for lumen mapping applications

- To build and test a rig which can verify the performance of the digit that can lead to a small scale digit

- To analyse and interpret information about tool-tissue interaction

- To test and demonstrate the overall system at the appropriate scale in a phantom device

1.2 SCOPE OF THE STUDY

A cochlear implant operates as an integrated system that includes intracochlear stimulating electrode array. Electrode array insertion in the cochlea is one of the key factors for restoration of hearing loss. The research is examined tool-tissue interaction of large prototype scale (12.5:1) digit embedded with distributive tactile sensor based upon cochlear electrode and large prototype scale (4.5:1) cochlea phantom for simulating the human cochlear which could lead to

small scale digit requirements. This flexible digit classified the tactile information from the digit-phantom interaction such as contact status, tip penetration, obstacles, relative shape and location, contact orientation and multiple contacts.

The distributive tactile sensors embedded the digit provided useful feedback information about the digit and the phantom interactions which resembles tool-tissue interaction during the surgery. This research is exploring feedback opportunities within minimal access surgery (MAS) with a view to minimising trauma during electrode array insertion of the cochlear implantation.

1.3   BACKGROUND

Studies have shown the need for developing steerable tools to aid palpation and navigation of corners and tight turns in lumen for clinical applications without excess force [1-2]. Although there have been remarkable advances in minimal access surgery instruments in recent years, these instruments are inadequate to perform path finding or lumen mapping which are challenging and demanding for many medical diagnoses and surgeries and where the surgeon does not have adequate information about what is happening inside the lumen or hidden tool/tissue interaction [1-6]. Minimally Invasive Surgery techniques, also called minimum-access surgery (MIS) allows access to the internal organs without the use of traditional open surgery [4]. These techniques have been introduced throughout surgery, including endoscopy, arthroscopy orthopaedics and traumatology. The surgeon is mainly reliant on a visual camera which gives important anatomic tissue information, however it is not sufficient and haptic and

tactile feedback information are crucial for these MAS operations [1, 2, 5]. For instance, cochlear implant (CI) electrode array insertion requires tool-tissue interaction information including any contact between the tool and object, feed force, shape and distance fed into the cochlea.

Modern cochlear implant surgery uses an electrode array which is inserted into the cochlea manually. The electrode arrays interact with auditory nerve during cochlear implant procedure and exert force on cochlea which has delicate spiral lamina and outer wall which has canal is filled with fluid (endolymph) and surrounded by fluid (perilymph) is needed [31]. The main challenge of cochlear implant is locating the electrode array closer to the spiral ganglion without tissue damage and exerted force on the scala tympani [6]. Trauma and damage during insertion of electrode arrays is related to lack of tactile or haptic feedback of the interactions between cochlear implant electrode and the cochlea during the insertion process.

Mechanical properties such as Size and stiffnes of the electrode arrays also contribute complications of the cochlear implantation. Small size which is not precluding small incision inside the human body and flexible of electrode arrays are needed to minimize exerted forces on the cochlea walls during electrode insertion.

Consequently, to avoid damage to delicate tissue, it is crucial to have instruments which have haptic ability, measure small and delicate tissue contact, determine obstacles and what is happening inside the human body during surgery, and can be used for diagnoses and preoperative procedures which the surgeon does not have the ability to see [2]. Moreover, tactile

tools/probes which provide feedback information from very soft tissues, such as inside a patient's body, to the surgeon during minimally invasive procedures are key components of current minimally invasive surgery including the cochlear implantation.

A flexible and steerable tool which can eliminate excessive force during the surgery has attracted considerable attention [2-5] in recent years due to its application in minimal access surgery procedures such as biopsies and cochlear implants which require tactile sensors that can provide tool-point interaction information for Minimally Invasive Surgery (MIS); however, these reports have focused on matrix tactile which uses more sensors and is not suitable for human body insertion because of the size which preclude to go inside the human body.

The expected benefit of these instruments/tools is that it will determine tactile feedback that can be used to assist the surgery for cochlear implant insertion procedures as well as other lumen mapping and diagnosis in minimally access surgery as well as lumen mapping and diagnosis procedures.

Prototype digit and phantom which resemble electrode array and human cochlear respectively but in a large scale were introduced in this research. Using the distributive sensing approach, texture, stiffness, shape, and relative motion and position of the tissue can be determined [1]. This digit will feedback to the surgeon the tactile information such as contact status, tip penetration, obstacles, relative shape and location, contact orientation and multiple contacts. Furthermore, the tool will provide tactile information feedback to the surgeon during microsurgery. This in turn will yield minimal interaction forces with the walls of the cochlea

and important information retrieved by the digit could map the lumen. This flexible digit has been demonstrated in a series of laboratory experimental phantom trials. It uses tactile feedback information as a performance to quantify the potential advantage of a flexible tactile digit for reduction of trauma in cochlear implant surgery.

The flexible digit produced tactile feedback information on interaction with the cochlea phantom such as contact direction and intensity, information about the digit shape, tip penetration, time and position of the contact during the digit insertion. In addition, this digit can be used for other similar applications like surgical and diagnostic tools which involve interaction of surgical tools with soft biological tissue in surgery. These could be guidelines to assist in the improvement of the surgical technique and to minimise trauma caused by excessive force application. Such a digit can help better the performance of cochlear implants with lower cost.

1.4   THESIS OUTLINE

This thesis is organised as follows:

Chapter 2 reviews the current state-of-the-art of existing research in the area of minimum-access surgery (MAS) and instruments. This chapter focuses on the challenges and problems of

current MAS instruments. It highlights some of the solutions that have been attempted and the main challenges that need to be solved, particularly cochlear electrode insertion procedures.

Chapter 3 describes the clinical environment, procedures, techniques, challenges and requirements of cochlear implants. This chapter provides the mechanics of the ear system, a brief history of cochlear implants, and presents the current state of minimally invasive cochlear implant technology with particular reference to the cochlear electrode arrays insertion techniques. The challenges and problems of existing techniques of cochlear implants will be highlighted at the end.

Chapter 4 provides an overview of tactile sensors, with the primary emphasis placed on distributive tactile sensing techniques. Concerning the interpretation of tactile information, this chapter describes the general overview of tactile sensing techniques and presents two case studies of distributive tactile techniques. The first involves cantilever tactile sensing, i.e., detecting the load of the object and estimating contact locations of the loads from the sensors. The second involves flexible probes for identifying tumours and voids or holes of an object, i.e., estimating the surface condition such as lumps or gaps and the direction of the contact.

Chapter 5 demonstrates the principle of operation and implementation of flexible tactile electrode arrays for a cochlear prosthesis. This digit is a hand held tool for enhancing the capabilities of surgeons. Design of an electrode which contains embedded sensors for wall contact and a digit that hugs the scala tympani wall of the phantom cochlea in order to minimise

tissue damage during array insertion is discussed. The digit collects signals related to tissue properties and provides tool-tissue interaction feedback to enhance surgeon's tactile capability. Effectiveness of a developed flexible tactile digit through different experiments and their results have been demonstrated.

Chapter 6 presents the results of the response analysis of the steerable tactile digit. Measurements of the frequency response under different surface conditions were made and are discussed. Also, touch characteristics of location with direction of the contact and shape characteristics of the digit were analysed. To verify the digit's performance an investigation of the contact conditions are required. During the digit insertion, desired output parameters needed for clinical applications including touch characteristics and shape characteristics are mentioned.

Chapter 7 presents results of a research study of evaluating efficacy of flexible tactile digits for cochlear implant surgery. It describes user studies which were performed with steerable sense touch digits inserted into the cochlear phantom. The user experiments will identify where the digit is and the pressing point where the contacts are taking place. It will provide tactile feedback that can be used to assist the surgery for cochlear implant insertion procedures for less trauma and sensitive tissue damage. The experimental method is presented in the first section, followed by different insertion procedures and tool/tissue interaction states and transitions analysis. In this study, we set the steerable digit as a contact and the cochlea phantom as a target to allow contact between the electrode and cochlea during the electrode insertion.

Chapter 8 In this chapter, thesis contributions and limitations are summarised, and the scope for future work is discussed.

2   Chapter 2 LITERATURE REVIEW

This chapter provides an overview of the minimally invasive surgeries that have been presented in the literature, with emphasis on instruments used by surgeons during the surgical operations. It highlights some proposals to the problems that have been attempted and the main challenges that need to be solved, particularly cochlear electrode insertion procedures.

2.1   MINIMALLY INVASIVE SURGERY

Minimally invasive surgery and minimal access surgery are becoming more and more common in medical and surgical practice and they have improved on the quality of surgery procedures and diagnosis as well as patient health, such as small incisions which cause less pain and trauma, less strain and reduced cost of health [4]. However, these procedures have drawbacks including limited vision information, lack of touch sense and haptic feedback/sensation, limited degree of mobility, and difficult hand-eye coordination [2, 4, 5, 7].

Instead of directly seeing and touching the tissues and organs as in open surgery, in these techniques, the surgeons rely on the images provided by miniaturised imaging systems inserted inside the patient, and use surgical instrumentation to perform the operations [4]. These surgical operations are carried out in procedures such as endoscopy, laparoscopy, thoracoscopy, arthroscopy, ophthalmic, orthopaedics and traumatology, hernia, gall bladder and thoracic spine. Endoscopic surgery (Figure 2.1) is now widespread in many fields and is used to treat and

diagnose many conditions including problems in the ear, gallbladder, knee, nose, and throat, and in tubal ligation and plastic surgery [8]. In most cases, manipulation of the endoscope is narrow and difficult due to the small diameter of the vessel, and causes excessive force and stress applied on the vessels [9]. Endoscope procedure has vision limitation due to the colon contract and this can cause problems for the surgeon [8]. Similarly, making an incision or to find hidden anatomical features of tumours and placing a sponge or inserting a suture is difficult for the surgeon to know the condition of the contacted tissue during the endoscope operation as well as the catheter operation [8, 9].

Figure 2.1: Different applications of endoscopic minimally invasive surgery [7]

Arthroscopy, shown in Figure 2.2, is used to diagnose and repair many joint problems and is one of the most common orthopaedic procedures which use a real-time image obtained by endoscopic camera during the invasive minimum surgery to get interaction between the tool and the tissue [11].

Similarly, laparoscopy (Figure 2.3) which is used to diagnose and treat many types of abdominal problems, including some cancers, obstetric/gynaecological problems, and urological problems uses a visual camera to enable the surgeons to look into the abdomen and at the reproductive organs [13]. Laparoscope and previous MAS/MIS procedures are needed for locating hidden anatomical structures and evaluating tissue properties to detect tumours.

Aston University

Illustration removed for copyright restrictions

Figure 2.3: Minimal invasive laparoscopy techniques [12]

In conventional open surgery procedures, it is the effect of haptic and visual feedback that controls the tool-tissue interaction, accessing hidden tissues and enables optimal surgical outcomes, however, all of these procedures, endoscope, arthroscopy, laparoscope, and others such as catheter and thoracoscopy share common problems: they lack tool-tissue interaction feedback, that is they lack tactile and haptic feedback information which could improve the quality of the operation [6,8,9,13]. Tactile and haptic feed can provide to the surgeon vital

information about hidden tissue characteristics as well as haptic perception of that part of the body compared to the visual camera feedback.

Minimally invasive cochlear implant (CI) surgery (Figure 2.4) which is one of the MAS operations, has achieved recognition as an approved medical procedure for the treatment of profound hearing loss in adults and children and has given rise to a great deal of many researches in last two decades [6, 14]. However, CIs need to reduce possible damage to the inner ear, deeper insertion for better hearing frequency spectrum and increased efficiency of reduction in comfortable loudness level charges [15].

Aston University

Illustration removed for copyright restrictions

Figure 2.4: Cochlear implant [14]

This improvement needs flexible tools with tactile and haptic feedback of the tool-tissue interaction during the cochlear implantation due to the anatomical cavity of the cochlea.

These MAS/MIS operations in general have challenges of tool point deployment to the working site or to navigate towards the working site, controlled interaction between the tissue and tool

[19], navigating through minimal access [16], path planning [17] or mapping [18], interpretation of haptics and reduced excessive force on the sensitive tissues. To solve these challenges, it is needed to examine current instruments/tools of the MIS/MAS. Research efforts are currently devoted to enhance the dexterity and sensory capabilities of surgical instrumentation for MIS, to improve visual and tactile rendering to the surgeon [1,4,5].

2.2   CURRENT RESEARCH ON MIS INSTRUMENTS

During minimally access surgery, the surgical instruments as illustrated in Figure 2.5 are introduced into the body through small incisions [8,9]. These instruments are fundamentally altered (size, flexibility) by the continuing development of minimally invasive surgical procedures.

Aston University

Illustration removed for copyright restrictions

Figure 2.5: Endoscopic surgery instruments (endoscope) [20]

To avoid the drawbacks of MIS, tactile sensory feedback instruments can play an important role. The tactile instruments will make it easy for a surgeon to get into inaccessible regions of the body by having information about the location, dexterity and tissue contact through tactile feedback.

A variety of hand-held instruments have been developed to improve MIS operations. A robot assisted by tactile sensing instrument (Figure 2.6) for minimally invasive surgery was developed for tumour detection [21].

Aston University

Illustration removed for copyright restrictions

Figure 2.6: Tactile sensing instruments [21]

This study has shown experimentally the difference between robot and human tissue palpation and indicated that tissue trauma is decreased while tumour detection is increased. However, this experiment used 60 sensing elements with a 385mm probe shaft length which is not suitable to incision surgery such as cochlea due to the size and wiring system. Also, this study analysed only force parameters instead of sense of touch, particularly tip contact.

Dario [2] has presented a novel mechatronic tool for arthroscopic surgery which is equipped with a position sensor and force sensor (Figure 2.7) to provide location and contact information.

Aston University

Illustration removed for copyright restrictions

Figure 2.7: Arthroscopy tool [2]

Although this tool provided more information compared to a traditional Arthroscopy surgery tool, no information about the contact object can be retrieved such as shape and stiffness.

To improve flexibility of MIS instruments and enhance the working site an active bending catheter tube which is made of Shape Memory Alloy (SMA) coil and metal spring coated with polymer [22] was developed. This tool is designed for catheter and endoscopic procedures and surgeons can control the bending motion of the tip of the tube from outside the body. However, it will not give information about the tissue contacted with the tool. Another study [23] has compared vision and force feedback for tissue characterisation of laparoscopic procedures which concluded that the force feedback plays a significant role in MIS.

Sensor-based position control for guidance in the advancement in tubular, compliant and slippery environment of colonoscopy was developed [24] and this Colobot (Figure 2.8) design has shown a possibility to guide the exploration of the tube with a sensor-based steering control method.

(a)   (b)   (c)

Figure 2.8: a) colobot ,   b) cross section of Colobot , c) kinematic parameters of the Colobot [24]

Although this approach of position control is showing improvement, this study uses only tip pressure information which can not be generalised to other MIS applications, also it uses a lot of parameters as shown Figure 2.8 (c) and lastly there is no sense of touch for the Colobot.

Shimachi [5] also has designed a new sensing method of force acting on an instrument for laparoscopic robot surgery (Figure 2.9) where gravity and acceleration forces of the instrument in motion are compensated for. This research focused only on force compensation. Other information about the tissue is needed for the surgeon to do a fine operation.

Figure 2.9: Active bending catheter tip (1.6mm) [5]

Sedaghati *et al* [18] designed and fabricated an endoscopic piezoelectric tactile sensor which only measures the applied force and softness of the tissue. Also, Javad Draghai *et al* [25] have designed a tactile probe for measurement of tissue softness. These investigations have focused on tissue softness which has many MIS applications but more tactile information about the shape and interaction tool-tissue, lumens, and contact directions are needed for intricate surgical operations.

Similarly, Oleynikova [13] designed *in vivo* miniature camera robots to assist a surgeon during laparoscopic surgery. Additional camera angles were provided that augmented surgical visualisation and improved orientation while abdominal procedures were performed. The *in vivo* miniature camera robots can provide surgeons with additional visual information that can increase procedural safety but lacks tactile feedback information. Navigation and mapping corners and tight turns without excess force are challenging areas in surgery. Murayama *et al* [26] have developed simple tactile mapping technology to obtain a contour image and topographical Young's modulus information rather than mapping the lumen or contacting the tissue directly. Brett *et al* [1] have designed a flexible digit with tactile feedback for invasive clinical applications. These works have shown good tactile feedback information; however, further work to collect more information that could be used for lumen mapping would be a significant advantage. Furthermore these works are limited to specific applications. Similarly, Onders *et al* [27] have done work on phrenic nerve motor mapping which has shown good results, however, this system is bulky and it requires electrode wires and external power.

Surgeons need to know more about hidden cavities as well as tumours and its depth to get better images or shapes of the tissue to carry out suitable surgical tasks [3]. Similarly, Current MIS instruments are inadequate to perform path finding or lumen mapping which are challenging and demanding for many medical diagnoses and surgeries. Human natural fingertips unlike MIS tools can detect multi-objects and their characteristics of mechanical features which can help the surgeon. Multi-axis force sensing arrays have been fabricated using Micro-Electro-Mechanical Systems (MEMS), but this is not suitable for soft and delicate tissue surgeries due to the size of the design [28].

All the above attempts share the goal of extending the surgeons' ability to perceive and act. The improvement can be dexterity and tactile perception enhancement or creating access, and that is what these instruments are lacking. A realistic tool-object interaction with collision-free contact position, which provides sufficient tactile information to perform lumen mapping, contact condition discrimination, and locate arteries and tumours hidden in the tissues is needed. At the same time these are likely to need to meet the additional requirements of miniaturisation, simplicity, disposability and to be cost-efficient. These tools/instruments embedded with tactile sensors can provide tactile feedback information which can be inferred features of the tissue and surrounding environment to perform difficult medical operations.

Thus, there is a need for a pragmatic approach to tactile sensing that requires: few sensor elements, few connections, good use of the cross-section of the instrument, is able to actuate sufficiently for controlled tissue-toolpoint interaction, toolpoint motion, tool-object interaction with collision-free position contact, toolpoint delivery and to react to tool point forces to

minimise excessive force applied on the delicate tissue. Furthermore, the means to feedback to the surgeon needs also to be pragmatic and to naturally give a clearer perception of interaction with the tissue and spatial awareness with respect to the tissue/ lumen and tool orientation.

2.3   COCHLEAR IMPLANT SURGERY

Cochlear implantation is an implant hearing technology for patients who are severely and profoundly deaf which has been expanding since last three decades. The current technology of cochlear implantation involves surgeons implanting a thin electrode array into the scala tympani canal [29] as shown in Figure 2.10.

Aston University

Illustration removed for copyright restrictions

Figure 2.10: Cochlea implantation [30]

Electrode array insertion which requires access to the cochlea plays a major role in hearing preservation. The position and how the electrode arrays (20-24 wires of each 20μm diameter or less) interact with auditory nerve during cochlear implant (size of 1.3mm diameter x 31.5mm

length) procedure without exerting force on cochlea which has delicate spiral lamina and outer wall which has canal is filled with fluid (endolymph) and surrounded by fluid (perilymph) is needed [31].

Thus, optimal success of the cochlear implantation probably depends on the electrode technology and insertion techniques. Wang *et al* [32] have developed a prototype position array sensor to overcome these challenges. There is no sense of touch feedback for this study that can cover all relevant tissue surfaces which can give tool-tissue contact information inside the cochlea. Although this study has indicated some improvements such as tip contact response, approximate position of the tip, and curvature equivalent to one turn, the report did not mention tool-tissue contact discrimination and complete shape of the cochlea with these many array sensors used. Similarly, Wise *et al* [33] have used tip sensor and position sensors to provide tip information and position sensors but many array sensors were used rather than few sensor-distributive tactile sensing methods which uses less sensing elements and less power.

Direction of the electrode insertion and excessive force need consideration during the electrode insertion of the CI operation. Roland *et al* [34] reported that deep and forceful electrode array insertion procedures can lead to severe destruction of the delicate intracochlear structure. Similarly, Donnelly *et al* [35] reported that insertion of a cochlear implant electrode into the scala tympani had a variable effect on stapes displacement, which may have an effect on residual low frequency hearing thresholds. Factors that may affect the incidence of the damage include mechanical properties of electrode design, variations in size and shape of each cochlea,

and the specific surgical techniques used for insertion [15]. Reducing forces on the cochlear outer walls, obtaining more consistent perimodiolar position should result in a favourable outcome. A number of approaches have been used to improve electrode array insertion to avoid cochlear trauma and increase depth of insertion. David Schramm [36] has revised one of the electrode array insertion techniques and highlighted that electrode location has reached only one turn of the cochlea turns (Figure 2.11). This is the typical depth of insertion while cochlea trauma was not reported in this study.

Figure 2.11: Intraoperative x-ray [36]

Frinjns *et al* [37] have shown a new electrode which is able to attain the desired position with minimal damage to the intracochlear structures. This electrode has contacts directed towards the modiolus. It has a very thin tip and is broader at the base. It is precurved with a large radius to follow the outer wall curvature. The electrode dimensions are chosen in such a way that it fits in even the smallest cochleae [37].

Furthermore, David Schramm [36] has implemented another electrode insertion (Figure 2.12).

Figure 2.12: HiFocus Helix Electrode

These attempts have tried to reach optimum insertion of the electrode cochlear, however these techniques can not reach the optimal position (full insertion of the inner depth of the cochlea) [6], but also with all electrode arrays inserted into cochlea, there is a risk of surgical trauma particularly to the basilar membrane, the partition on which the organ of hearing rests as reported by Chen *et al* [38].

Today, all the cochlear implantation operations insert the electrode array into the cochlea manually where insertion is stopped until further advancement of electrode array could not be made [39]. However, this manual insertion which is required to insert or to reach sensitive regions of the cochlea wall can damage the tissue or the walls [4].

Successful electrode array insertion requires further improvement of the insertion tools which can reduce trauma damage and can be inserted more deeply. Companies like Med-El have manufactured flexible electrode array (Figure 2.13) which have played a significant role in reducing excessive force. However, Adunka *et al* [41] carried out experiments and reported that all insertions were atraumatic and covered one cochlear turn. Besides limited insertion depth, intracochlear trauma could happen due to lack of tool-tissue interaction feedback.

Aston University

Illustration removed for copyright restrictions

Figure 2.13: FLEX^{EAS} electrode array [40]

Also, increased electrode insertion to a depth of up to two turns have been reported recently [42] which improved speech reception, however insertion technique is still using force without tactile feedback and that will have an effect on the delicate tissue of the cochlea. Also this study did not report trauma effects. Wilson and Michael [43] have a remarkable review of cochlear implants and mentioned future improvements including continued development of electrical simulation patterns and new designs or placements of electrode arrays. Similarly, Andress *et al* [44] proposed an automation tool to reduce trauma during the electrode insertion. Nevertheless, the proposal did not use tactile feedback which is essential to avoid cochlear trauma.

Surgical instruments which provide sufficient tactile information to perform lumen mapping, tool-tissue interaction and at the same time are flexible, disposable and cost effective are required by major MIS techniques including cochlear implants. These tools can provide tactile feedback information which serve as an extension of the surgeon's ability to do fine operations and by these efforts MIS will get safer in the future.

3   Chapter 3 COCHLEAR IMPLANTS

The aims of this chapter are to provide the anatomy of the ear system and principal causes of hearing loss, along with a brief history of cochlear implants and the current state of minimally invasive cochlear implant technology. Lastly, this chapter highlights challenges and problems of the electrode insertion procedure of the cochlear implantation.

3.1   ANATOMY OF THE HUMAN EAR

The human ear is made up of three basic structures [46] shown in Figure 3.1: the outer ear, the middle ear, and the inner ear. The outer ear consists of:

- o   the ear lobe (pinna or auricle)

- o   the ear (or auditory) canal, through which sound waves pass to the ear drum

- o   the ear drum (which separates the outer ear from the middle ear)

The outer ear collects sound waves and directs them into the ear canal. The ear canal carries sound waves to the eardrum [45, 48].

Aston University

Illustration removed for copyright restrictions

The middle eFigure 3.1: Human ear anatomy [47]

- o the inner part of the ear drum

- o the hammer (malleus)

- o the anvil (incus)

- o the stirrup (stapes).

The main task of the middle ear is to ensure that sufficient sound energy is conveyed to the fluid within the cochlear [49]. It transmits sound from the outer ear to the inner ear where it is processed into a signal that the brain can recognise.

The inner ear consists of: cochlea for hearing, vestibular labyrinth dedicated for balance and semicircular canals for letting us if we are moving. With its series of winding interconnected chambers and tubes (fluid-filled), the inner ear has been called a labyrinth. The inner ear (Figure

3.2) is responsible for interpreting and transmitting sound and balance sensations to the brain [45].

Aston University

Illustration removed for copyright restrictions

Figure 3.2: Inner ear structure [47, 50]

The human hearing system has an ability to detect, collect and amplify and encode acoustic information to hear a sound [45, 51]. Sound waves are collected by the outer ear and are funnelled through the ear canal to the tympanic membrane (eardrum) and cause the tympanic membrane to vibrate. The vibration from the tympanic membrane is transmitted to the bones in the middle ear. Then the bones in the middle ear amplify the sound and transmit it to the inner ear. The middle ear also matches the impedance between sound from the air and water (fluids in

the inner ear) for the optimum sound transfer [45, 49]. These vibrations pass through the oval window to the inner ear, setting the fluid inside the cochlea in motion. Special nerve cells or spiral *ganglion* (hair cells) within the cochlea then turn the sound waves into electrical impulses and the auditory nerve sends these electrical impulses to the brain's auditory cortex, where it is processed as sound [45].

3.1.1   Concept of Hearing Loss

A problem in any part of the ear may cause a reduction of sound transmission due to the hearing disorder or hearing loss. When describing hearing loss, generally three attributes are considered: *type of hearing loss*, *degree of hearing loss*, and the ***configuration of the hearing loss.***

There are a variety of diseases that can affect the ear, causing a hearing loss. The root causes of the hearing loss are severed, missing, compromised or complete loss or destruction of the sensory hair cells [45]. In general, hearing loss is categorised by three basic types depending on the area of the ear or auditory system that is damaged or compromised and Table 3.1 shows these types and their area of auditory system with possible causes [49].

Table 3.1: Types of hearing loss and possible causes

Type of hearing loss	Position/location of the ear	Possible causes
Conductive loss	outer or middle ear	wax in the ear canal, a perforation in the eardrum, or fluid in the middle ear disruption or fixation of the ossicles.
Sensorineural loss	the inner ear or along the nerve pathway between the inner ear and the brain	ageing, infection or other disease, noise exposure, or it may be related to a genetic disorder.
Mixed loss	Conductive loss and a sensorineural loss occurring at the same time	

Conductive loss can often be treated by medical management or minor surgery whereas sensorineural hearing loss due to the result of damage to the inner or outer hair cells within the cochlea or the hearing nerve (or both) is irreversible and cannot be cured [49].

The severity of hearing impairment experienced is referred to as the degree of hearing loss and is measured in decibels (dB). Table 3.2 is one of the more commonly used classification systems with their technology intervention [49]. Decibel is the scale of amplitude of sounds. The larger the decibels, the louder the sound are. For example, speech range is between 0 and 15 dB is a whisper while 100-110 dB is how loud a motorbike engine is and a jet plane in close proximity is heard at a painful level of 140 dB or louder. 0dB is defined as the faintest sound that a young sensitive human ear can hear. As such the dB hearing level numbers are representative of the patient's thresholds, or the lowest sound intensity they can perceive. Normal ear can detect a range of pitches or frequencies over a wide range of loudness or intensity. The normal threshold is of 20 dB for very quite sounds to very loud sounds of 120
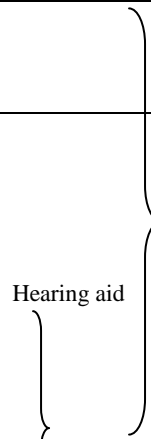
dB. In another way, the audible range of frequencies is usually to be 20 Hz to 20 kHz. Similarly, frequency (pitch) threshold of low pitch is 125 Hz to high pitch of 8000 HZ.

The configuration of the hearing loss refers to the pattern or shape of the hearing loss on the hearing thresholds and normal healthy auditory person can pick up and process a wide range of sound frequencies but profound or deaf person do not have that ranges and this could be hearing loss of high frequencies or low frequencies or both of them [49]. Situation is different from one person to another, a person with high frequency hearing loss or the inability to hear higher pitched sounds may have a bad hearing in the low frequencies but poor hearing in the high frequencies. If only the person's low frequencies are affected, the configuration would indicate poorer hearing for low tones and may have better hearing for high frequencies. Also, some people may have affected low and high frequencies and this person has no ability to hear sounds of all ranges of frequencies (low and high) [49].

According to the Royal National Institute for Deaf People (RNID) [52], there are around 9 million people who are deaf or hard of hearing in the UK. Most have lost their hearing gradually with increasing age, with over 50% of people aged over 60 are hard of hearing or deaf. Hearing loss can also occur at a younger age, with approximately one in every 1,000 children showing a profound hearing loss at three years old, rising to to two in every 1,000 children between the ages of nine and sixteen. These people have a lower quality of life compared to those without hearing impairments shown in Figure 3.3.

Table 3.2: Degree of hearing loss and technology intervention

Degree of hearing loss	Hearing loss range (dB Hearing Level)	Technology intervention
Normal	-10 to 15	None
Slight	16 to 25	None
Mild	26 to 40 (soft sounds may be difficult to distinguish).	
Moderate	41 to 55 (conversational speech is hard to hear, especially if there is background noise such as a television or radio).	Hearing aid
Moderately severe	56 to 70 (it is very difficult to hear ordinary speech).	
Severe	71 to 90 (conversational speech can't be heard).	
profound	91[+] almost all sounds are inaudible. Most people with profound hearing loss benefit from a hearing aid, while some don't.	Cochlear implant

People with moderate, severely moderate or severe hearing loss may use hearing aids of different technology, but people with severe and profound hearing loss require cochlear device implantation.

Figure 3.3: Position of the deafness in the quality of life [53]

In patients with severe to profound sensorineural hearing loss is resulted from damage to the sensory hair cells or to the nerves that supply in the cochlea, the inner ear. [45]. A cochlear implant, however, bypasses these damaged sensory cells and directly electrically stimulates the nerve responsible for hearing through series of microelectrodes inserted into the cochlea, which directly electrically stimulates the auditory nerves to the brain as a sound [45, 49].

3.2   COCHLEAR IMPLANT DEVELOPMENT

Many scientific discoveries and research has contributed to the current design and development of the cochlear implant. Figure 3.4 shows a timeline history of the cochlear development [45, 54-57]. This timeline starts in the 8th century (1790), when a researcher named Volta stimulated

his own ears electrically by placing metal rods in his ear canal, and connected them to an electric circuit generating an unpleasant jolt sound and it is considered the first known attempt at using electricity to hear [45, 54, 55].
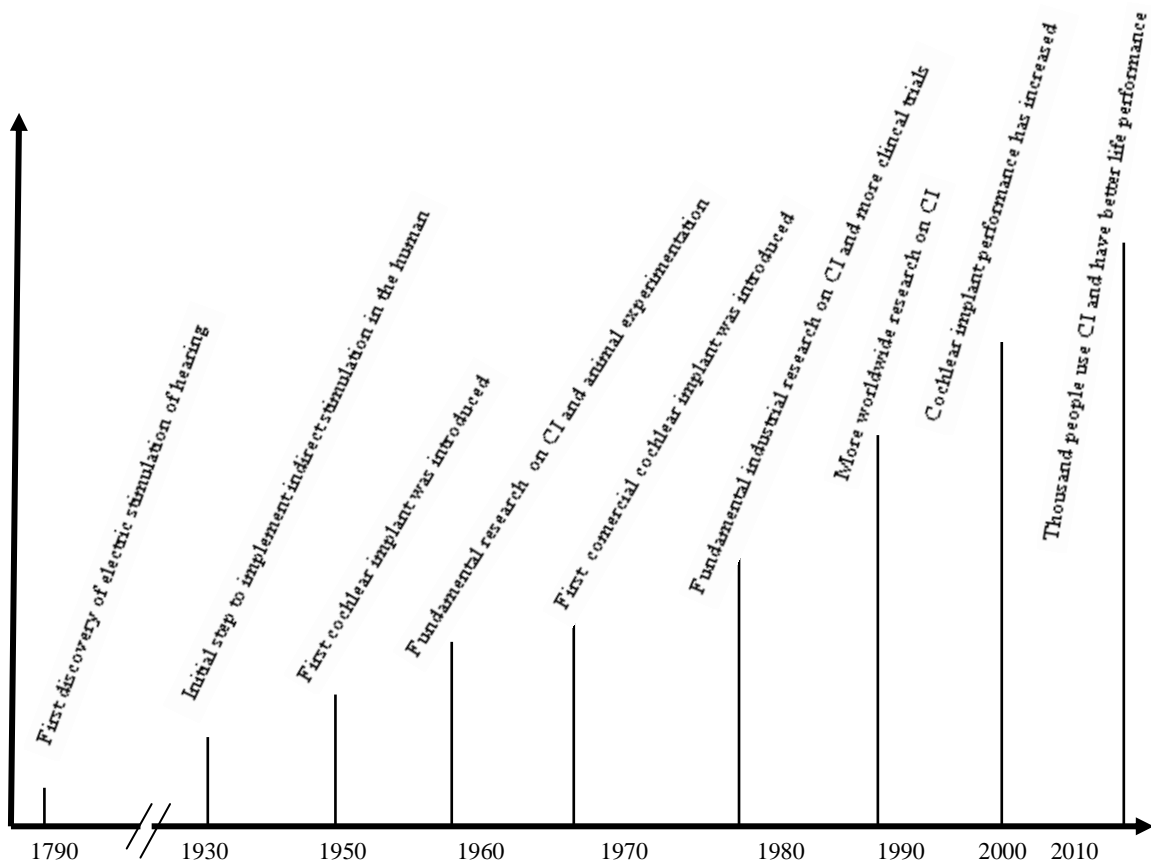
Figure 3.4: Timeline history of cochlear implants

In the nineteen thirties, an important advance was made when Weaver and Bray discovered that electrical energy can be transformed into sound before reaching the inner ear [54]. This was indirect electrical simulation in the human. It was in the year 1957 when the first cochlear implant concept was introduced through direct electrical stimulation in the human with an

electrode by the scientists Djourno and Eyries [55]. In that experiment, the patient whose nerve was being stimulated, could hear background noise but could not discriminate and understand speech. They continued experiments but could not achieve speech comprehension by means other than through lipreading and noise hearing [55].

The important legacy of this period was the first clinical application of this technique.. Dr. William House took the work of Djourno and in 1961 he implanted the first single electrode cochlear implant in two patients [55]. Dr. William's initial results indicated that the patients could perceive the rhythm of speech. These successful discoveries encouraged many scientists around the world in attempts to restore the hearing of deaf people. A few years later, in 1964 to 1966, better results were observed when an array of electrodes was placed in the cochlea [54]. These developments made a significant impact on the development of cochlear implants, and implant technology leaped forward in the seventies due to the speech processor development. In the early seventies the patient could only understand lipreading and could recognise environmental sounds [54], but in 1972, the single-electrode implant was the first to be commercially marketed by House 3M which the Food and Drug Administration (FDA) approved in the late eighties [56]. In the eighties, the FDA started cochlear implant regulations and Dr. House implemented the first cochlear implant on children and after that more children followed on receiving cochlear implantation [55]. These activities triggered fundamental research in industrial development and clinical trials where the activities involved electrical stimulation of the auditory system using an electrode or array of electrodes inserted into the scala tympani [55].

Through the 1990's, researchers learned even more about the positioning of electrodes and the impact of that positioning on speech frequencies. These researchers were looking at more flexible and smaller devices including different electrode arrays and speech processors to produce higher performance levels of hearing [1, 6]. Continual development of multichannel signal processors, higher stimulation rates and more efficient electrodes such as perimodular contour electrodes and split electrodes resulted in dramatic improvement of cochlear implants in the late 1990's and early 2000's [29, 32, 36]. These efforts brought practical solutions to thousands of deaf people.

Currently, feedback from thousands of cochlear implant users has indicated remarkable increases in speech perception and this has improved their quality of life [33, 35, 55]. Improved performance is due to a number of factors including improved cochlear implant technology such as speech processors, electrode array insertion techniques and the size of implant, which as the technology advances the cochlear implants demonstrate better performance, as shown in Figure 3.5 [57]. Beyond that, it has been reported that many patients have achieved more than 90% score on standard tests of sentence intelligibility in quiet conditions [55]. The significance and role of the cochlear implants to overcome severe-to-profound hearing impairment problems is now well accepted and is available in the market.
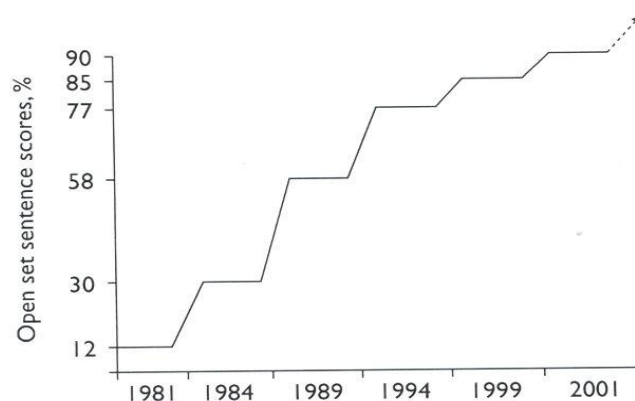
Figure 3.5: Cochlear implant performance

Three forerunners of the current cochlear implant providers are: 1) Advanced Bionics; 2) Cochlear Corporation; and 3) The Med-El Cochlear Implant. Also AllHear, Nurobiosys, MXM laboratories and House 3M companies produce cochlear implants. Because all implants have differences as well as similarities in their design, there is no clear indication about superiority among them. These companies manufacture basic parts of the cochlear implants. The basic parts of the device are grouped into external and internal components (Figure 3.6)

Aston University

Illustration removed for copyright restrictions

Figure 3.6: Cochlear implant components [58]

External parts consist of a microphone, speech processor and transmitter. The microphone which picks up the sound is worn behind the ear and replaces the function of the outer ear; a speech processor which is worn externally on the body analyzes and digitizes the sound signals and sends them through a thin cable to the transmitter; a transmitter, which is a coil held in position by a magnet placed behind the external ear (Figure 3.7) transmits the processed sound signals to the implanted receiver just under the skin.

Figure 3.7: Cochlear implant parts [59]

Internal parts are: a receiver and stimulator which convert the signals into electric impulses and send them to electrode arrays through an internal cable; an array of up to 22 electrodes (diameter of ≈ 0.5 mm at the apex (distal **tip**) to ≈ 1.3 mm at the proximal with length of ≈ 13mm and the total length is 31.5mm) [60] serve to send the impulses from the transmitter to the nerves in the scala tympani and then directly to the auditory nerve. The internal parts are used to implant into the scala tympani of the human cochlea using invasive surgery with different ways of transmitting electrical stimuli to the electrode array [61], and the surgical procedure of implantation plays a significant role on cochlear implantation.

The way in which the cochlear implant replaces the human hearing organ (functions of the cochlea) may be summarised as follows: the concept of the cochlear implant is that early scientists positioned wires on bare nerves during an operation and applied an electric current, and reported that the patient heard sounds like "a roulette wheel" and "a cricket"[62]. Today, Microphone detects speech and sounds from the surrounding environment and these signals are

sent to the speech processor. The speech processor translates the information received by microphone and converts into an electrical impulses by decomposing the input signal into audible frequency components. These electrical impulses are delivered directly to the transmitting coil in the headset through a cable. Radio waves from the transmitter coil carry the coded signal through the skin to the implant inside. The internal implant decodes the signal where the signal determines how much electrical current will be sent to the different electrodes. These code signals are used to determine the stimulus characteristics which are sent to the suitable electrodes. The suitable amount of electrical current determines the intensity of the sounds and sends these electrical currents to the appropriate lead wires to the chosen electrodes. The number of electrodes and the spacing between the electrodes within the cochlea determine the frequency or pitch of the sounds. The coded signals are sent to the brain where the electrodes stimulate the auditory nerves. Finally, stimulated information is sent to the brain for interpretation as a meaningful sound [62].

3.3   MINIMALLY INVASIVE SURGERY FOR COCHLEAR IMPLANTS

Modern cochlear implant surgery uses an electrode array which is inserted into the scala tympani (Figure 3.8) in order to stimulate the nerves of the inner ear.

Figure 3.8: Cochlea implant cross-section [63]

The electrode array is inserted into the cochlea smoothly (Figure 3.9) through a cochleostomy near the round window as far as possible using a claw instrument provided by the manufacturer [64] and precise technique specific to each manufacturer's device is followed. The challenge for the cochlear implant surgeon is to place the electrode arrays close to the scala with minimal insertion trauma [39, 65]. Exciting different auditory precepts through stimulation of electrodes on different locations inside the cochlea made successful current multichannel cochlear implants.

(a)   (b)

Figure 3.9: Cochlear implantation; a) electrode insertion [65]; b) electrode insertion with insertion tools [36]

It is generally noted that intracochlear insertion of the stimulation electrode contributes significantly to the performance of the cochlear implants [39]. Dimensions and three dimensional arrangements of the cochlea and the ganglion cells have influenced the design of electrode arrays. Electrodes located near the round window evoke a high pitch of hearing frequency, whereas electrodes at the pitch end (electrode's front tip) of the cochlea transmit low pitch sensations [65]. It is vital that the electrode arrays are placed in close proximity with corresponding auditory neurons that goes along with the length of the cochlea.

Mathieu *et al* [66] reported that that deeper insertion of the electrodes arrays into the cochlea can improve hearing performance. Current electrode array manufacturers include significant features of the electrode to bring better results such as easy insertion, biocompatibility, long-term reliability, safety during insertion, exert no static forces on intracochlear tissue and be relatively simple to manufacture [67]. Similarly, some of the considerations associated with electrode design in the literature include [61]: (1) electrode placement, (2) number of electrodes and spacing of contacts, (3) orientation of electrodes with respect to the excitable tissue, and (4) electrode configuration.

In an attempt to develop a suitable electrode array which lies close to the modiolar wall but does not cause damage to the delicate tissues in the cochlea has been the focus of research for many decades [67]. Different electrodes have been developed to improve the performance of the cochlear implants and some of the forerunner companies that manufacture electrode arrays of the cochlear implant are shown in Table 3.3. At present electrodes differ in overall length,

diameter, contact design and distribution as well as stiffness and can be classified based on their shapes such as straight, contour, curved and spiral electrode shapes as shown in Table 3.3.

First generation, straight electrode arrays (Figure 3.10) such as the Banded array of cochlear Limited and FLEX^{EAS} electrode of MED-EL use different techniques to insert into the cochlea with a claw instrument provided by the manufacturer such as an electrode plus space filling positioned and an array with positioning wire [67-69]. These straight electrode arrays are not curved at all before they are placed into the cochlea.

Table 3.3: Electrode array manufacturers

Company	Electrode /Internal implant	Electrode array type
Cochlear Limited	Cochlear banded^{TM} Cochlear contour^{TM} Contour advanced^{TM} Nucleus^{R24} Nucleus^{R24}	Straight Spiral Spiral Contour Straight
Advanced Bionics	Spiral clarion^{TM} HiFocusII^{TM} Helix^{TM}	Spiral Straight/Curve Spiral
MEDEL	Combi 40^{+} Flex^{soft}	Straight
Nurobiosys	Nurobiosys	Straight

(a)   (b)

Figure 3.10: First electrode array generations:
a) banded electrode (Cochlear Limited) [6]; b) FLEX^EAS electrode (MED-EL) [68]

Second generation designs (Figure 3.11) including the contour electrode array of Cochlear Limited and spiral clarion electrode of Advanced Bionics are designed to coil or follow the shape of the cochlea during or after insertion to occupy a position closer to the modiolar wall of the cochlea to increase operating efficiency and channel selectivity and to reduce damage and trauma of the cochlea [6, 66, 67, 69].

(a)   (b)   (c)

Figure 3.11: Second electrode array generation   a) Nucleus Contour^{TM} electrode array (cochlear limited) [67]; b) Spiral clarion electrode (Advanced Bionics) [70]; c) HiFocusII^{TM} electrode (Advanced Bionics) [70]

(a)   (b)

Figure 3.12 : Contour electrodes :(a) contour electrode and contour advance electrode
with stylet. b) The contour advance after advancing off the stylet [64]

In these electrodes, the precoiled electrode array is straightened with a stylet (Figure 3.12a) and is pushed off the stylet as the electrode is advanced into the cochlea. Then, the precoiled electrode array returns to a spiral shape intended to facilitate insertion and ultimately position the electrode array near the modiolus as shown in Figure 3.12b [36]. This technique has been termed advance off stylet (AOS) [6].

3.3.1 Electrode Array Insertion Problems and Challenges

In spite of the considerable progress of the cochlear implant procedures, the electrode insertion procedures have recommendations [6, 71] such as to increase electrode insertion of depth of up to two turns, inserting electrode arrays in to the cochlea without any trauma or damage and to be cost effective. These have faced some challenges and problems.

Standard straight electrode arrays cause tissue damage and this mostly happens due to the penetration of the basilar membrane or lateral walls, which is caused by the mechanical property (stiffness) of the electrode [6, 29, 49, 72]. Twisting and compression forces exerted on the

electrode array are another cause of the trauma or damage of the cochlea [44, 72]. It is reported in the literature [73] that in cases using the straight electrode trauma happens at two points during insertion: first, when the straight electrode tip lies against the outer wall upward (Figure 3.13), it can burst the basilar membrane; secondly, when the electrode is pushed to its final depth. Another challenge for the straight electrode array is that it is still not reaching optimal frequency [46]. That is, it will not cover whole frequency due to the limited depth insertion.
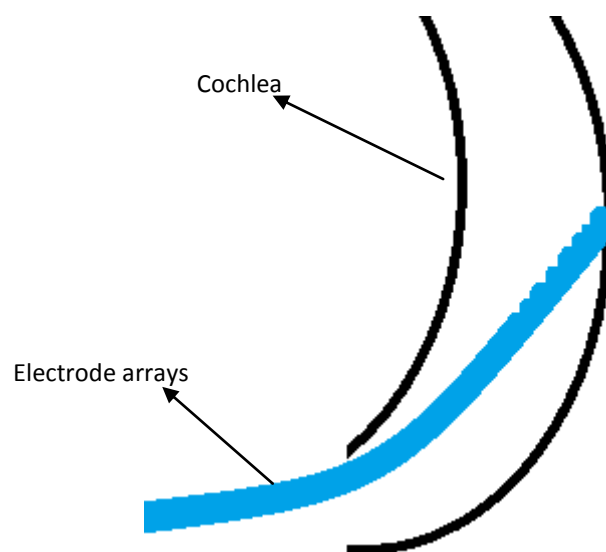
Figure 3.13: Possible cochlea damage of the straight electrode arrays

Second generation electrodes can be placed well in the basal and middle cochlear turns using different insertion devices [51, 71]. Contour and flexibility features of these electrodes made it possible to reach a greater depth into the cochlea compared to a straight one [45]. Adunka *et al* [39] highlighted that deeper electrode insertion increases the trauma and damage of delicate tissues of the cochlear. Similarly, Catherine [74] reported that Nucleus® 24 Contour™ and Nucleus® 24 Contour Advance™ electrode insertion has indicated that forces transmitted on

the scala tympani during insertion are coming from the electrode strength, trajectory and frictional forces between the tool-tissue interfaces, and these can cause trauma and damage to the cochlea. However, contour electrode arrays have fewer traumas compared to straight electrodes in the basilar membrane and it is reported that the minimal force application was achieved using the Contour Advance electrode in an AOS technique insertion [70]. Other studies mentioned that there is no significant difference between the trauma caused by these two generations [48, 73].

Studies on standard straight and contour electrode have shown that stiffness of the electrode array has a great impact on the trauma and damage during the insertion of the electrodes array into the human cochlea [71]. Some companies manufactured a flexible electrode tip to minimise trauma, however, Adunka *et al* [39] reported that increased flexibility could impair the surgeon's perception of intracochlear resistance and the approach depth exceeding one full cochlear turn was not achieved. Other studies have recommended that the pre-curved electrodes discussed earlier could solve extensive damage observed in deep insertion of the cochlea in the middle turn (first one –half turn) stage [39, 74]. In contrast, other studies have shown that the contour electrodes can be inserted easily and can be deeper into the scala tympani but have the same rate of trauma as straight banded electrodes [66]. Deep insertion of the contour electrode takes place in the middle turn and that force can cause trauma [39]. It means, extensive damage due to the deep insertion has link with the dimension of the cochlea in the middle turn stage as well as the greater forces which usually are necessary to place an array in the middle turn [39]. In addition, latest studies have reported that none of the current electrodes (i.e., Spiral, straight,

curve, or curved with positioner) have met all the criteria for an ideal CI electrode including insertion without damage to the cochlear [14]. Flexible contour electrodes have shown better performance compared to straight techniques but optimum electrode array insertion has not been achieved so far to produce optimal hearing [39].

Some of the common electrode arrays and their limited insertion depth are shown in Figure 3.14. One of the latest studies on the Med-El Combi40+ has suggested the possibility of covering the whole range of the cochlea [66].

Aston University

Illustration removed for copyright restrictions

Figure 3.14: The images of the final position of the banded [68], contour^{TM} [68], HiFocus helix [36]and COMBI40+ electrodes [55]

A further study suggested that both the *Clarion™* spiral and *HiFocus II™* with positioner can be inserted with minimal trauma, but in many cases not to the maximum depth allowed by the design, and significant insertion trauma was observed attempting full insertion [70]. The study added that injury appeared in the majority of temporal bones when full insertion into the scala

tympani is attempted. Attempting full insertion of the scala tympani, it is hard for the surgeon to feel electrode resistance and that can cause trauma [70].

Other factors that may affect the incidence of damage besides the mechanical properties of a particular electrode design include variations in the size and shape of each cochlea, the specific surgical techniques used for insertion [14], forces that are applied on the tissue and dimensions of the fluid space [38].

It is noted that current electrode cochlear insertion techniques are manual and do not have any tool-tissue feedback information, similarly electrode insertion is stopped at the depth specified by the manufacturer or after resistance to the insertion was felt by the surgeon [69, 70].

Many studies suggested different ways that can minimise trauma and increase the depth insertion as well. Initial studies by Zhang *et al* [75] mentioned that a proposed steerable electrode array and robotic insertions with a phantom model can reduce insertion forces. Similarly, Wise *et al* [33] have used tip sensor and position sensors to provide tip information and position sensors but many array sensors were used rather than few sensors-distributive tactile sensing method.

To avoid any cochlea damage rather than using surgeon's hand during the depth insertion, there should be a way to detect this force that is imparted on the scala tympani during insertion which is dependent on the electrode strength, trajectory and frictional force between tool/tissue interfaces [71]. Trauma and damage during insertion of electrode arrays is related to lack of tactile or haptic feedback of the interactions between cochlear implant electrode and the cochlea

during the insertion process. Without the feedback of the insertion trajectory and electrode/tissue contact feedback, the problem will continue to exist.

Development of a new steerable or flexible electrode array with embedded sensitive touch feedback is proposed and described in this thesis. This approach will provide tactile information feedback to the surgeon during the precise surgical task, working through sensitive and minimal access regions of the cochlear. The information retrieved by the tool can be used to map the lumen in real time. That is, current existing flexible contour electrode arrays and AOS technique with tactile feedback approach could eliminate trauma and damage of the cochlea and can facilitate deeper insertion of the electrode arrays. Similarly, the risk of damaging the basilar membrane during insertion of the electrode array into the human cochlear is expected to be significantly reduced with the ability to redirect the tip of the electrode array at the critical hook region. The bending behaviour of the steerable electrode array and its trajectories during insertion into the scale tympani could be predicted and the final position of the electrode array can also be adjusted to lie beneath the basilar membrane inside the scala tympani.

4 Chapter 4 FLEXIBLE TACTILE DIGIT

This chapter demonstrates the ways in which the digit can be constructed including the specification, the materials required for construction of a digit and the process of manufacturing of the digit.

4.1 SPECIFICATION

Current electrode arrays of the cochlear may be classified based on their shapes such as straight, contour, curved and spiral electrode shapes as discussed in section 3.3. The contour electrode has flexibility as well as being pre-shaped to match the form of the cochlea. The contour and flexibility features of these electrodes make it possible to reach a greater depth into the cochlea compared to a straight one [45]. Flexible contour electrodes have shown better performance compared to straight techniques but optimum electrode array insertion has not thus far been achieved to produce optimal hearing [39]. Roland [63] reported that current perimodiolar electrodes have some additional advantages over straight electrodes such as reducing damage to the cochlear, lower power consumption and more selective stimulation of the cochlea. It can therefore be assumed that the future development of cochlear implantation electrodes will be in the direction of flexible forms, and as such this research will use prototype prosthesis similar in form to a conventional flexible cochlear electrode. The prototype will hitherto be referred to as a `digit'.

Flexible cochlear electrodes are held in a straight configuration prior to insertion by inserting a stylet into the lumen (Figure 4.1).
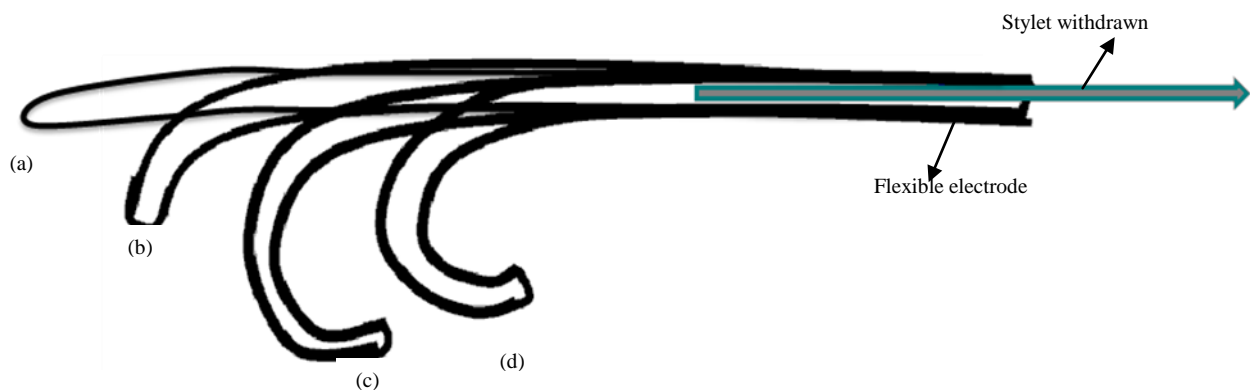
Figure 4.1: Sequence insertion plot of the flexible cochlear electrode; a-c: curving stages of stylet withdrawn

This then relaxes to a shape matching the curvature of the cochlea when the stylet is removed (withdrawn). This action will be replicated in the digit enabling investigation of the effect of the stylet on the geometry of and loads exerted upon the digit, but also the interaction of the digit with the structure of the cochlea, or cochlear phantom, throughout the insertion process.

When the tip of the digit comes into contact with the wall of the cochlea phantom (Fig 4.1(a)) it is expected to deform and bend as it slides around the wall due to the manual withdrawing of the stylet (Fig 4.1(b)). The digit will need to detect any contact of the tissue in order to prevent any inadvertent tissue damage.

As the digit is inserted further into the cochlea (Fig. 4.1(c)) the tip will touch the wall where it will need to detect curvature (wall) contact and tissue contact, and the digit bends and conforms

to the curvature of the cochlear wall by pulling out the stylet further. If the digit touches the cochlear phantom, the digit can be withdrawn and re-inserted (Fig.4.1(d)) such that the digit is not touching the walls of the phantom. As the digit progresses through the first and second turns of the cochlea this process will continue until the flexible digit reaches the optimum electrode array location. This concept demonstrates the benefit of controlling insertion through sensing and control of the digit during insertion into the cochlea (phantom).

Besides contour shape and flexibility feature of the digit, the digit requires tactile sensing to feedback information about contacts between the digit's tip and the side walls of the cochlea phantom, as well as contact points along the digit and the side walls. Similarly, the digit needs ability to give information about relative position of the electrode insertion (location) in the cochlea. Furthermore the digit will be required to detect when a force occurs at the tip arising from contact with obstacles in the cochlear.

Mathematically, the morphology of the digit prototype can be considered to be similar to a slender beam (aspect ratio > 25). As such a relationship between the stresses, strains, radius of curvature and the material of the digit can be accurately predicted using the Bernoulli-Euler bending moment-curvature relationship for a slender rectangular beam of uniform-section composed of a linear elastic material and expressed in equation 4.1 [75]:

$$\kappa = \frac{1}{\rho} = \frac{\varepsilon_m}{c} = \frac{\sigma_m}{Ec} = \frac{1}{Ec}\frac{Mc}{I} = \frac{M}{EI} \qquad (4.1)$$

where E is the Young's modulus of the material (N/M^2), M and κ are the bending moment and the curvature at any point of the beam respectively, (1/ρ) is a radius of curvature, σ is the stress,

ε is strain, *c* is distance from the neutral axis of the beam and I is the moment of inertia (the second moment of area) of the beam cross-section about the neutral axis.

Furthermore, since the behaviour of structure can be modelled, it can also be scaled up for ease of manufacture and manipulated whilst preserving geometric similitude.

This could also allow the prototype digit appropriate for application to access different areas at a surgical site such as the catheter and endoscope insertion processes where tool-tissue/object interaction without damaging the soft tissue is of potential concern.

4.2 TACTILE SENSORS

Tactile sensors are becoming increasingly important in many fields and several tactile sensors have already been developed for handling objects in robotics and automation as well as minimum access surgery (MAS) [76-78]. Eltaib and Hewit [76], and Nichols and Lee [76] provided comprehensive early surveys of tactile sensing technologies whilst Howe [77] has done more surveys recently. One of the clearest definitions of tactile sensor is given by Lee and Nicholls [77]:

"a device or system that can measure a given property of an object or contact event through physical contact between the sensor and the object."

Tactile sensing plays a significant role in gathering information about an object and contact conditions as well as in grasping. Tactile sensors can coordinate a group of sensors and measure

surface contact parameters between the sensor and object to get feature parameters such as touch, vibration, pressure and tickle senses [79].

The importance of tactile sensing for exploration and response are most evident for fine surgery of MAS/MIS operatoins where the surgeon copes with loss of direct contact information and reduced visual information. This is particularly applicable when dealing with the mapping of lumen within the body (Figure 4.2) [79, 80].

Tool tip

Lumen Path
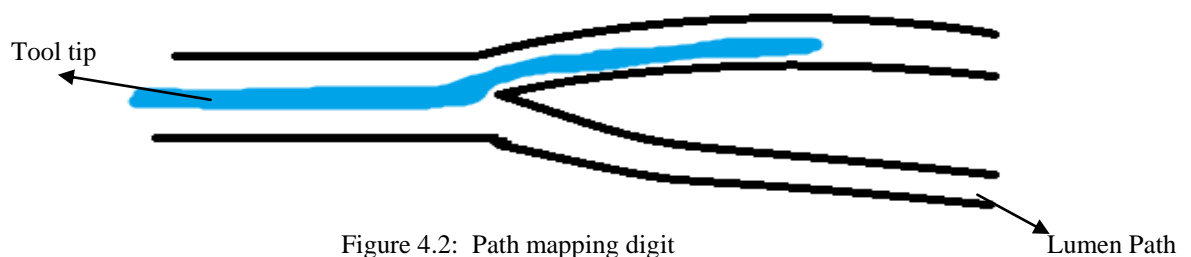
Figure 4.2: Path mapping digit

The constituent elements in a tactile sensing and feedback system are shown in Figure 4.3 [76]. The digit collects signals related to tissue properties and provides tool-tissue interaction feedback to enhance the surgeon's tactile capability. Tactile sensing technology and tool-tissue interaction information are the key elements of this design.

Aston University

Illustration removed for copyright restrictions

Fig 4.3: Basic components of the tactile sensing system [73]

Humans employ tactile sensing to support different activities such as manipulation, exploration and response. The information provided by tactile sensors are used to detect and measure manipulation activities such as identifying contact location and object shape, measuring contact forces, stiffness, assessing surface condition and determining contact conditions [81, 82]. On the other hand, lack of tactile information increases the risk of tissue damage and sometimes amputation [82].

The following general specifications of a touch or tactile sensor are proposed in the literature which can be used as an excellent basis for defining the basic requirement of a touch or tactile sensor suitable for the majority of industrial applications [76, 82]:

- small spatial resolution (1 to 2 mm): small spatial makes easy for coverage area of distributive sensing system

- minimum installation space: smaller space will reduce body insertion if any)

- as large as possible area coverage: more coverage cover will minimise the number of sensors and hence reduces needed space

- biocompatible: required to function in intimate contact with living tissue

- small sensing element size: contribute less overall space of embedded tool

- toughness against impact and shear forces.

- easy to manufacture

- low Cost

- miniaturisation

4.3   TACTILE SENSOR TECHNOLOGY

Industrial tactile sensors may be divided into the following categories to accomplish manipulation (grasping), exploration (texture) and response (detection) operations [81, 83]:

- Proprioceptive: provides information about the individual's touch and movement through muscles and joints (robot appendage).

- kinematic: provide geometric information for manipulation and exploration of finger *movements* in a normal subject

- force: forces exerted by or on a robot appendage

- dynamic tactile: provides information about motion of a moving or displacing object.

- array tactile sensors: grid or matrix of sensing elements coordinating together to provide information about a measured pressure or deflection of an object.

- distributive tactile sensors: small number of sensors which can estimate the nature of a surface through a measured pressure or deflection of an object

 Tactile sensors can provide information about a simple contact, magnitude of force, slip, shape, texture and thermal properties [84-86]. Although the basic function of tactile sensors remains the same, a wide variety of technologies have been applied to solve the problem of tactile sensing in robotics and medicine. The most popular tactile sensor technologies use conductive elastomer, strain gauge, piezoelectric effects, capacitive and optoelectronics [82, 85]. These technologies can be further grouped by their operating principles into two categories: force-sensitive and displacement-sensitive. The force-sensitive sensors (conductive elastomer, strain gauge and piezoelectric) measure the contact forces, while the displacement-sensitive

(optoelectronic and capacitive) sensors measure the mechanical deformation of an elastic overlay [81, 85].

4.3.1 Tactile Array Sensors

Tactile sensing devices are simple contact measurement devices where one parameter or one sensor can be used to measure or detect changes in an object. These tactile sensors are used to describe:

- presence of an object

- object's contact area-shape, location and orientation

- pressure and pressure distribution

- force magnitude and location.

Tactile array sensors consist of a grid or matrix of sensing elements that can measure force distribution or mechanical deformation and they are used for gripping and guiding robot manipulation tasks [80, 81]. This type of sensor provides higher spatial resolution but they have some disadvantages such as [86]:

- large number of sensing elements

- high computational load

- complex construction

- higher power consumption than single element sensor equivalent.

These sensors typically consist of individual sensors arranged in a rectangular array over the contact surface. The majority of applications can be undertaken by an array of 10-20 sensors

square, with a spatial resolution of 1-2 mm and are typically used in conjunction with one or more parameters such as touch with vision or audio [79, 83]. For instance, Medical Tactile Inc. has produced SureTouch, the world's first Food and Drug Administration (FDA)-approved device using tactile sensing for breast cancer documentation [88]. Hsin-Yun Yao and Vincent Hayward developed a surgical probe with tactile and auditory feedback [80].

4.3.2 Distributive Tactile Sensors

Distributive tactile sensing is different from the array tactile sensing approach. The principle of this novel approach employs deformation of a substance monitored by a small number of sensors that can estimate (or predict) the nature of a surface on the substance or object and this type of tactile sensing offers many advantages over tactile array sensors including [89-92]:

- lower data processing speed requirement
- can cover large area with fewer sensors for equivalent spatial resolution
- lower computational load
- lower cost than tactile array equivalent
- less space and wiring requirement

The distributed tactile sensing technique is well suited to many clinical applications which need tactile information feedback such as detection of anatomical features for navigation and diagnosis and this applies to surgical tools such as endoscopes, laparoscopes, catheters and some implants such as cochlear electrodes [1,76]. These current tools provide vision information while there is no haptic feedback information. Effectiveness of this technique relies on the interpretation algorithm, and optimum location of the sensors and this tactile sensor

depends on the distributed deformation of the surface response where few sensors are applied on the surface area [93]. These issues are needed to emphasis to get appropriate design.

Brett was the first to name this approach "*Distributive*" where Stone & Brett used the distributive approach to derive information describing the distribution of contacting force directly from the sensory data [89].   Ma and Brett [90] have extended this approach and used it to measure force distribution in minimally invasive surgical procedures. Eight strain gauge tactile sensors were used to detect slip and other movements of the surface of contacting objects using a trained neural network as an interpreting tool. This approach integrated actuators and sensing elements using a neural network algorithm. Brett and Li [94] have extended this further for 2-D contact position of normal force applied on a planar surface. This system combined a high-level interpretation method of a neural network and hardware with real time information which enables automatic determination of the contact position in real time.

Tongpadungrod *et al* [91] used a similar approach to determine the type, position and orientation of an object using the distributive sensing method. This system describes an optimisation technique through sensor placement using a genetic algorithm rather than equal pitch spacing.

Further extension is distributive tactile perception with a neural network which is investigated at Aston University [95] has shown good estimation of load as well as its position. Ma and Brett [89] and Tongpadungrod *et al* [91] have used similar approaches to determine the description of a load in contact with a surface of 1-D such as the type, position, weight and orientation of an object using the distributive sensing method. Also, Ma *et al* [96] investigated a flexible digit with tactile feedback for invasive clinical applications and Petra *et al* [97] added an embedded

system with distributive tactile approach using a flexible digit for clinical applications. Similarly, Brett *et al* [98] have used distributive tactile approach to track moving contact load in real-time.

A distributive tactile sensing system was selected for this research due its benefits of few sensors, small space and wiring requirements with larger covering area ability, and reduced data processing overhead.

Strain gauge technology was selected for the tactile sensors as they require minimal space and are readily available in comparison with other technologies such as conductive elastomer and piezoelectric force sensors.

Dimensions of the tactile sensors drive diameter of the digit and consequently the digit dimensions also drives the dimension of the cochlea phantom. The width of the sensors controls the width of the digit-------smaller sensor width, smaller digit width size. Consequently, the width of the digit controls the width of the cochlea phantom. The size of the sensing material has impact overall dimension design of the system. This interlink dimensions have caused limitations and the sizes of the prototype. From there, the size of the was digit depend on the size of the strain gauges and the embedding techniques while the cochlea phantom dimensions was controlled by the digit size. Nevertheless, the concept of digit-cochlea interaction contacts can be applied besides the size.

4.4 DESIGN

4.4.1 Geometric similitude

Before attempting to design the digit or try to perform any operation on or with it, the outcome of size reduction or enlargement has to be considered. A model is a representation of a physical system that may be used to predict the behavior of the system in some desired respect. There are three types of similitudes (geometric, kinematic and dynamic) that constitute the complete similarity between problems of same kind but it is often difficult to achieve all types in a single study. In this study, geometric similitude is considered.

The basic requirement for the physical similarity between two problems is that the physics of the problems must be the same. This similarity or similitude as sometimes called can be geometric, kinematic or dynamic similarity but geometric similarity is perhaps the most obvious requirement in a model system (*Model*) designed to correspond to a given prototype (*Prototype*) system [75].

Geometric similarity exists between model (real or existing design) and prototype (proposed one) if the ratio of all corresponding dimensions in the model and prototype are equal. For the length similarity, we have

$$\frac{L_{Model}}{L_{Prototype}} = L_{ratio} \quad \text{and} \qquad \frac{L_m}{L_P} = L_r$$

And the diameter similarity, we have;

$$\frac{D_{model}}{D_{prototype}} = D_{raio} \text{ and } \frac{D_m}{D_p} = D_{ratio}$$

The model geometry must be in the same proportions as the real or prototype condition.

$$\frac{L_m}{L_p} = \frac{D_m}{D_p} = L_r = D_r$$

$$D_r = L_r$$

Currently existing cochlear implants have different dimensions. For instance one cochlear [MED-EL standard] has the length of 31.5 mm with a diameter of 1.3 mm and another cochlear implant [MED-EL FLEX20] has length of 20 mm with diameter of 0.8 mm [44,101,102]. In this study, the cochlear which has length of 20 mm with a diameter of 0.8 mm was considered as the dimensions of the model where the prototype has length of 250 mm and diameter of 10 mm. The geometry similarity was calculated as follows:

$$\frac{31.5 \ mm}{250 \ mm} = \frac{1.3 \ mm}{10 \ mm} = 0.13 = L_r = D_r$$
$$20/50 = 0.8/10 = 0.08$$

In that case, this prototype design has a geometric similarity with scale ratio of 0.08. In another way, the prototype is 12.5 times bigger than the actual (model).

Table 4.1: Cochlear sizes with model ratio

Cochlear implant	Length $L_m/L_p=(L_r)$	Diameter $D_m/D_p = D_r$	Scale ratio $L_r = D_r$
MEDEL-STANDARD	31.5/250	1.3/10	0.13
MEDEL- FLEX[20]	20/50	0.8/10	0.08

4.5 MATERIALS

One of the key requirements of the digit's material is flexibility. Smaller size with flexibility will make the digit better design to match future design. The main requirement for the material of the design is that it should have high allowable strain, high stuffiness and high strength to match the functionality of the digit.

4.5.1 Silicone substrate material

Based on the required features (shape and flexibility) of the proposed digit, silicone was selected as the material of the substrate because of its high allowable strain, and its high stiffness and strength in comparison to rubber or plastic materials. The prototype digit is constructed from RTV C250[1] silicone. This material has following features [104]:

- available as an easy-to-apply single-component coating

- cures at room temperature, yet is usable over a temperature range of -60°C to +290°C

- has a low modulus of elasticity (flexible structures)

- provides good short-term protection from water; resists many chemicals

Silicone moulding compounds are used to coat sensors with flexible silicone. A flexible silicon substrate provides a biologically compatible [103].

---

[1] Alchemie Ltd, Warwick, UK

4.5.2 Silicone Substrate

Flexures of the digit play a significant role whenever a minimum contact touch is detected and fed back to the surgeon, remedial action can be taken by manipulating position of the digit and a risk of trauma could be avoided. Taking out the stylet or using any other form of actuation based on the feedback information will facilitate easy insertion within the cochlea by deforming/curving the electrode slowly around the scala wall.

The prototype flexible lumen digit, the design for which is shown in Figure 4.4 consists of a flexible silicone substrate that is bent to the required anatomical shape, but which is held straight by a rigid stylet. The stylet will make it easy to advance the digit and keep the pre-curved shape of the digit during or after it has been released. Stylet withdrawal results in the digit returning to the precurled state as shown in Figure 4.4 b.

Sensor 1   Sensor 2   Sensor 3

Silicone substrate   (a)   Single Lumen tube
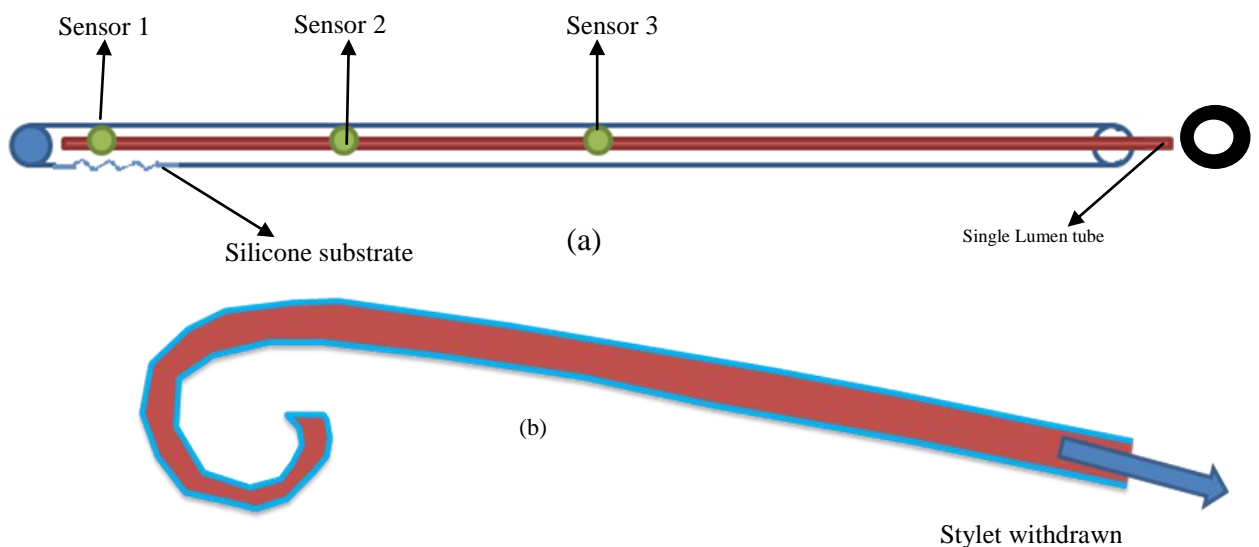
(b)

Stylet withdrawn

Figure 4.4: Main parts of the Flexible digit: a) straightened through stylet during the insertion   b) the digit with original pre-curved shape (stylet off) before the insertion.

The flexible digit contained a single lumen that was 3 mm in diameter into which the stylet was inserted in order to control the digit curvature. To enhance the bending flexibility of the digit a serrated section shown on the end tip was added to make tip deflection easier as the digit was guided along with the basilar membrane wall of the cochlear phantom. In addition, the end tip should bend earlier than the other parts of the whole digit when stylet is removed to shape the curve shape of the cochlea.

The main function of this digit is to detect any tool- tissue contact and obstacles during insertion process of implant into the body (phantom), monitor the position of the digit and return object shape information. Sequential insertion of the flexible digit causes a curling trajectory of the flexible digit which conforms to the inside of the spiral shaped cochlear. For instance, the tip of the flexible digit should be able to detect the tissue contact of the CI as the electrode array (EA) goes deeper inside the cochlea in order to avoid any tissue damage. When the stylet is withdrawn, the deformation of the digit will be non-linear, however the curve shape and size of the tip are kept unchanged. This is the key point of the design as when the tip contacts with the basilar membrane wall the sensors will feedback the status of the contact and the digit is expected to deform and bend as it slides around the wall by pushing back the stylet. Using the sense of touch, the digit could obtain information about important parameters during the procedure such as penetration, contact and its direction, location and magnitude, and shape of the path or the digit.

4.5.3 The sensors

The tactile sensors used in this design were strain gauge sensors[2]. Using strain gauges is one of the simplest methods of measuring small deformations of relatively soft tissues. Three strain gauge sensors are used as tactile sensors to collect information about the interaction between the digit and the phantom. Furthermore, strain gauges could be used to measure bending strains, which are proportional to curvature, allowing a distributive tactile sensing approach that can monitor both contact and shape through the bending strains induced by flexure. These sensors have a gauge factor of 2.09 ± 1.0 %, gauge length of 2 mm, gauge resistance of 120.2 ± 0.2 Ω and adoptable thermal expansion of 11.7 PPM/$^{\circ}$C [103]. The strain gauges have small strain changes and they need signal conditioning and an amplifier.

These strain gauge need to be integrated into the digit where proper placement of the strain gauge then becomes important ensuring accurate and repeatable measurements of micro touch/contact. Although the optimal location to place a strain gauge is where the largest strain occurs, the location of the sensor is important and sensitive when using few sensors. The locations of the sensors within the digit prototype (shown in Figure 4.5) are based on the contact locations of the typical cochlear electrode array insertion along the outer wall into the scala tympani of the human cochlea.

---

[2] Model KFG-2-120, manufactured by KYOWA, Japan
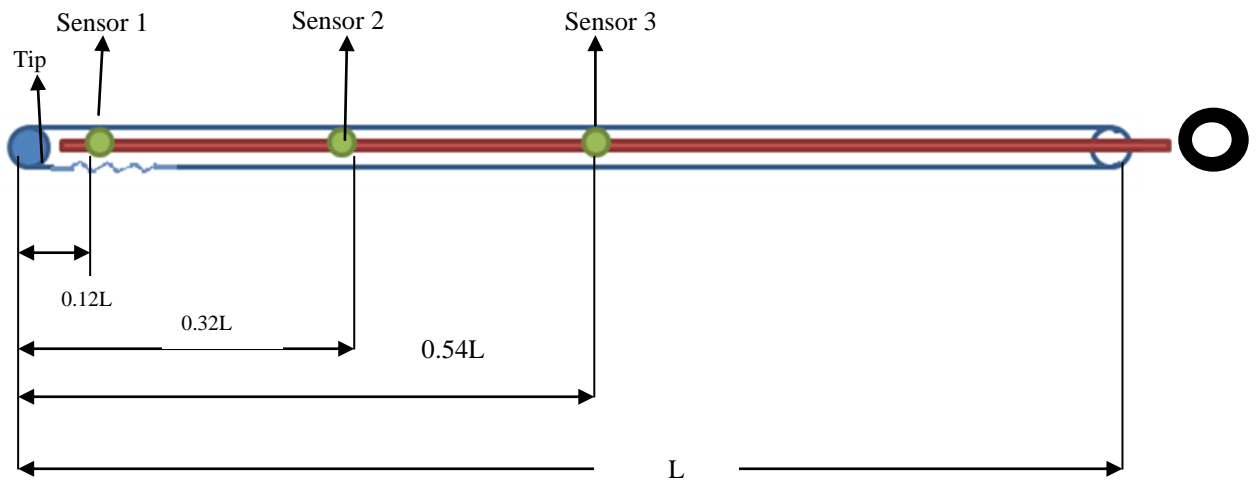
Figure 4.5: Locations of the sensors along the digit

Normally assuming 2 ¼, 2 ¾ or even one turn of the cochlear, there are three insertion stages: basal turn, second turn and the last turn. The optimal sensor locations were identified as being *0.12 L, 0.32 L* and *0.54 L* when measured from the fixed end, which are very close to 58%, 29% and 13% respectively of the anatomical measurements of the organ of Corti [103] as well as three stage locations which could cause contact with the electrode array insertions [31,44]. These positions could show possibility of sensing the contacts along the digit during the digit insertion into the phantom through tactile sensing system feedback.

These three stages can cause contacts with cochlea as shown in Figure 4.6.

Based on these contacts three sensors were allocated along the digit to detect any contact between the digit and the phantom. 1st sensor (tip sensor) can detect any tip contacts, inner wall contacts as well as outer wall contact as shown Figure 4.6 (A,C). The 2nd sensor can detect outer

wall contacts of the basal turn and the final turn of the digit as shown in Figure 4.6(C). The 3rd

sensor senses outer wall of the last (rest) turn of the digit.
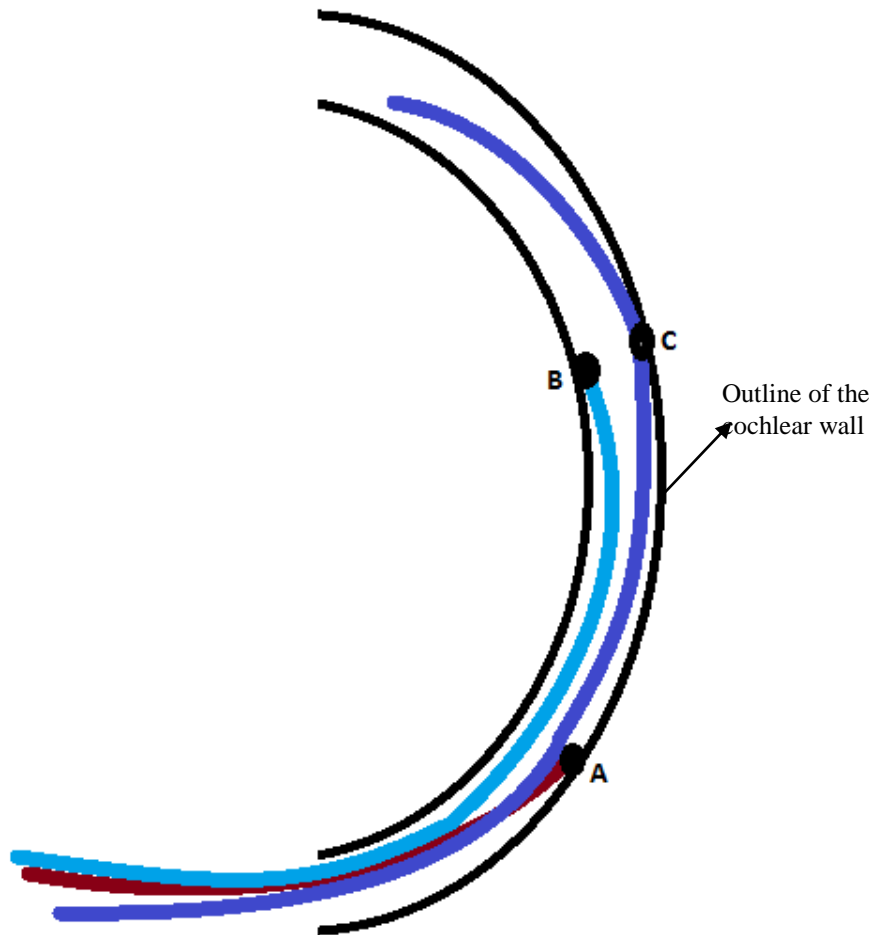
Figure 4. 6 possible contacts between the digit and the cochlea: (A,C) outer wall contact，B) inner wall contact．

4.5.4 Single lumen tube

A steel stylet wire of 2.5 mm diameter is required to actuate the digit manually or control the curvature of the digit. Flexible lumen is needed within the digit where the digit can be straightened, and held in a straight configuration by inserting the stylet into the lumen; the digit relaxes to a shape matching the curvature of the cochlea when the stylet is removed (stressless shape). A soft PVC single lumen tube of 3 mm diameter (Figure 4.7a) was selected to be the lumen for the stylet. The soft PVC has relative similarity with the silicone substrate in terms of flexibility and elongation at break. This lumen could also be used for hydraulic or fluid control instead of manual control (stylet). The lumen tube was used so that the stylet will go through this lumen to control the shape of the digit and depth insertion of the digit.

Silicone substrate

Single Lumen tube
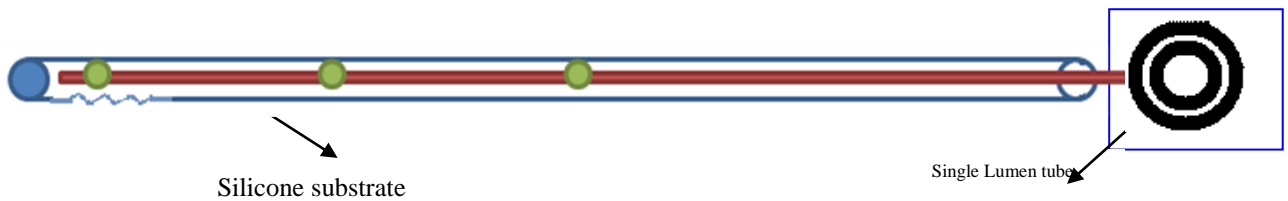
Figure 4.7: Main parts of the Flexible digit: a) straightened through stylet during the insertion   b) the digit with original pre-curved shape (stylet off) before the insertion.

4.6   MANUFACTURING THE FLEXIBLE DIGIT

A correspondingly simple, low-cost and easy manufacturing process was developed where sensors were attached to a thin sheet metal with silicone lumen tube and a room-temperature vulcanizing RTV silicone was moulded into the desired shape (cochlea shape).

Three strain gauge sensors were glued (Sil-Poxy-Silicone Adhesive) on a thin sheet metal (0.3 mm) to keep the space between the sensors as well as alignments of the sensors in one direction (Figure 4.7). Connectivity and sensor resistance were checked before the sensors were glued on a PVC tube. The three sensors with sheet metal were glued on a PVC lumen tube (3mm diameter) as shown Figure 4.8.
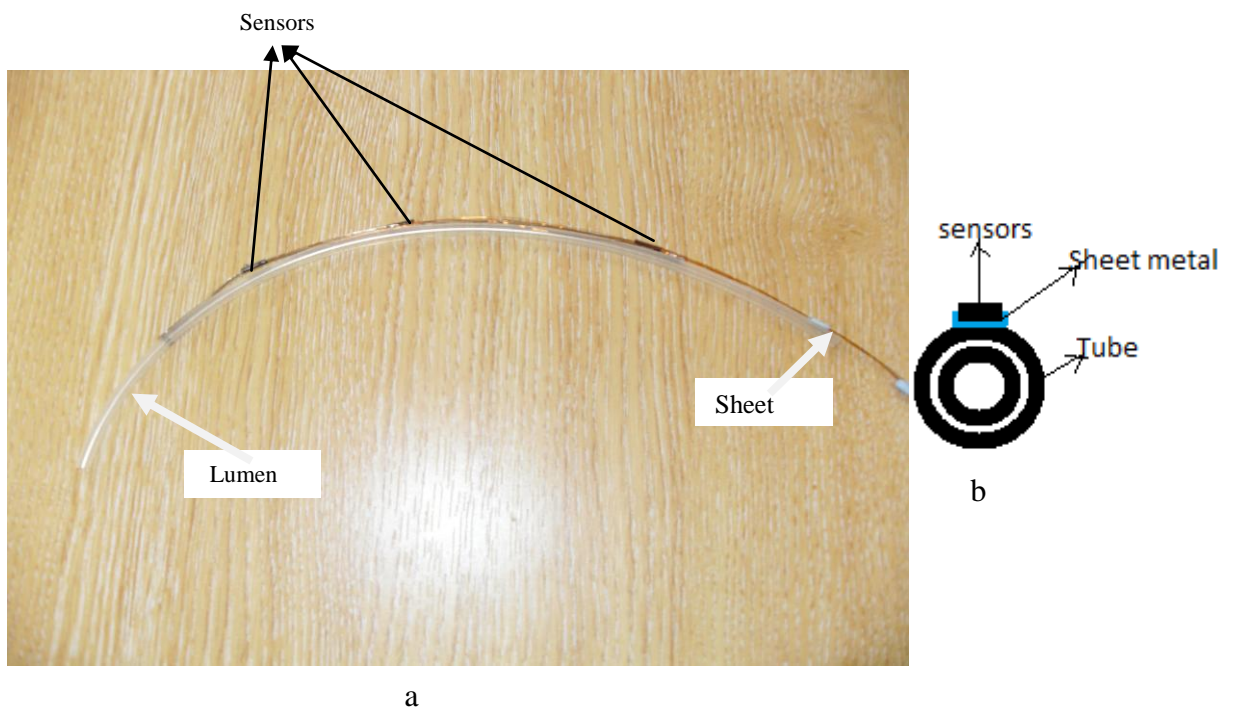
Figure 4.8: a) Lumen tube glued on three sensors with thin sheet metal
b) cross-section of the tube with sensors and sheet metal

The overall digit was manufactured using a 2 part split mould. The mould was constructed from Accura Si10 photocuring resin using a Viper Si2 Stereolithographic Apparatus from 3D Systems Inc. The instrumented lumen was located within the lower mould and then overmoulded with RTV 250 silicone as shown in Figure 4.9.
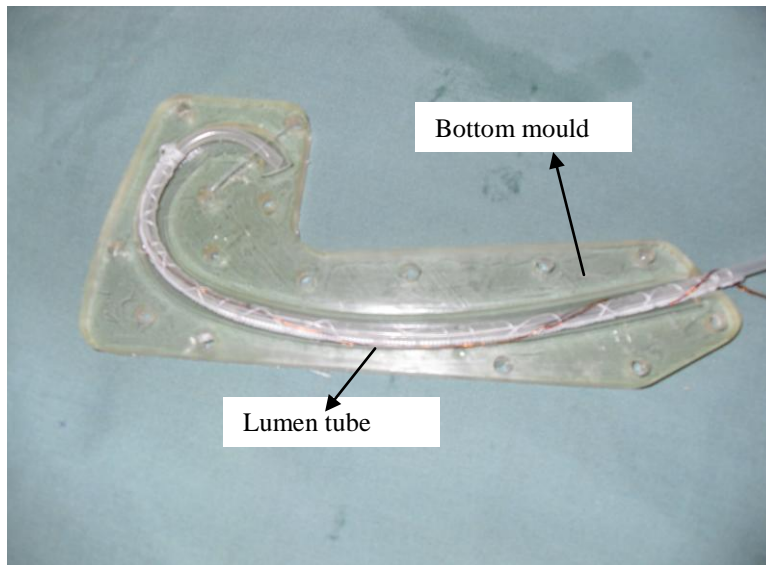
Figure 4.9: Lumen tube with sensors lied down on the bottom mould

Then the sensors with silicone tube were over moulded by a 250 silicone. Room-temperature vulcanizing (RTV) 250 silicone was poured into the bottom mould and then sealed with a top mould to have a pre-curl shape as shown in Figure 4.10.
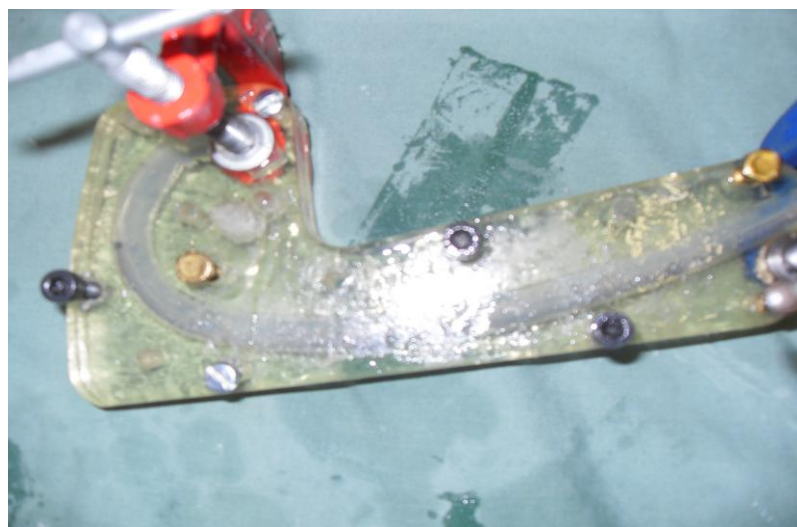
Figure 4.10: Silicone digit inside complete mould

Pouring uncured silicone liquid rubber into a mould was the process which was chosen since it was the simplest shaping process to perform. After curing, the digit is shown in Figure 4.11.

Figure 4.11: Flexible digit after cured

With 10% catalyst added to the base material, the curing time was about 48 hours. Two-part RTV silicone rubbers must be stirred which causes air bubbles to become trapped in the rubber, creating voids in the cured product which tend to accumulate near the surface. These voids change the mechanical properties of the rubber, which makes accurate testing of the sensor difficult. To mitigate this, the silicone rubber was degassed using a partial vacuum.

4.6.1 Manufacturing process

The shape of the cochlea is one of the roots of the challenges of cochlear implantation operations. The cochlea (Figure 4.12) is the auditory part of the inner ear and it is 'snail-shaped' structure which is roughly 2½ to 2¾ turns around its axis (the bony core of the cochlea). The shape of the cochlea affects the human hearing range, for instance, the basal affects high-frequency hearing frequency where the apex shows low-frequency range [108].

In CI insertion experiments, different phantom models are used such as making casts of human cadaver cochleae using epoxy and silicone elastomer and silicone only [109] to resemble the cochlea of the inner ear. In this research, it is focused the shape of the cochlear rather than the stiffness (or filled fluid) properties. The 1st turn of the cochlea was considered which can give us tool-tissue contact information of the cochlea phantom.

Figure 4.12 cochlea shape with its frequency spectrum [107]

The phantom cochlea (Figure 4. 13) was designed using Solidworks[3] software and then manufactured using a Viper Si2 stereolithographic apparatus (SLA) from Accura Si10[4].

Figure 4.13: Cochlear Phantom

A 4.5:1 scale prototype which has a length of 158 mm, thickness of 1 mm and a varying diameter of 24.5 mm – 26 mm was used in this study where the human cochlea has the length of about 35 mm and diameter of 2mm [109,110]. The phantom is large compared to real size of the cochlea (4.5 times bigger) but it is only conceptual to investigate the interaction between cochlea and the digit during the cochlear implant operation.

The shape of this cochlea prototype resembles the human shape and this makes comparison analysis for the inserting electrodes into cochlea. The main parameter was detecting the contact between the cochlea and the digit.

---

[3] Solidworks V 2010, Dassault Systèmes SolidWorks Corp, Massachusetts, USA
[4] Viper™ SLA® System, 3D systems corporation, Rock Hill, USA

4.7 EVALUATION EXPERIMENTS

Data acquisition and signal processing were used with a PC to collect the measured data (Figure 4.14). FLYDE[5] signal processing circuits were attached to the digit's strain gauge sensors. Data from the FLYDE amplifier is acquired using Computer Board's NI PCI-6034E data acquisition board (DAQ) and recorded using MatLab[6] software.

Figure 4.14: Flexible tactile digit system

---
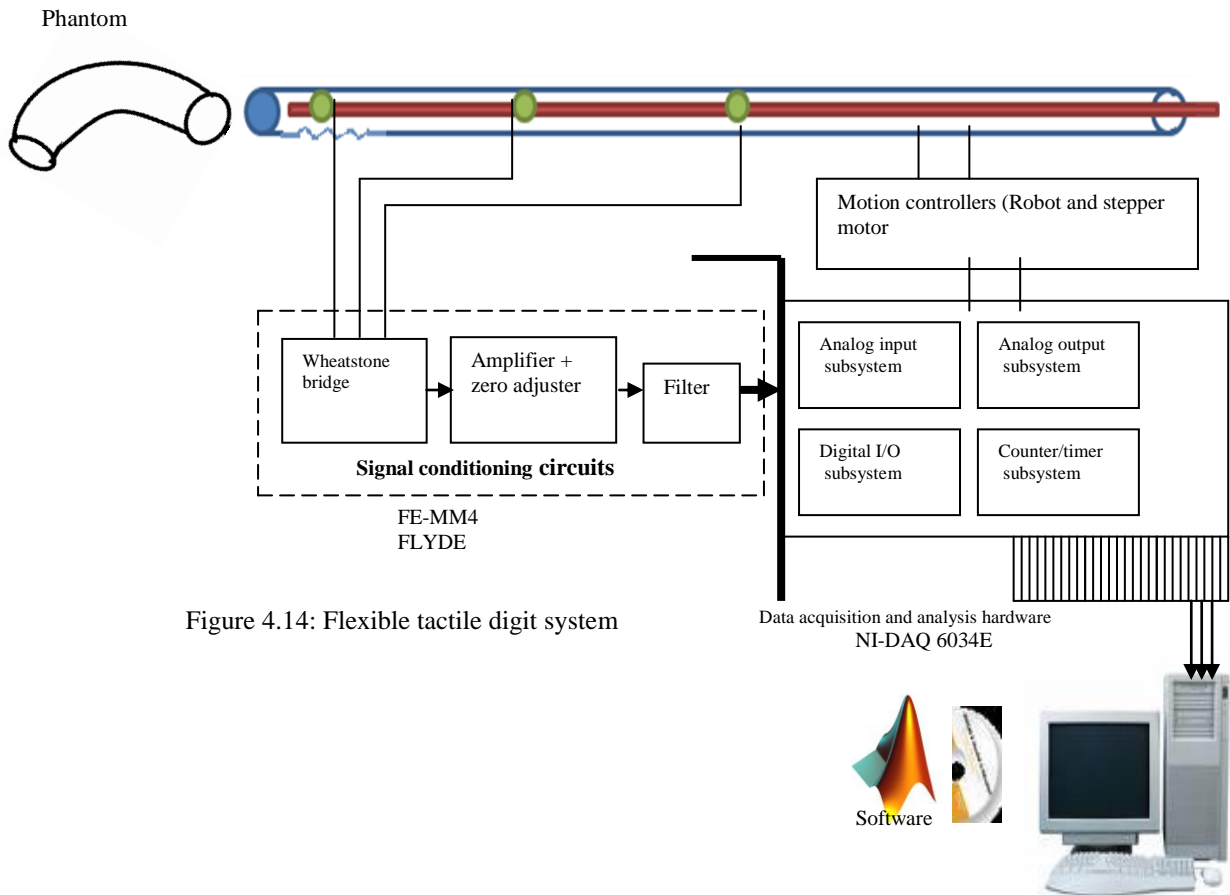
[5] FF-MM4 FLYDE, Fylde Electronic Laboratories Ltd, Preston, Lancashire, UK

[6] MATLAB V6.5 R13, 2002, Mathworks, USA

That data is analysed to obtain information about digit–phantom contact. The Output signal of the DAQ can be expressed in different parameters such as voltage, force and strain. The digit is subject to a bending strain which varies in a linear way with the output voltage

The output voltage, *Vo* of the quarter bridge (Figure 4.15) as a function of the strain is given by [102]:

$$Vo = \frac{V_i G_f}{4} \varepsilon \qquad (4.2)$$

Where V_i is the excitation voltage (input voltage), G_f is the gauge factor and ε is the strain.
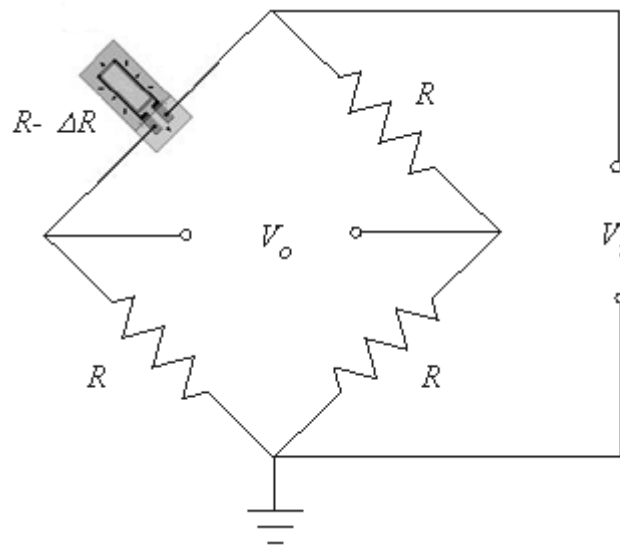
Figure 4.15: Quarter bridge (one-active gauge) configuration

With gain, *G* included, equation (4.2) becomes

$$Vo = \frac{GV_i G_f}{4} \varepsilon \qquad (4.3)$$

And the strain, ε becomes

$$\varepsilon = \frac{4V_o}{GV_iG_f} \qquad (4.4)$$

Knowing that stress, σ and strain are related by Young's modulus, E and is given by

$$\sigma = E\varepsilon \qquad (4.5)$$

Consequently, axial force that is normal to the contact tissue becomes

$$F = \sigma A = E\varepsilon A = \frac{4V_o EA}{GV_iG_f} \qquad (4.6)$$

Where A is the cross sectional area of the digit.

An equation that describes the relationship between bending strain and curvature with sensor output is detailed in [111]. Let us consider the strains experienced by a single gauge-pair with substrate as shown in Figure 4.16(a). It is possible to directly relate the radius of curvature of the substrate, r_{ave}, to the original length of the strain gauge, L0 (L0 = Lg, the gauge length). Assuming a constant curvature in the localised area of the gauge-pair, gives the relationship:

$$s = r_{ave}.\emptyset \qquad (4.6)$$

where s is the arc-length and θ is the angle inscribed by that arc length. However, since the substrate mid-line is inextensional, the portion of the substrate corresponding to the length of each strain gage is always equal to L0. Therefore, the inscribed angle for that portion of the sensor is simply:

$$\emptyset = \frac{L_o}{r_{ave}} \qquad (4.7)$$

Output voltage in terms of the strain gauge and substrate thickness (Figure 4.15) could be approximated by assuming current length, L of the arc length of the curve with substrate thickness t_s and gauge thickness, t_g.

$$L = (r_{ave} + \frac{t_s + t_g}{2}).\theta \qquad (4.8)$$

Where r_{ave} is the curvature of the membrane centreline, t_s is the thickness of the membrane substrate, t_g is the gauge thickness, and θ is the angle inscribed by arc length.
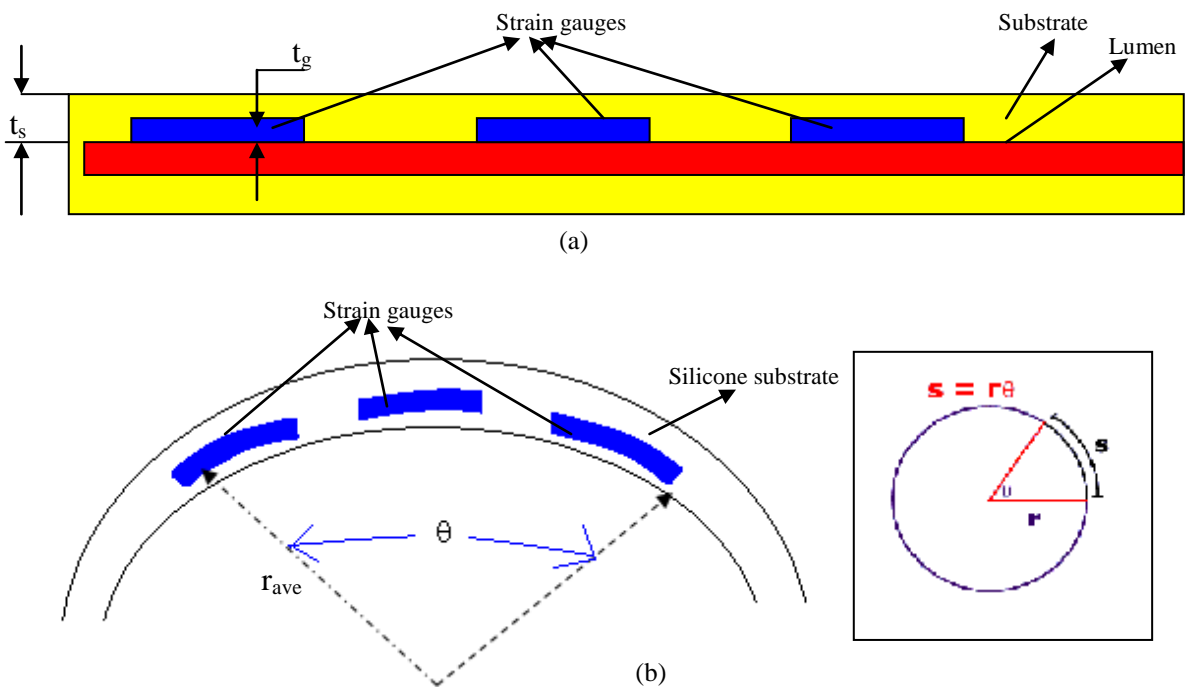
Figure 4.16: Modelling the digit (a) dimensions of the sensor substrate and strain gauge in flattened view. (b) The radius of the curve of object related with curvature of the substrate.

The current length, L of the curve could be expressed

And knowing that $\theta = \dfrac{L_o}{r_{ave}}$ equation 4.8 is

$$L = (r_{ave} + \frac{t_s + t_g}{2}).\frac{L_o}{r_{ave}} \qquad (4.9)$$

To compute the strain of the gauges, the formula for strain and equation are used to get

$$\varepsilon = \frac{L - L_o}{L_o} = \frac{(r_{ave} + \dfrac{t_s + t_g}{2}).\dfrac{L_o}{r_{ave}} - L_o}{L_o} = \frac{t_s + t_g}{2r_{ave}} \qquad (4.10)$$

The change in resistance is given by

$$\Delta R = \frac{R_g G_f (t_s + t_g)}{2r_{ave}} \qquad (4.11)$$

where R_g is gauge resistance before strain is applied.

The output voltage of the quarter bridge strain gauge can be obtained by substituting equation 4.10 into a standard Wheatstone-bridge configuration, the equation for measuring bending strains with quarter-bridge strain gauges becomes;

$$V_{out} = \frac{V_{in} G_f (t_s + t_g).G}{8r_{ave}} \qquad (4.12)$$

The average curvature κ of the digit for ith gauge could be estimated by

$$\kappa(i) = \frac{1}{r_{ave}} = \frac{8V_{out}}{V_{in}.GF.(t_s + t_g).G} \qquad (4.13)$$

4.8   GENERAL DESIGN CONSIDERATION

The digit was easily manufactured and still has room for additional functionality. First, it has a very simple physical structure. So, all electrical parts are readily available at low cost and mechanical parts are simple to procure or produce. Secondly, the digit is large scale. This design is intended to serve as proof of concept, but it can be miniaturised to fit the purpose. Micromachining processes could be used to fabricate the digit integrated with tactile sensors.

As shown in equation 4.11, decreasing the thickness of the substrate and strain gauge t_s, and t_g respectively, will decrease the curvature, κ of the digit. Also Stoney's equation which is used to describe thin film curvature is given by [103]

$$\frac{1}{R} = \frac{6(1-\nu)\sigma}{E}\frac{t}{h^2} \tag{4.14}$$

Where R is the radius of curvature; σ is the film stress; E is the Young's modulus, ν is the Poisson's ratio of the material; t and h are thicknesses of the film and the substrate/plate, respectively. This equation indicates that decreasing substrate thickness, h will decrease the curvature of the digit.

4.8.1 Configurations

The design of the steerable tactile digit allows for several different configurations. Besides the original purpose for electrode insertion for cochlear implants, it is also possible to use it for path navigation, surface condition sensing and as a guiding feedback tool.

In summary, this steerable digit incorporating tactile sensors will facilitate insertion of the tip into the scala tympani as it is subjected to resistance (force). In this design the main features include, continuous sense touch feedback with a flexible curling path of the tympani, simplicity in design, few sensors (effective distributive tactile), cost effectiveness and few complications. These concepts will be implemented in the next chapter.

5 Chapter 5 FLEXIBLE DIGIT ANALYSIS

After optimising the design parameters and phantom design, it was necessary to determine the response of the prosthesis and empirically assess its viability for determining the required categories of manual stimulation. This chapter presents the results of the response analysis of the flexible tactile digit. Experiments leading to understanding the proposed flexible digit under different surface conditions conducted. The sensing characteristics of the digit to stimuli of varying lumen contact conditions (including location, direction and shape) were analysed and used to formulate a functional specification of the digit.

5.1 FUNCTIONAL ANALYSIS

To verify the performance of the digit, investigations on the tool/tissue interaction in lumen contact conditions were investigated. The tactile digit signal-response strategy is summarised in Figure 5.1:
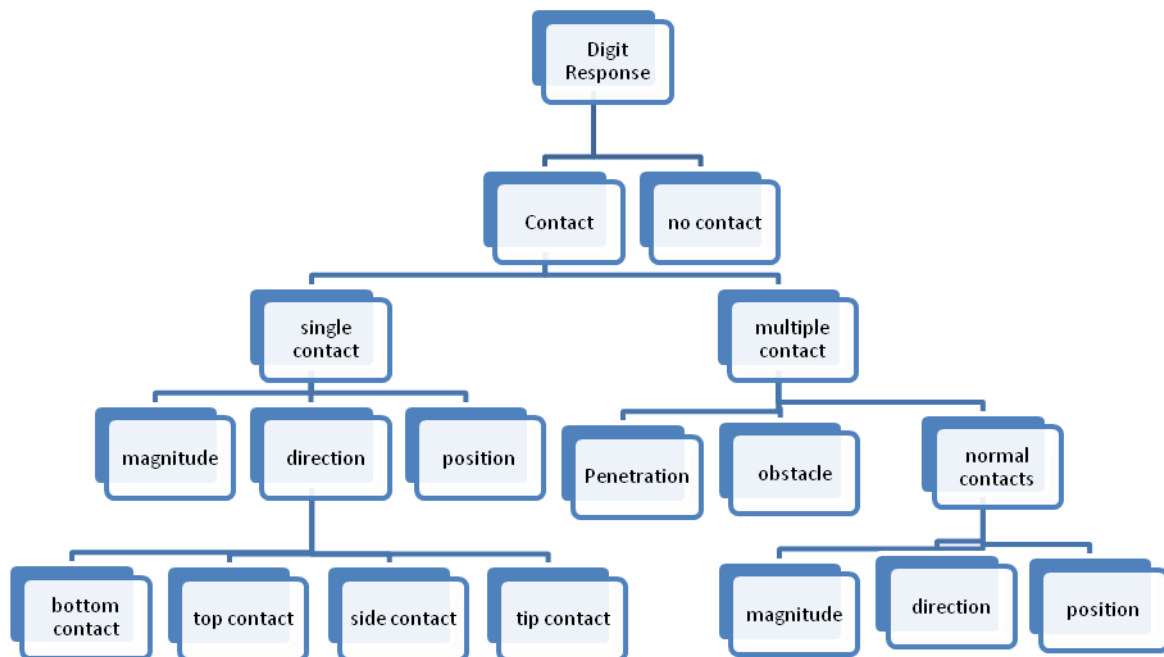
Figure 5.1: Signal discrimination strategies

Although there are other potential signals for the digit such as texture/stiffness of the contact and lumen mapping, contact conditions, their directions and the relative position parameters of the digit are essential to minimise trauma during electrode insertion. Based on these parameters, a series of experiments were devised to evaluate the digit's performance. Many of these characteristics are common in path navigation, lumen mapping and palpation procedures.

5.2 FUNDAMENTAL TOUCH CHARACTERISTICS ANALYSIS

The aim of this experiment was to ascertain the ability of the digit to identify the basic touch characteristics that discriminate between contact versus no-contact status, tip penetration, obstacles, and contact locations. For instance, the insertion force due to contact between the digit and the cochlear phantom depends on the contact angle or the relative orientation of the digit with respect to the walls of the cochlear. Before the digit was inserted into the phantom, a few experimental tests were done to discern the digit's ability to detect the position of the contacts with time. In this situation the flexible digit with stylet in place was tested outside of the cochlea phantom, the digit was then stimulated at various locations along its length, and the strain gauge tactile sensors were used to detect these contacts (taps) and their locations.

Experiment 5.1: validating and calibration of the experiment

To minimise measurement errors a calibration process was undertaken through applying the known loads to the system and observing the resultant sensor output voltages. Once this relationship was established or verified, the load types and magnitudes could then be inferred from the measured voltages.

Aim: To calibrate the digit to detect surface conditions of an object.

Method: A number of known loads were suspended from the digit using a hook apparatus as shown in Figure 5.2, and the resulting voltage signals were recorded.

Results: results of this experiment were shown in Figure 5.3 and 5.4, as well as Table 5.1.
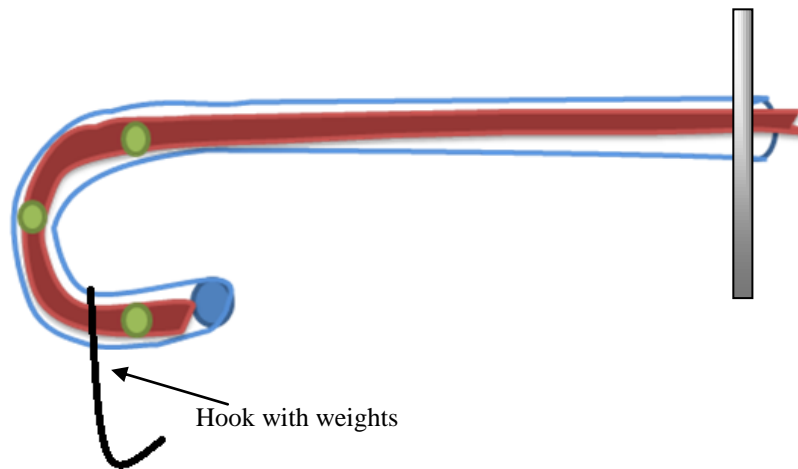
Figure 5.2: Testing the digit with different loads

Figure 5.3 shows response of the digit when 208g was applied to the digit suspended on the

hook. The experiment was repeated 5 times and the result was -0.042V ±0.001V. The difference

is negligible and this has verified that the digit can identify specific loads.
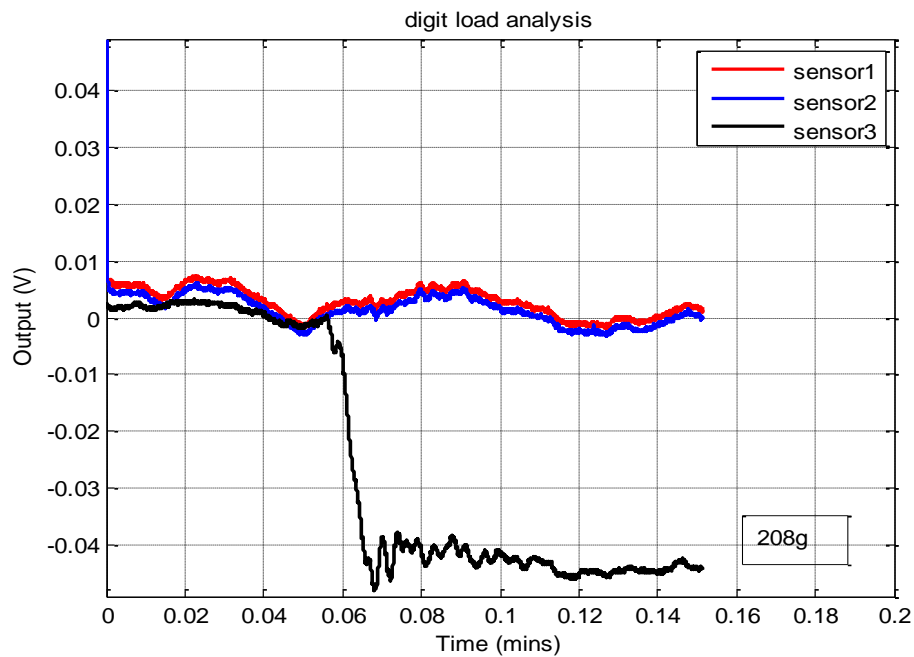
Figure 5.3: Digit responses when 208g of load was attached on to it.

Figure 5.3 shows response signal of the digit with and without loading. The graph shows that initially the system was monitored in an unloaded condition in order to establish a no-load reference. This methodology was repeated for each load case in order to observe the effect of self-load. After approximately 4 seconds (0.06 min) figure 5.3 shows the effect of applying a 208 g (2.0 N) load to the digit. At this point the result shows a change in Sensor 3 of -0.045V from the no load state of the digit. There was no significant change to the readings from sensor 1 and 2. The applied load (weight) caused the digit to bend down. The bending effect is greatest under the location of sensor 3 which is the furthest sensor from the point of loading, and the most sensitive due to its position. This location has the largest extension effect compared to other positions of the sensor 1 and 2.
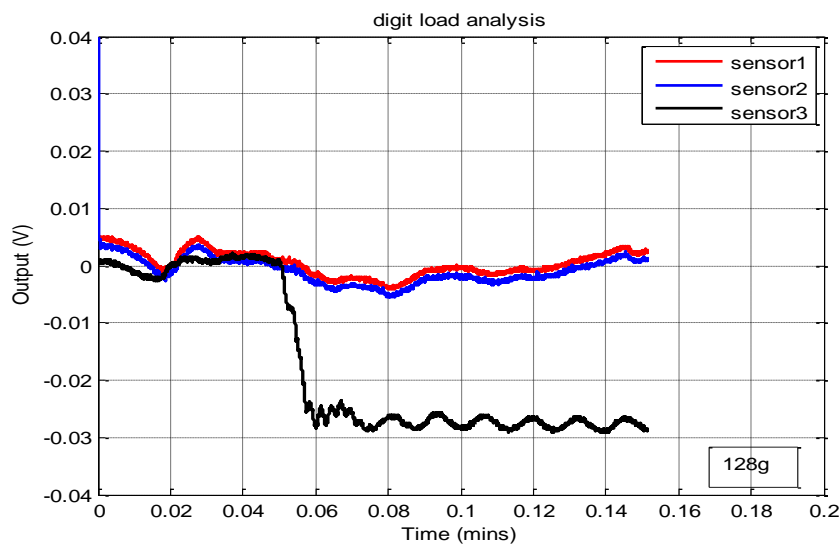
Figure 5.4: Digit response when 128g of load was attached on to it.

Figure 5.4 shows the loading process for a 128 g load (60% of that applied previously), again it may be seen that only sensor 3 has significant deviation as a consequence of the applied load,

and the magnitude of the deviation from the no-load condition is approximately 60 % of that found for the previous load. These results are shown in Table 5.1

Table 5.1 Loading for digit calibration			
Load	Output signals		
	Sensor 1	**Sensor 2**	**Sensor 3**
No load	0.005 V	0.004 V	0.002 V
128 g	0.002 V	0.001 V	-0.029 V
208 g	0.002 V	0.001 V	-0.045 V

Analysing this experiment, using known inputs (Loads), a strain and the young's Modulus of the used material was calculated.

Using equation 4.4, $\varepsilon = \dfrac{4V_o}{GV_iG_f}$ strain, ε caused by 128 g (V_0 =-0.032 V) is 0.00128 = 1280 µstrain where input voltage (excited voltage) , V_i = 5 V, gain of the system, G, is 10 and the gain factor, G_f of the strain gauge is 2.00.

Young's modulus, E or Tensile modulus of this experiment can be expressed as follows:

Area of the digit ($A = \pi d^2/4$) with diameter (d) of 10 mm is 7.85 x 10^{-5} m^2. Load is expresses as weight /force (w=mg) =0.128*9.81= 1.25 N. Based on the force, area and strain calculated above, the Young Modulus, ϵ ($\epsilon = F/\varepsilon A$) of this material, is 0.0124 GPa where F is the applied force (N).

Through the same methodology the strain caused by the load of 208 g which produced -0.042 V can be said to exhibit a strain ε of -1680 µstrain.

Experiment 5.2: multiple contact locations

During the cochlear implantation or endoscope insertion, there is a contact between the tissue and the endoscope or electrode arrays. These contacts could be single or multiple contacts with different directions and knowledge of the nature of the contacts between the tool and the tissue could reduce the risk of excessive force being applied to the sensitive structures within the ear during implantation.

Aim: to detect any momentary contacts with the outer surface of the digit and establish directions of these contacts.

Method: three different locations along the digit were momentarily stimulated whilst the digit was held in its straight position through the use of the stylet (Figure 5.5). Different methods could be used to represent analogy of momentary tissue contacts but manual tapping was selected as a contact method for simplicity. Tapping on the outer surfaces of the digit was used to approximate delicate tissue-tool contacts. Each time before the contacts are made, the reading of the system is set to zero.
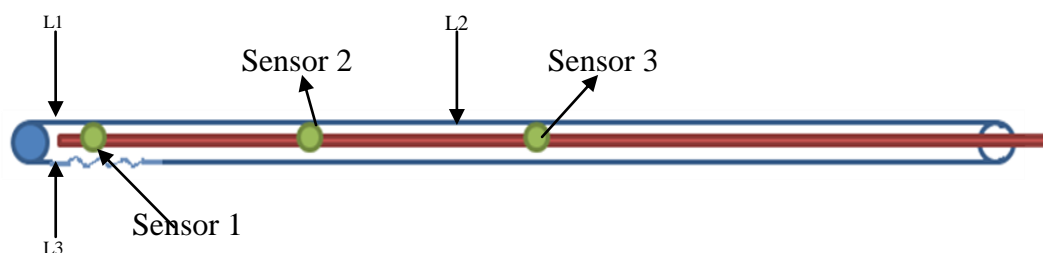
Figure 5.5: Diagram of the instrumented digit. Tap contact locations L1, L3 (distal) and L2 (medial) are indicated with respect to the Sensor locations.

The three tap contacts were made in the sequence of L1, followed by L2, and lastly L3; As shown in Figure 5.5, Ll and L2 were top contacts which caused bending strain, resulting from a

linear force exerted in the vertical direction where L3 is bottom contact, and all contacts were made in a direction normal to the surface of the digit. The location and magnitude of the applied force were different and were random, just to see how sensors can detect different contacts with their directions was the aim of this experiment. It was expected that the strain at the top in bending (L1 and L2) or tensile side will have increase in resistance which produces positive signal of strain and stress, where compressive side (L3) will have negative signal of stress and stress due to decrease in resistance.

In that way, the top contacts would result in a positive signal, a positive curvature of the digit (reporting a positive strain in the strain gauge sensors and a subsequent reduction in the output sensor voltages) and vice verse for bottom contacts due to the strain gauge deflection behaviour.

Results: The output responses of the digit with above contact locations are shown in Figure 5.6. The experiment was repeated five times to test repeatability and the result was statistically significant ($p=0.0703$) showing different contacts with their locations. The experiment has shown same results of directions of these contacts.
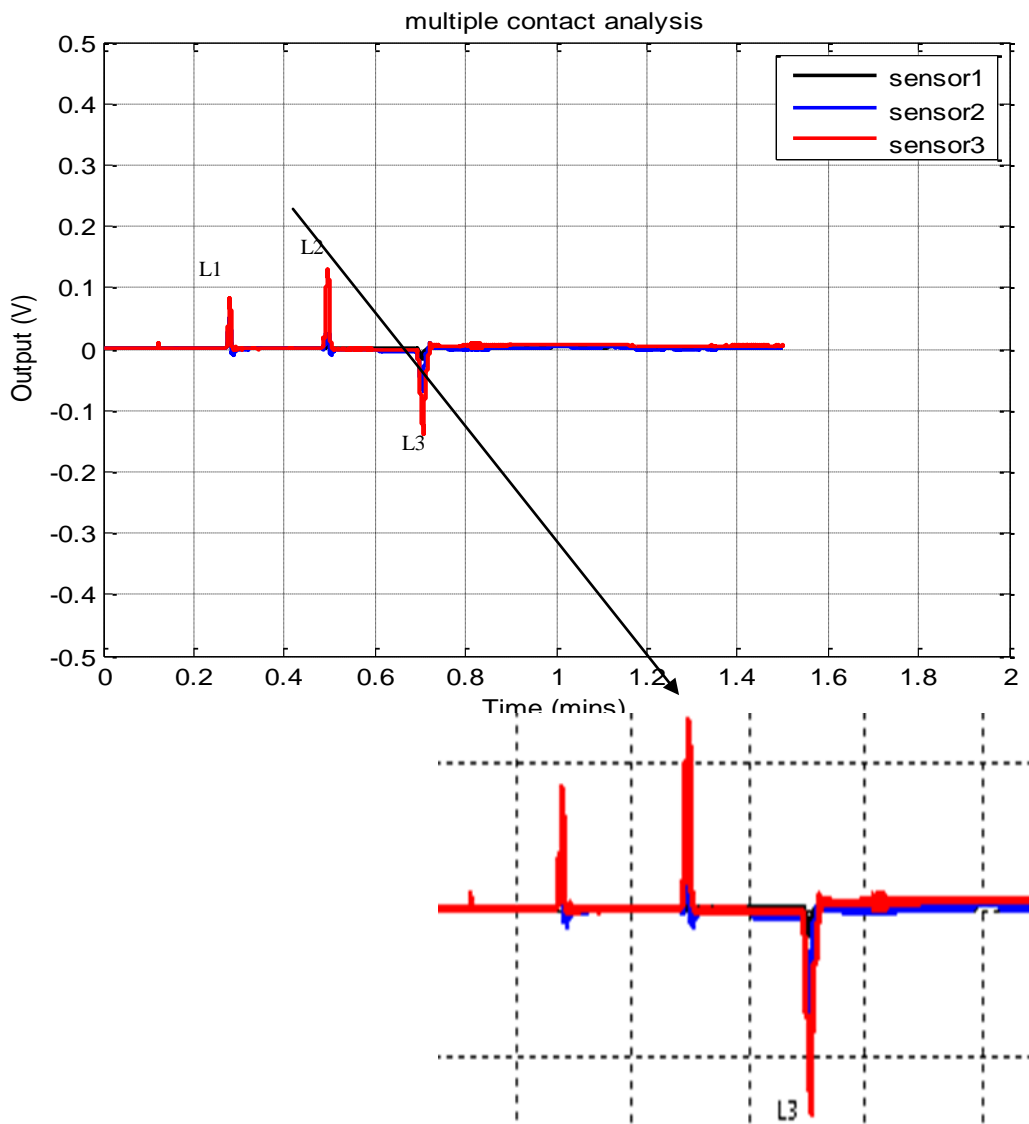
Figure 5.6: Digit response with style in place (multiple contacts and their directions); L_i: tap contacts

As can be seen, the result conveys rich dynamic information about the sequence of contacting stimuli, the time at which each contact begins and ends, and the magnitude (bending forces exerted by each digit on the object). These output signals indicate direction of the three tap contacts *L1*, *L2*, and *L3* respectively. The magnitudes of the response indicate that there are three contact locations that have different directions and magnitudes. In addition, it can be seen that contact with the L3 occurs later than contact with L2, L3 and L1. The timeline of these three signals happened different time and this shows that the contacts occurred differently.

Additional observations were made from the digit's responses (Figure 5.6) where L1 and L2 signals have positive (upward) direction while *L3* has a negative (downward) direction. This coincides with the directions of contact indicated in the Figure 5.5; positive spikes show top contacts whereas negative spikes indicate bottom contacts. The magnitudes and directions of the output signals depend on location of the sensors along the digit and force applied on the digit. In this case contact L3 were applied higher force through tapping compare to other contacts. Further study of sensing algorithm is needed that can incorporate the magnitude of the applied forces and the location of the sensors with contact status and their directions.

Another multiple tap experiment with its results is shown in Figures 5.7 and 5.8 respectively. Like the previous experiment the contacts with the digit were made sequentially at different locations, but two additional contact locations were considered, most notably an axially acting tip contact.
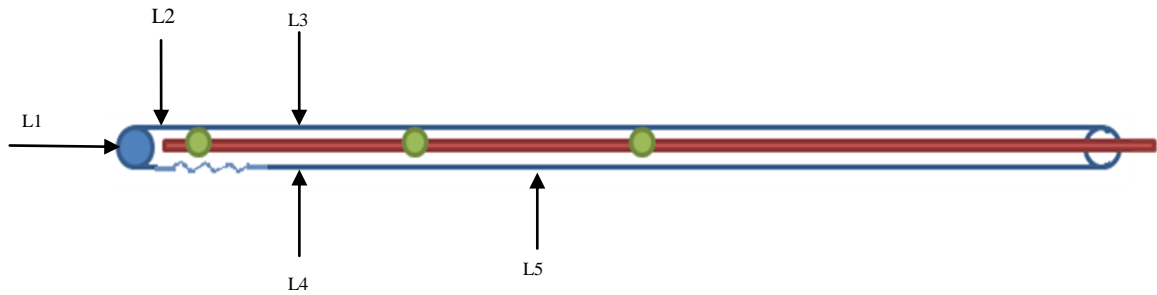
Figure 5.7: Identification of the contact locations: L_{is} are tapping contact locations

These output signals are similar to the previous experiment (section 5.7) except that there is an extra tip contact (L1). Although the tip is subjected to an axial load (compressing the digit), the axial load made the digit bend down (flexible digit) rather compressing and subsequently reducing the length of the strain gauge which reduces the resistance and therefore voltage goes up (positive signal) at the same the digit bounced back and caused an upward force. This upward force created the negative signal shown in Figure 5.8.
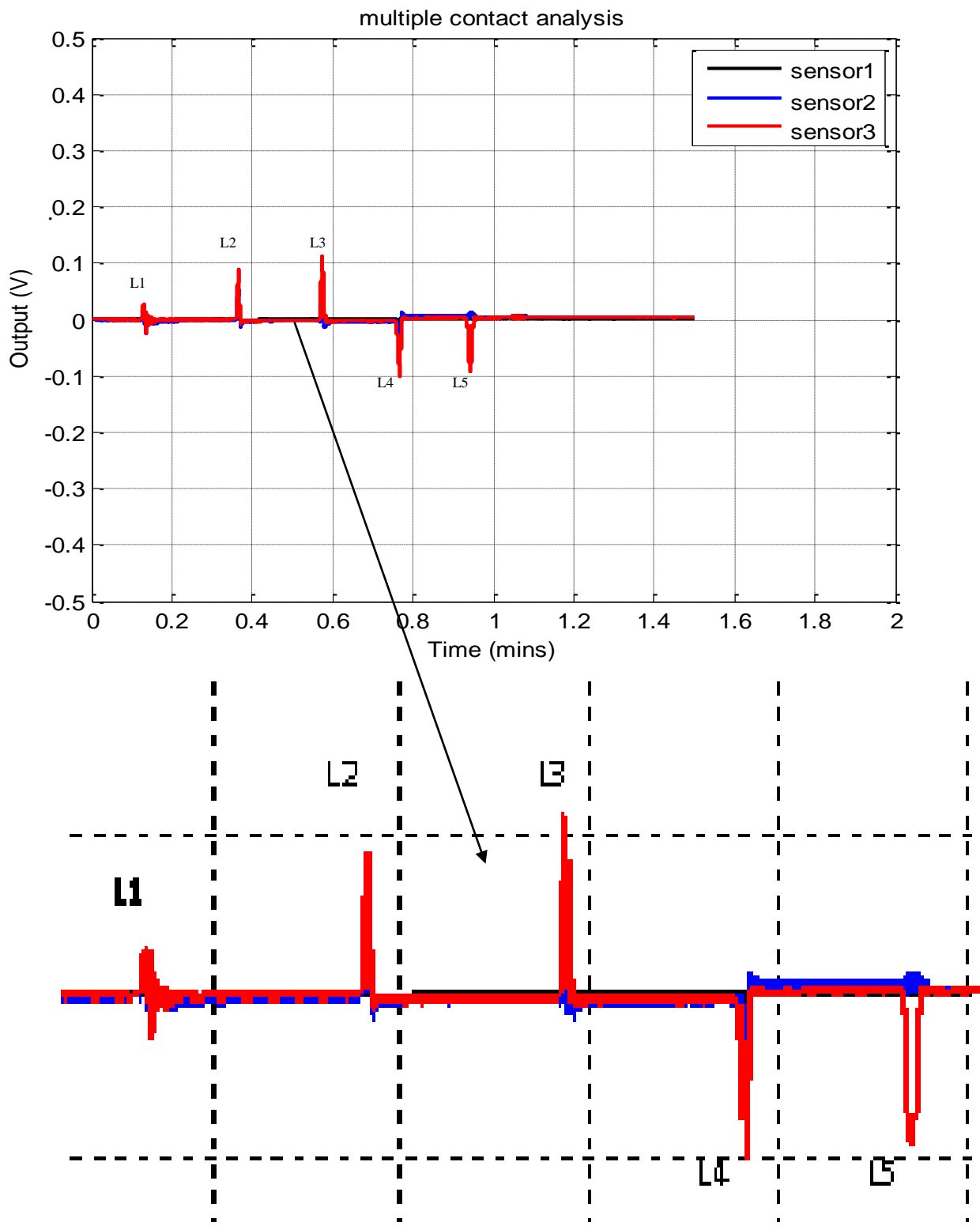
Figure 5.8: Digit response with tip and multiple contacts

Experiment 5.3: multiple contact locations with partially removed stylet

Electrode insertion during cochlear implant processes can have different stages and each stage can make contact with the cochlea as discussed in section 4.1.2. Electrode straight insertion can cause tip and side contacts, similarly second stage (1st curve) can make different direction contacts.

Aim: to detect any contact of the digit through tapping contacts. This experiment aims to detect digit contacts that can occur during the electrode insertion procedure for the first turn or second turn.

Method: three different locations along the digit were manually stimulated (tapped) whilst the digit was in a curved configuration (with the stylet partially withdrawn) as shown in Figure 5.9. The reading of the system is set to zero before the contacts were made.
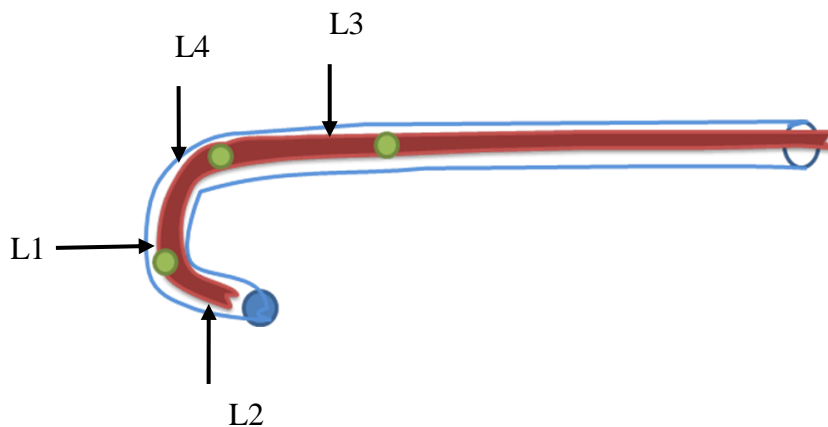
Figure 5.9: Multiple tappıng contacts of the digit with partially stylet withdrawn, L1-L4: tapped contacts

The contacts with the digit were made at different times – first location L1 of the probe were touched, afterwards location L2 of the probe was touched, and then L3, and lastly L4. The

output transient signals from the sensors were recorded. The experiment was repeated five times to test repeatability.

Results: The output responses of the digit with above contact locations are shown in Figure 5.10. The three positive signals correspond to stimulation at locations *L1*, *L3*, and *L4* whilst the negative signal corresponds to location *L2*. The negative voltage at L2 is caused by bottom tap contact of the sensor 3 where the tap caused an upwards flexure in the digit, inducing a compressive strain to be induced across sensor 3 thereby reducing resistance and increasing the voltage signal. This confirmed that the digit was able to detect different position along the digit in any situation. However, in this case, the digit can classify direction contacts (top and bottom contacts) only and needs further investigation algorithm which can classify radius contacts from top and bottom contacts. The tap contacts were very soft and the digit is flexible, this feature suggested further algorithm investigation for radius and compression contacts classification.
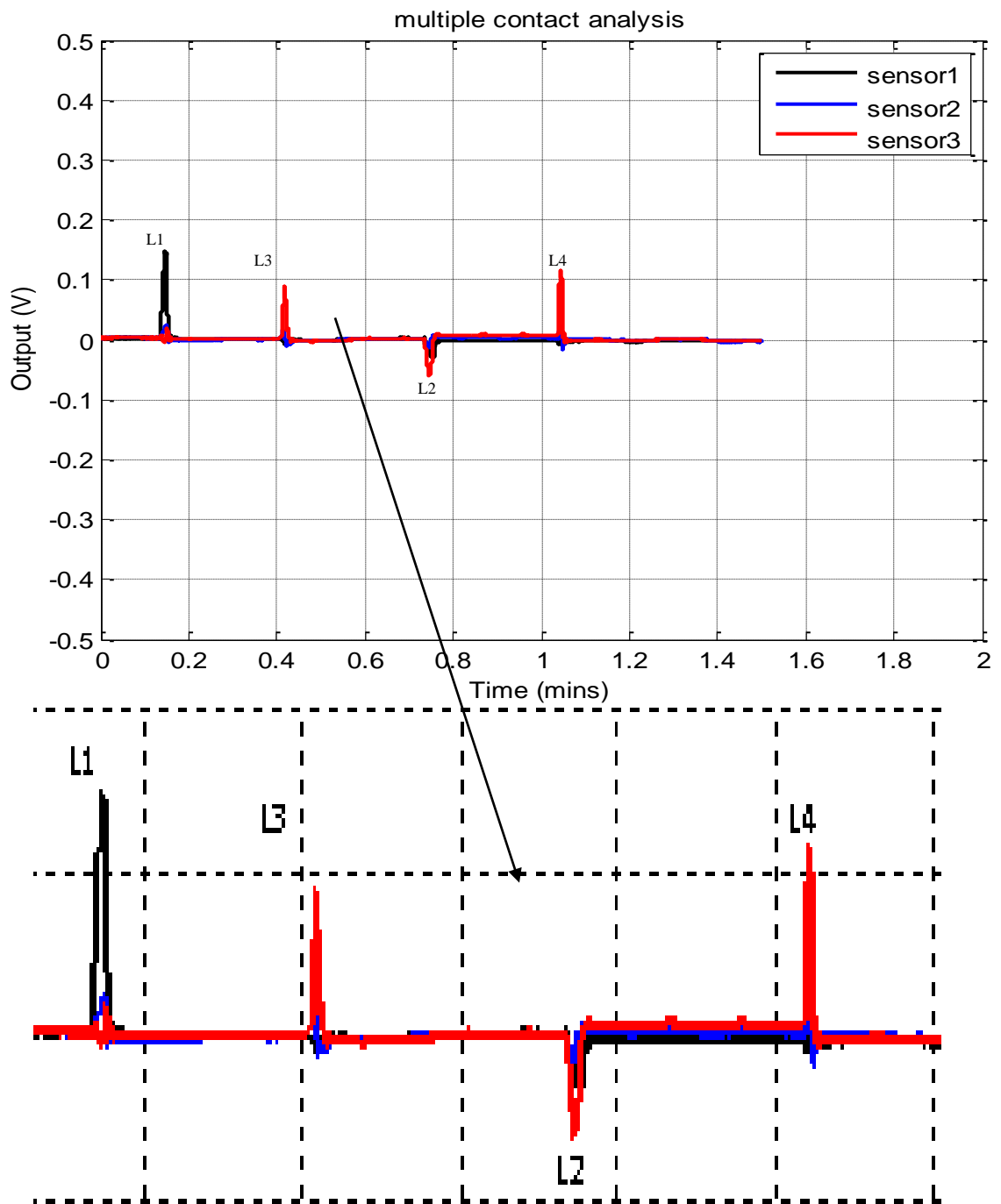
Figure 5.10: Tactile response of tapping contacts

Finally, results depicted on Figure 5.10 showed statistically significant (p =0.007) of detecting different contact conditions of the digit. Although these results are preliminary, there is evidence of measurable change in sensor voltage as a consequence of momentary contact in both straightened and flexed conditions. The results are useful prove for the tissue contact detection. The compression force was not detectable easily due to the flexibility of the digit which is easier to bend down or up rather than compressing and needs further investigation.

5.3 SURFACE CONDITION ANALYSIS

Three surface conditions were considered; tumour detection, gap/crack detection and surface condition. This analysis was performed as a way of assessing the effectiveness of the digit for the determination of tumour and crack presence.

Experiment 5.4: crack/hole detection

The human ear has cavity in the middle ear (tympanum) and inner ear (the bony labyrinth). In the case of inner ear, the winding tubular cavity within the inner ear can have a crack or hole (a perilymph fistula) which must be detected for appropriate treatment. Similarly, other MIS applications can have cracks in the body. This experiment is expected to identify the difference between normal contact of output of smooth continuous surface and the output of the crack or hole phantom contact. This could potentially help the surgeon to identify surface conditions including holes or cracks in a hidden anatomy such as within the cochlea.

Aim: To be able to obtain information about consistency of tissue structures (particularly hole/cracks) by investigating the effects of the tissue/object on the tactile digit and thus to be

able to recognize and assess anatomical or pathological structures, even if they are hidden in the tissue.

Method: A stationary digit was placed in contact with a rotating target object (connected to a electrical motor). The target incorporated two notches of 2 mm and 3 mm (Figure 5.11) each representing cracks in the human body or any abnormality gaps/cracks in the cochlea during the electrode insertion. The digit was clamped at the root and orientated horizontally such that the front tip of the digit was placed under the rotating target with speed of 10 mm/s. This target was selected for simplicity, reproducibility and in order to avoid any manual disturbance or uncontrolled contact through manual movement of the digit. The data from the sensors of the digit was collected through MATLAB and a data acquisition computer card, 6034E NI DAQ. Like the previous experiments, the reading of the system is set to zero before the contacts were made.

The digit was brought into contact with the target until a deflection of less than 3 mm was observed at the tip to avoid any physical deformation of the digit. At that point sensors were ready to detect any force/pressure changes. After about 2900 degrees rotation of the target, with the digit in continuous contact, the target was stopped and the data from the digit sensors was recorded.
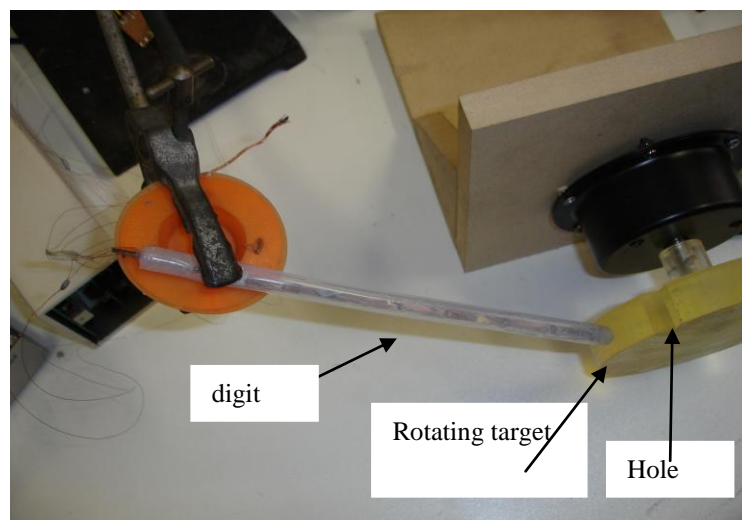
Figure 5.11: Tactile digit used to detect holes/notch of an object

To verify that this result was reproducible this experiment was repeated five times and each time the digit response was observed and results were recorded. Results were 0.083V±0.001V. This readings (0.083V) refer to the average difference between the notch and non-notch across all 3 sensors and the hole or crack detecting was statistically significant (p=0.03125). This result verifies that the digit possibility of identifying notches/cracks or gaps.

Results: Figure 5.12 depicts a response of the digit to the holes of the object.
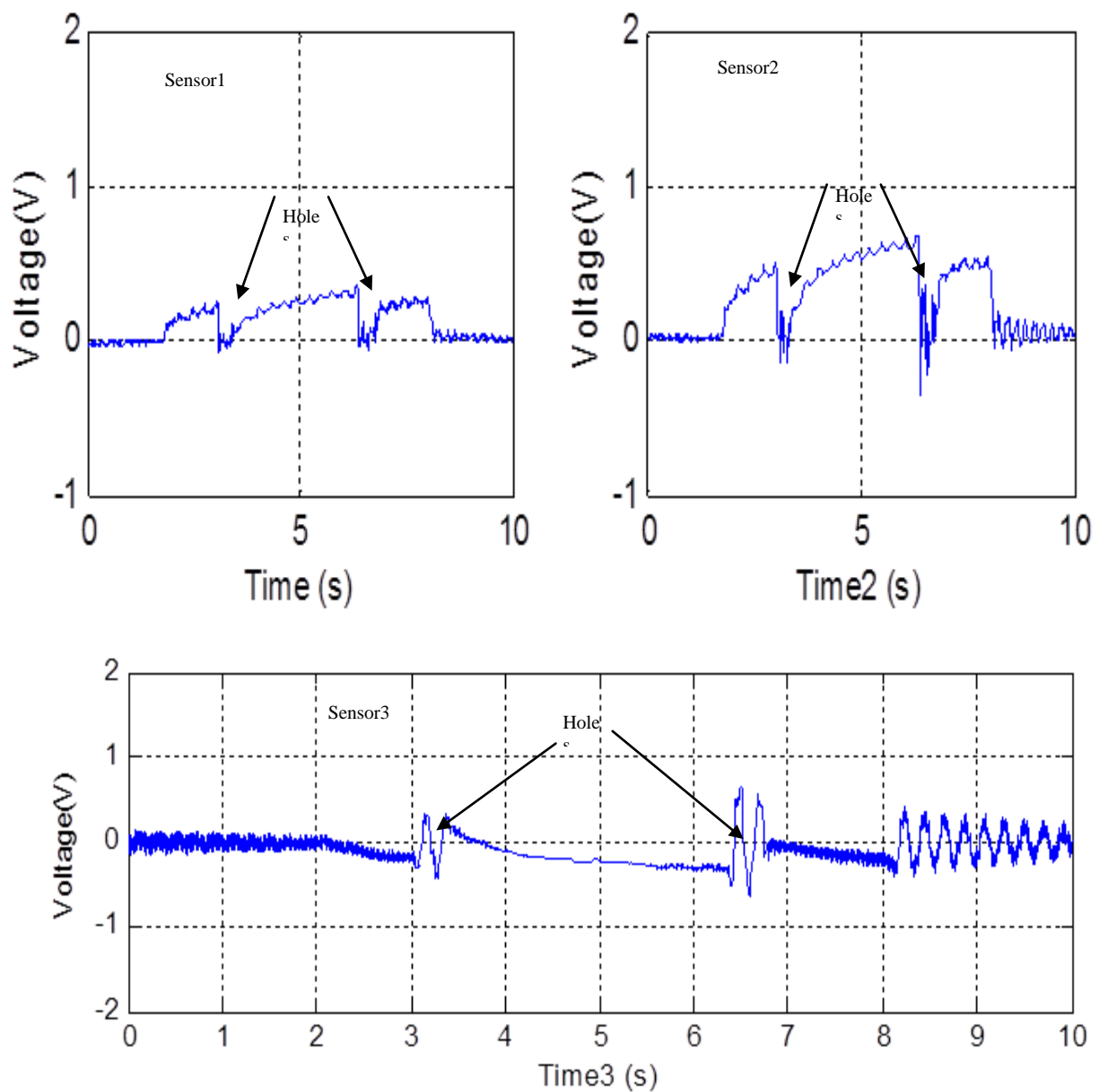
Figure 5.12: Tactile sensor response for Gap contact detection condition

The digit was placed under the object (direct contact) in order for a longitudinal load to be maintained with a positive output flexure signal. Similarly, constant output voltages represent unchanged surface condition where different signal rise indicate change of surface conditions. Outputs were analysed and the transient signal demonstrated the amplitude and temporal spacing of excitation of the digit. The positive rises of the signal of the two sensors indicated contact between the digit and the object. However, whenever there was a notch/hole in the surface, the tip of the digit dipped slightly in to the hole and this produced a transient signal that was detected by the flexure of the tip which goes down to the zero. No doubt whenever the output signal changes (either goes up or down) there is a indication of object surface change. If continuous positive signal indicated contacts between the object and the digit due to the upward force of the digit, the other part of the signal which goes down to zero showed that the surface condition has changed (upward force has disappeared)- a hole/notch indication.

These results, and other cues, suggest that they could be used by surgeons to detect and characterise surface anomalies. This will help the surgeon to identify if there are normal/abnormal cracks which exist in the cochlea and this could improve the cochlear implant surgery compare to lack of detecting any analogy of the cochlea. Similarly, information about surface anomalies can be applied to other invasive surgeries such as endoscopic instruments.

Experiment 5.5: tumour detection

The cochlear nerve is involved with the tumours in most cases. One of them occurs distal end of the tumour in the inner ear structures (vestibule and cochlear). Similarly, other operations such as thoracoscopic are used to detect mediastinal tumours. Besides these normal existing tumours,

there could be abnormal tumours in the human body such as lung tumour and colon tumour that also need to be detected. Knowing the contact surface conditions could make it easier for the surgeon to locate tumours during MIS and locating these underlying tumours during MIS procedures would reduce collateral tissue trauma.

Aim: the aim of this experiment was to detect a tumour (Figure 5.13) in a hidden anatomy such as within the cochlea. It is expected to show positive signal for any tumour phantom on the object.
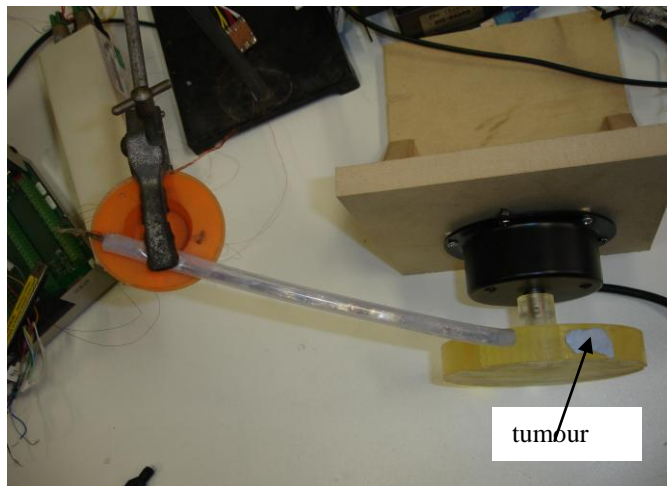
Figure 5.13: Experimental set up to detect a tumour on an object

Method: this experiment employed a stationary digit with rotating target featuring an irregularly shaped protuberance. The digit was placed under the object, as in the preceding study (experiment 5.4) and the object was rotated at same speed in the preceding experiment 5.4. Placing the tumour to contact with the top surface of the digit is considered as top contact (downward force). The experiment was repeated five times to test repeatability. Like the previous experiments, the reading of the system is set to zero before the contacts were made.

Results: Figure 5.14 and 5.15 show tactile response for tumour phantom detection. Figure 5.9 shows top location tumour detection response. The experiment was repeated five times to test repeatability with result of 3.9 V (increase above a normal non-tumour baseline) $\pm$ 0.08 V for sensor 2. The experiment was repeated five times to test repeatability with results of 2.01V $\pm$ 0.05V for sensor 3. The results showed that the results were very close to each other. The result was found to be statistically significant ($p=0.0313$).

When the digit touched the protuberance, sensor 1 and 2 have showed positive signal. The object behaves like a bending load (downward force) on the digit and that way the tactile sensors (shown in Figure 5.14) behave as if exposed to a contact from the top (positive signal) by placing the tumour to contact with the top surface of the digit.
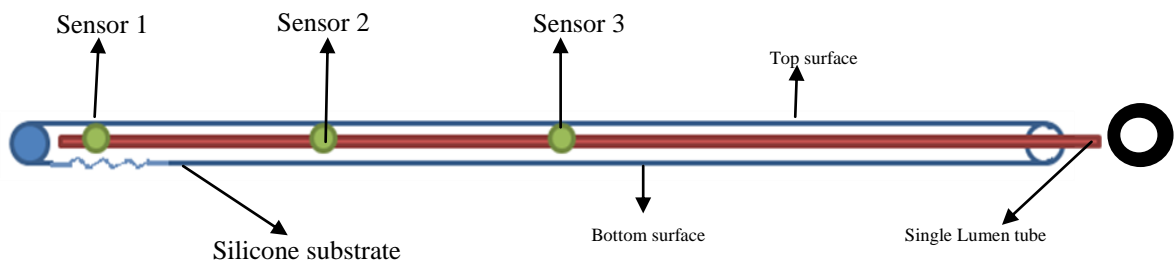
Figure 5.14: Steerable digit (straightened through stylet during the insertion)   with sensor locations

Sensor 3 shows a negative voltage due to the compressive pressure during the tip contacts. The digit was subject to a compressive load with buckling which made sensor 3 behave as if exposed to a bottom contact.
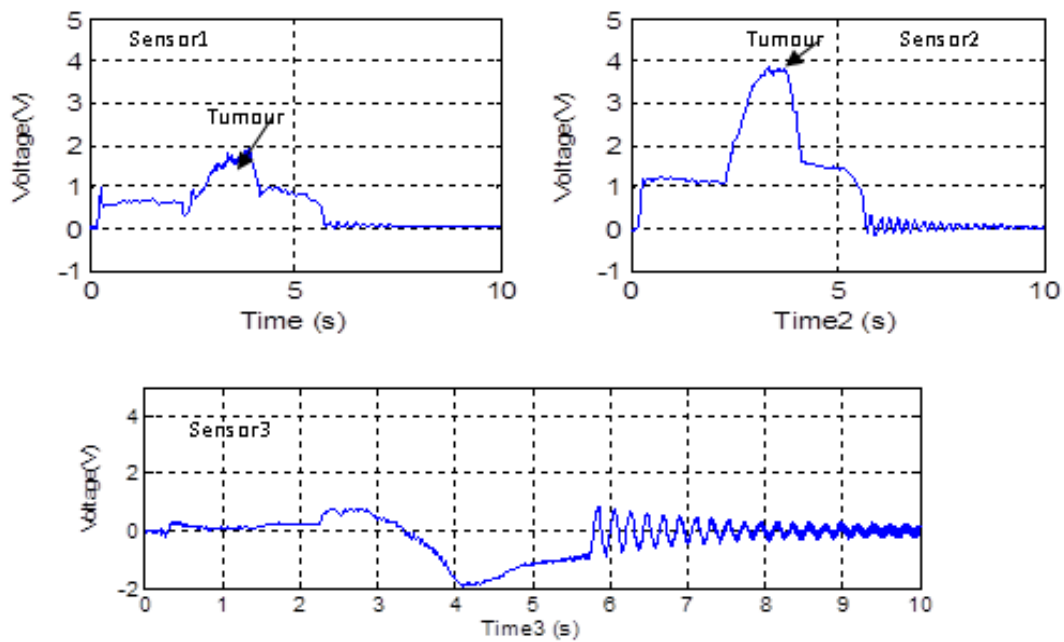
Figure 5.15: Tactile digit responses of top location tumour contact detection

Figure 5.12 shows bottom tumour detection response. The digit was placed on the object and contacted with the tumour phantom. Placing the tumour to contact with the bottom surface of the digit is considered as bottom contact (upward force).

Placing the tumour to contact with the bottom surface of the digit which was considered as top contact (downward force) has shown opposite signal direction. It was seen that contact with the tumour phantom induced a change in voltage at all 3 sensor locations. The negative direction of the measured voltage change in each sensor indicated that the tumour phantom was in contact with the bottom surface (upward force) of the digit.
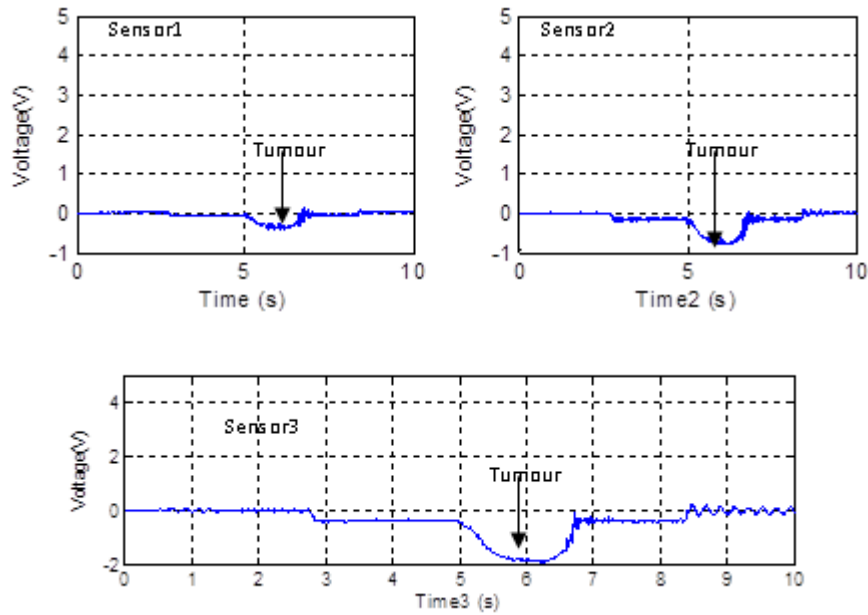
Figure 5.16: Tactile digit responses of bottom location tumour contact detection

By showing responses of the sensor output to surface conditions, it is clear that this tactile digit would be able to detect different surface conditions of a tissue.

The results were expressed in voltage output signals but the contacts can be expressed as a strain. For example, top contacts of the experiment 1 have shown 0.14V (L1). Using equation 4.4 in chapter 4, the magnitude of this signal is equivalent to strain of 5600 mmε. This strain has caused by magnitude force (F = E.ε.A) of 5.5 N where the L3 showed 0.09V which is -3600 mmε and force of 3.5 N. Experiment 2, signals were close to each other. L4 = -0.1V which correspondents to -4000 mmε and has a force of 4 N.

A more logical continuation of your discussion would be to make use of your mathematical models to explain the magnitudes of the voltages and how they relate to the forces experienced

in the studies. This would address one of the examiner's comments on how you do not appear to have applied your mathematical models to your results, and it would not require as much work as recreating your plots in other physical units.

These results demonstrate that the from interpreting the data from the 3 sensors together, although not entirely independent, can be used to infer the presence, applied force, and direction of action of protuberance in moving system. Curvature contact classification needs further investigation. In this case, the sensor will detect contacts and their respective directions. To identify the curvature contacts, it needs to make link the position of contact along with the active length of the sensor with the output sensor signals. An algorithm that can analysis the angle of the contact based on the contact information of the sensors can be derived curvature contacts.

Experiment 5.6: obstacle detection.

There is a significant chance of intra-cochlear damage by penetration of the digit. Such injury may occur if the tip of an electrode strikes the modiolar wall during insertion or if the body of the array is pushed into contact with the modiolus by a positioner device. Thus, it is crucial to discriminate obstacles from other contact conditions.

Aim: the aim of this experiment was to assess the possibility of detecting an obstacle in the hidden anatomy such as within the cochlea.

Method: This experiment uses Kawasaki FS03N robot with D controller, a linear drive system supplied by Baldor (LMSS0602-2WW0) which consists of a stepper motor[7] on a linear etched platen and NextMove ST[8] controller using Mint ActiveX. Moving digit (10mm/s) with stationary object was set up. The digit was moved towards the object until contact occurred (Figure 5.17)
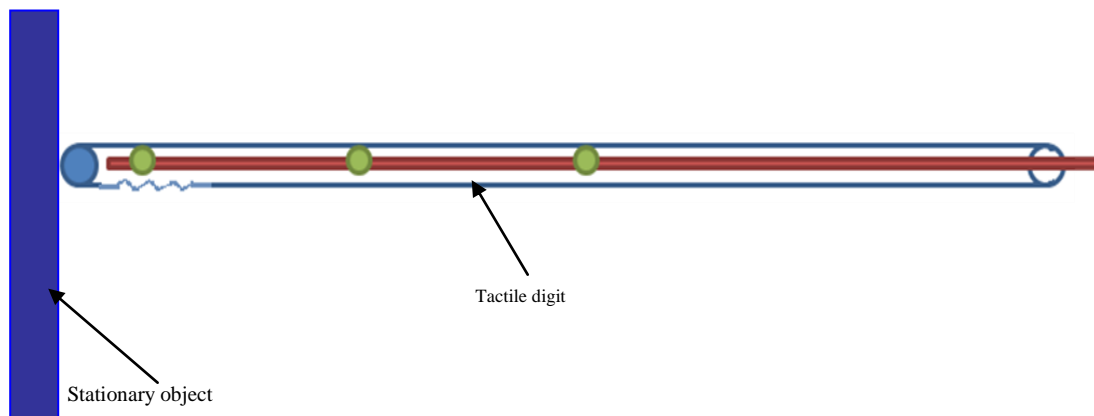
Figure 5.17: Tactile digit is pushed towards stationary object to test obstacle detection

Results: Figure 5.15 shows digit's response. The experiment was repeated five times to test repeatability with results of $0.16V \pm 0.05V$ and showed statistically significant (p=0.0083).

---

[7] LMSS0602-2WW0, Baldor, Fort Smith, Arkansas USA

[8] NST002-501, Baldor, Fort Smith, Arkansas USA
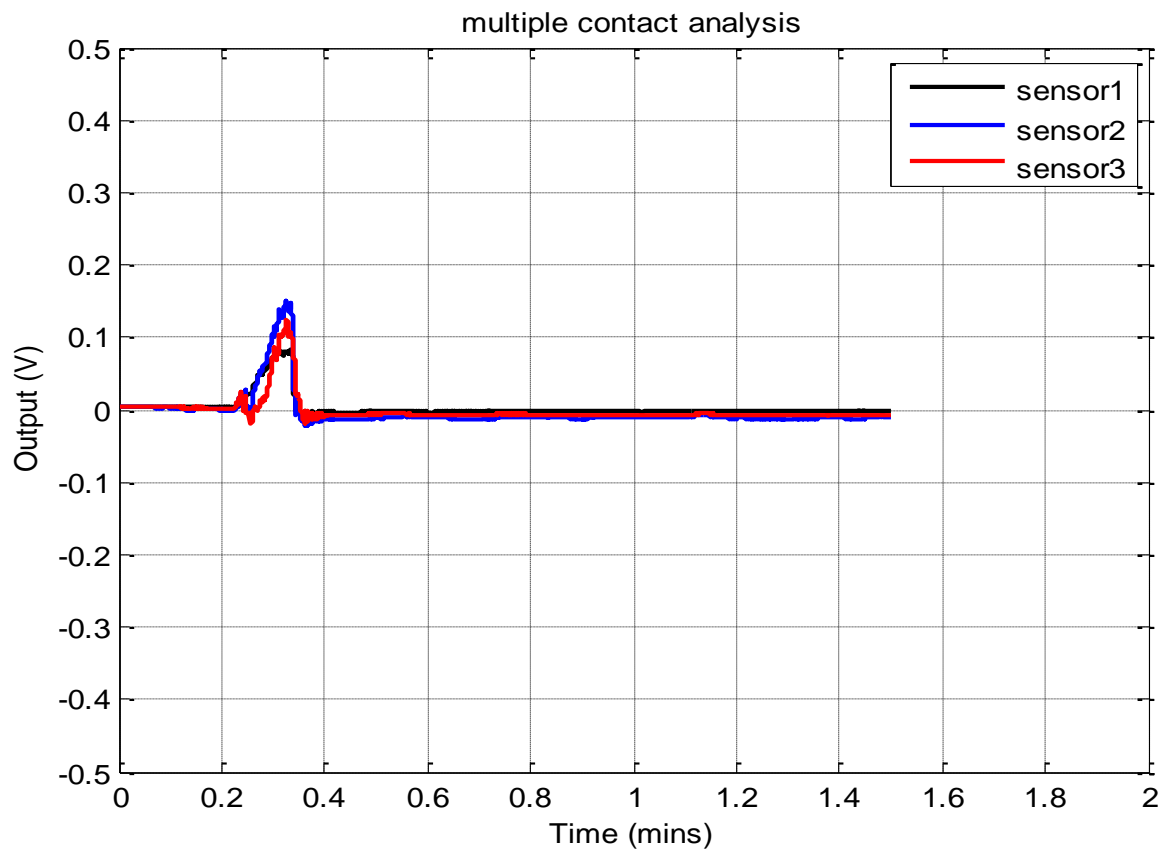
Figure 5.18: Tip obstacle responses

Quantitatively, the result depicted on Figure 5.18 is different from the previous digit responses in terms of timeline frame. All the sensors had output response at the same time. The small difference between the sensor responses indicates that all sensors are experiencing approximately the same loading, and consequently are indicating the same change in resistance.

The experiment was repeated five times to test repeatability and it has shown same pattern response. In normal contact conditions (as in the preceding studies), signals had different

directions and magnitudes and occurred at different times whereas when encountering obstructions at the tip, the signals from each transducer occurred simultaneously and were of similar magnitude and operating in the same direction. That is, if they all have the same pattern (voltage rise) at the same time, the obstruction is at the tip. The typical directions of the signals are positive whenever there is tip obstruction due to the buckling direction of the digit.

In this experiment, Figure 5.15 shows an output signal of 0.15 V. This voltage which is created by the bounce (obstacle contact) has a force of 6.4 N. The digit's response of the obstacle detection and tap contacts are close to each other. It is can be deduced that, that is possible to detect obstacle contacts before more force are applied on the tissue.

When an axial force is applied on a strut, this axial force causes buckling (deflection) if the load is critical. This critical load, P_{cr} depends on the end conditions of the strut, column dimensions (actual length, L, and area moment of inertia, I) [75]:

P_r = critical force/load

E = Modulus elasticity

I = Area moment inertia, $\quad I = \dfrac{\pi d^4}{64}(circle)$

n = column effective length factor (dependent on end conditions)

$$P_{cr} = n^2 \frac{\pi^2 EI}{L^2} \qquad (6.1)$$

In this experiment, one end of the digit is fixed and the other is unrestrained (n=2). The critical load of this experiment can be calculated using above equation (6.1) where Diameter of the digit, d= 10 mm (0.01 m)

Elastic modulus, $\epsilon = 0.0124$ GPa

Length of the digit, L = 250 mm (.25 m)

Moment inertia, $\quad I = \dfrac{\pi d^4}{64}$

The critical load, $\quad P_{cr} = n^2 \dfrac{\pi^2 EI}{L^2} = 24N$

The applied force of the digit was calculated as $\quad F = \varepsilon.E.A$

where A = 0.0000785 m^2, the Young Modulus, $\epsilon = 0.0124$ GPa

strain, $\varepsilon = 0.00064$ (Vo = 0.16 V)

The applied force F = 6.9 N.

Buckling will happen when applied force (F) is greater than the critical load, P$_{cr}$ $\qquad (F \geq p_r)$

and buckling did not happen in this experiment.

5.4 SHAPE CHARACTERISTICS ANALYSIS

This analysis was performed with a goal of determining whether the digit can discern the difference between normal curling responses whilst the digit is not inserted into the phantom cochlear compared with the response to contacts made by the digit during the insertion processes. In that way it is possible to minimise the interaction forces between the digit and the walls of the cochlea. In order to achieve the electrode array position close to the inside wall of the cochlea, the electrode was designed in such a way that it can resemble the shape of the cochlea easily during the electrode insertion into the cochlea. The morphological design of the electrode is a particular challenge as it must resemble the form of the cochlea, conforming to the shape of the modiolar whilst permitting a simple insertion process which causes minimal trauma

to the sensitive structures of the cochlea. In this sense it has been found to be desirable for the electrode array to be generally straight during the insertion procedure before the curl shape is reached.

The digit has been designed such that the stylet keeps the digit straight during initial insertion and then through withdrawing the stylet, the flexible tactile digit returns to its non-stressed (curled) shape that will match/hug the modiolar wall of the cochlea phantom which allows the wall position to be determined. Response of the tactile sensors attached along the digit can be used to determine the relative shape of the digit. Three tactile strain gauge sensors were used to measure the local deflection of the digit, allowing overall array shape to be determined.

This approach was demonstrated in Figure 5.19; this figure shows successive stages of curling of the flexible digit and the relative position of the stylet. The states *a1*, *a2,* and *a3* indicate different amount of digit curvature.
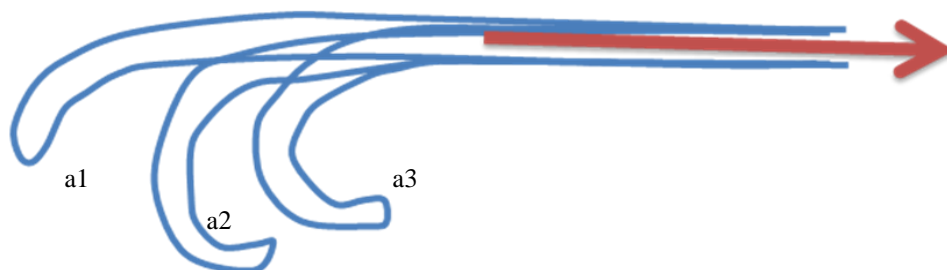
Figure 5.19: Curvature stages of the digit and relative stylet position

Experiment 5.7: digit shape identification

Aim: the aim of this experiment was to determine the relative shape of the digit.

Method: First, the digit was straightened through stylet insertion and the strain gauge amplifiers were all zeroed. Then the stylet was withdrawn from the digit slowly whilst data was recorded.

Results: Figure 5.20 shows read-out voltages (all the three sensor readings are combined) observed during stylet withdrawal without inserting the digit into the cochlea phantom. Five replicates were made of this experiment with results of 1.25V ± 0.03V. This variance is small and it came from the digit's self-weight. This result showed self bending strain of 50 mm strain.

Figure 5.20: Digit responses with smooth stylet release (standby): normal down facing digit response.

The peak outputs of three signals (*a1*, *a2* & *a3*) decreased quickly show when the stylet has passed by the location of each sensor as it was withdrawn. When the stylet passed the location of a sensor, the digit curled to its original shape. For sensor 1, the first spike falling indicated that the first curl of the digit has taken place and the sudden positive rise exhibited the beginning of the curl.

The three peaks (a1, a2, and a3) of Figure 5.17 show curving stages which are depicted on the right side of the figure. These peaks are caused when the stylet has passed by the location of each of the sensors. For instance, when the stylet passed the location of a sensor 1, the digit curled to its original shape in that part which has no stylet which is shown as *a1*. Similarly, the other peaks *a2* and *a3* are caused by sensor 2 and 3 respectively when the stylet passed by their locations.

Overall pattern of this signal showed subsequent curling shape stages of the digit. These results presented three spikes (*a1, a2* & *a3*) which represent three locations that the stylet has passed and three different stages of the flexible digit's shape. More tactile sensors could make monitoring of the shape more accurate. Knowing how far the stylet was withdrawn and with responses due to contacts, the depth to which the digit was inserted into the cochlear could be inferred. Having information of how far the digit was inserted in to the cochlear phantom and this is correlated with information from the tactile sensors, the relative positions of the stylet and digit could be inferred from the output results. This showed how far the digit is advanced, which is 83 mm, unless there is an obstacle or resistance.

In summary, the signals of the digit experiments have shown that the flexible tactile digit has the ability to detect and identify any load contact condition whether it is single or multiple contacts as well as their directions. However, some tool-digit contact classifications such as the curvatures and close boundaries of the signal locations needed more complex algorithm and needs further research. In this experiment it was seen that having strain gauge sensor outputs other parameters such as direction of the contact, magnitude of the contact, applied force, stress and strain of the contact can be deducted. This information is useful in many surface and diagnosis clinical applications. The sensing scheme often has the potential to provide tactile information feedback to the surgeon during precise surgical tasks, working through minimal access. Important information retrieved by the digit such as texture, relative shape of the object, location and direction of different contact conditions can be used to determine the lumen in real time. Using the distributive sensing approach, the texture, stiffness and shape can be discriminated.

These analyses could be typical tool/tissue interactions of surgical procedures in MIS and these findings are relevant to the design of future implant devices and to various important issues regarding the surgical technique used for implantation. Furthermore, the features of position detection and wall contact sensing should improve the depth of insertion possible in cochlear implants and hence the range of pitch perceived by the patient as well as reducing any insertion damage to surviving structures.

Further experiments of digit- cochlear phantom insertion intersection will be discussed in the next chapter.

6 Chapter 6 SIMULATION   EXPERIMENTS

This chapter presents the experiments that have been carried out in order to evaluate the digit performance. Experiments were performed with a flexible tactile digit inserted into the cochlear phantom and the resulting contact data was recorded. The experiments identified digit location within the phantom, and the points where contact with the phantom was made. The digit provided tactile feedback that can be used to assist the surgery for cochlear implant insertion procedures yielding less trauma and sensitive-tissue damage. The experimental method was presented in the first section, followed by different insertion procedures and digit/phantom interaction states and transitions analysis. In this study, the steerable digit was set to insert into the cochlea phantom as a target to allow contact between the electrode and cochlea during the electrode insertion analogically. It should be noted that this system is an up-scaled prototype and is not a stage at which it can be used clinically.

6.1   EXPERIMENTAL METHOD

The experiments designed in this chapter aim to investigate the ability of the flexible digit to provide tactile feedback in terms of the contact intensity, time and position of the digit, and tool and phantom interaction for the process of inserting the digit into the cochlea phantom. In this study, different insertion techniques with the steerable tactile digit were performed; 1) digit insertion without stylet; 2) manual stylet withdrawal during insertion; 3) and semi-automatic

digit insertion. All of the experiments demonstrated the interaction between the digit and the phantom during the digit insertion process.

The experiments were performed using the apparatus shown in Figure 6.1. The phantom was clamped in position and orientation using a retort stand and adjustable clamp. The fixed distal end of the flexible digit was connected to the end effector of a Kawasaki FS03N robot and its position with respect to the phantom was controlled using a computer linked to a D series controller. The root of the stylet was connected to a linear drive system supplied by Baldor (LMSS0602) comprising of a stepper motor[9] on a linear etched platen which is mounted on the top of the Robot so that it moved dependently of the robot and NextMove ST[10] controller using Mint ActiveX controls through MATLAB[11]. All strain gauge signals were amplified using FE-MM4 FLYDE[12] and recorded into MATLAB using and a National Instruments 6034E data acquisition board.

The flexible digit with tactile sensors was 250 mm in overall axial length and the sensors were placed at *0.012L, 0.032L* and *0.054L* as measured from the fixed (distal) end.

[9] LMSS0602-2WW0, Baldor, Fort Smith, Arkansas USA
[10] NST002-501, Baldor, Fort Smith, Arkansas USA
[11] Solidworks V 2010, Dassault Systèmes SolidWorks Corp, Massachusetts, USA
[12] FE-MM4 FLYDE, Fylde Electronic Laboratories Ltd, UK
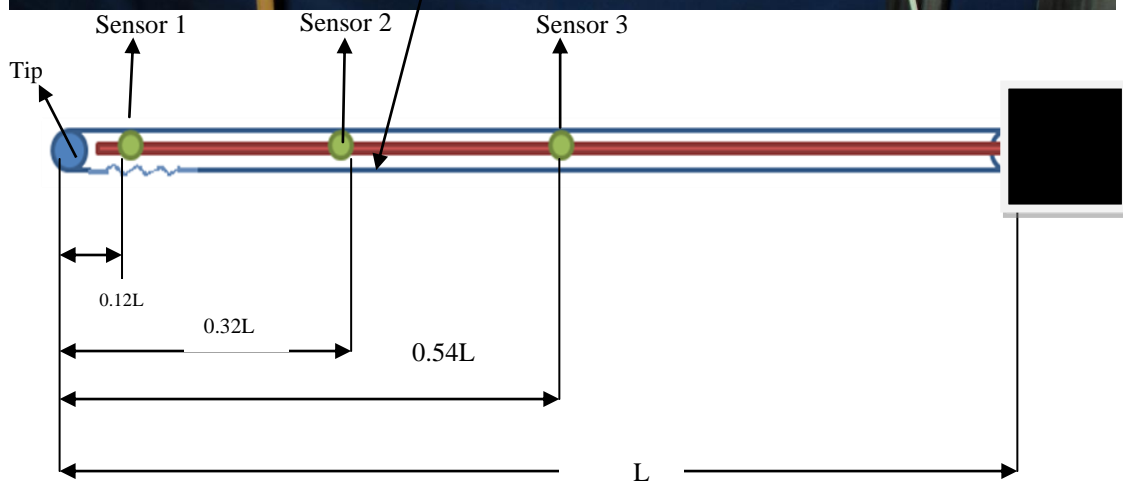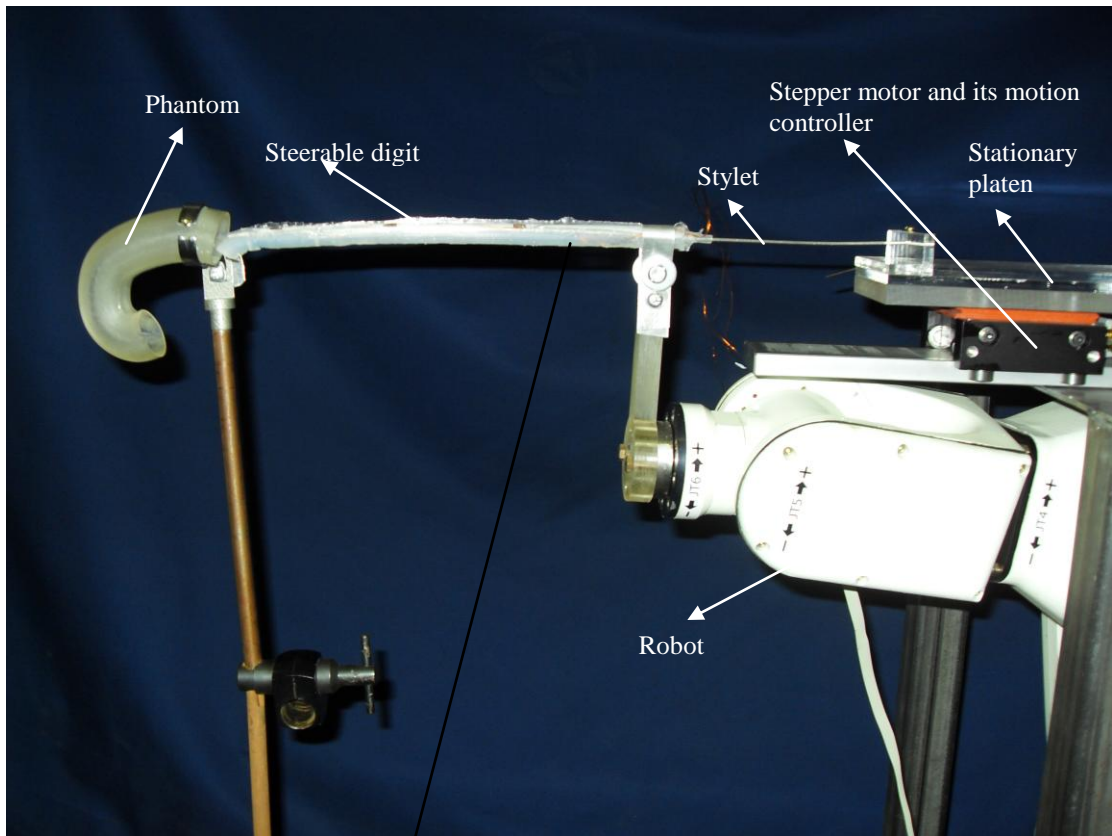
Figure 6.1: Experimental set-up for steerable tactile digit

Experiment 6.1: Digit insertion without Stylet

Aim: The aim of this experiment was to investigate the interaction between the digit and the cochlea phantom when a stylet was not used to aid insertion.

Method: In this experiment the steerable digit without stylet was inserted into the cochlea phantom; thus its bending was not controlled. Initially, the tip of the electrode was positioned at the beginning of the cochlea phantom before the electrode was pushed forward into the cochlea phantom. The digit was moved slowly forward into the cochlea a predetermined distance by the robot. As the digit moved into the cochlea, the digit slid along the inner wall and touched the lateral outer wall of the phantom. During the insertion, the geometrical curvature of the digit and the digit/phantom interaction can be recovered from the output signals of the sensors.

Results: Figure 6.2 depicts the contacts between the digit and the phantom during the digit insertion into the phantom. Generally, negative signals indicate where the bottom of the digit made contact with the phantom, and positive signals indicate contacts with the top of the digit as detailed in Chapter 5. However sometimes curvature location could affect the direction of the contact (as seen experiment 5.5).
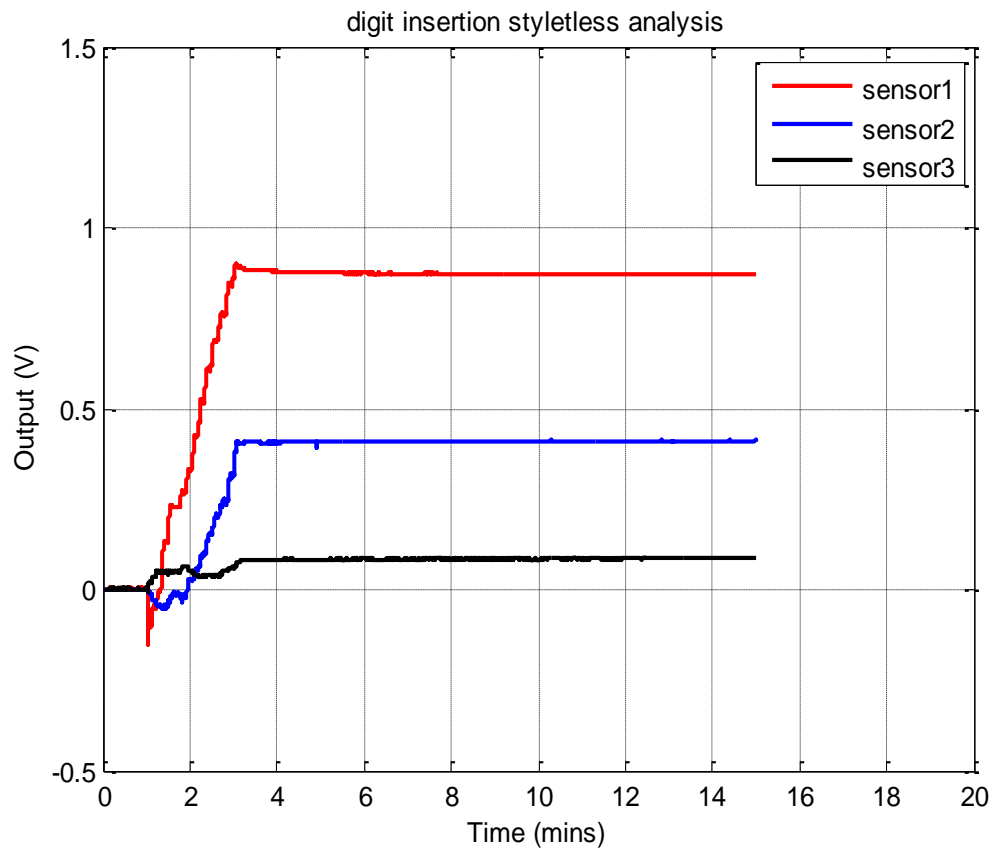
Figure 6.2: Interaction response of the digit and phantom during the phantom insertion (styletless insertion)

The result of Figure 6.2 versus the pictorial representation of the Phantom and location and curvature of the digit are shown in Figure 6.3.
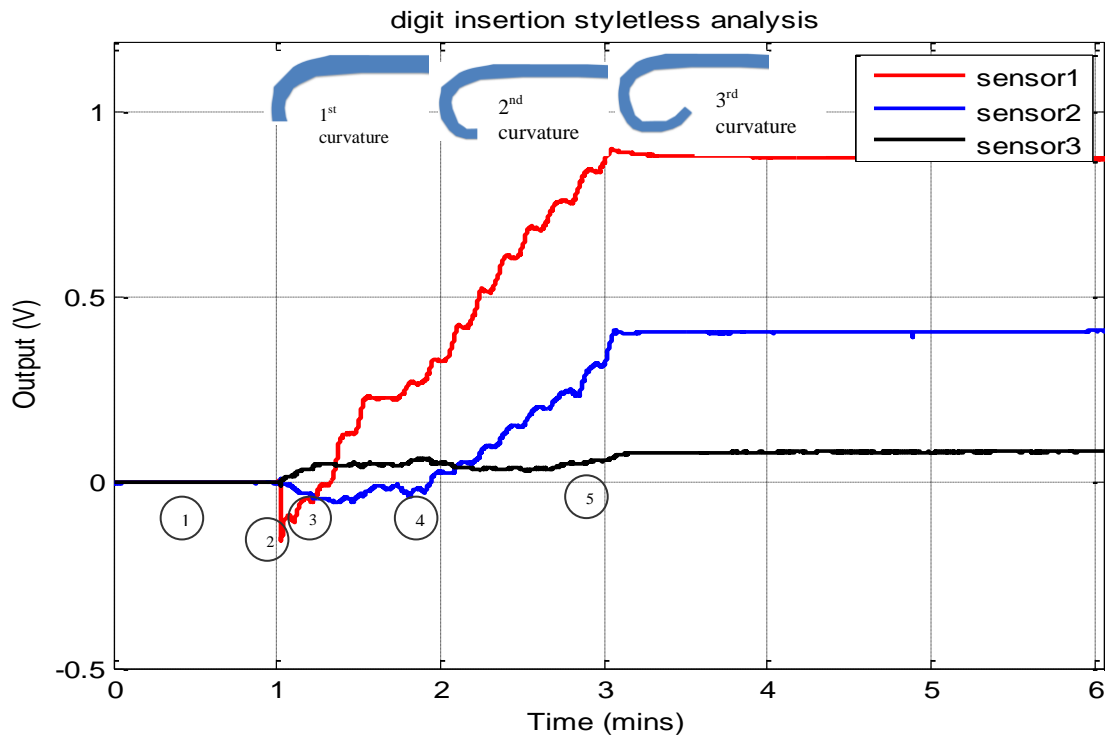
Figure 6.3: Interaction response of the digit and phantom versus pictorial of the digit and phantom

Here is a summary of the contact conditions of the digit and the phantom shown in Figure 6.3:

1. digit has made initial contact but was not moving

2. bottom contact (negative peak)

3. tip curling of the digit started (1st curvature)

4. 2nd curvature of the digit started

5. 3rd curvature of the digit started

Initially after the digit started to move, the tip pressed against the phantom causing a negative strain as detected by sensors 1 and 2. Sensor 2 has a lower magnitude when compared with sensor 1 which indicates a bias in the location of the contact towards sensor 1. As the digit

advanced, the digit moved against the outer wall (sensor 1 and 2). Peak output signals followed by immediate decrease (*sawteeth*) indicate the digit is following the shape of the modiolus. For example, sharp rises in the strain measured by sensor 1 at position (3) of figure 6.3 indicates the digit starting to curve and continues to rise until the first part of the curve is complete where this signal shows steady output. Since the locations of the sensors on the digit are known the 1st curvature occurred at 0.01L (2.5 mm) from the proximal/distal end of the digit.

 The negative strain as reported by sensor 2 at position 2 on Figure 6.3 shows a sliding contact with the inner wall (bottom). The second stage of the curvature trajectory (0.032 L) starts at the position of the second peak (4) but rises sharply due to the outer wall contact of the digit as reported by a positive strain. The final stage of curvature (0.54 L) was shown by step 5. The output response of the sensor 3 depends on contact force/load as well as how far the digit goes into the phantom. The higher the load and the further the digit goes inside, the higher the magnitude of the sensor 3 signal. In this case, there was a small curve of step 5 which showed by sensor 3.

The continuous steady output of the signals after peak rises indicated modiolus-hugging curvature. That is, the continued rise of sensors 1 & 2 confirm that the digit was taking its unstressed trajectory curve with inner wall contact (negative signal). The deep negative signal indicates a strong inner contact but the digit immediately takes its path and there was no significant resistance compared to its weight. If there was no inner wall (bottom) contact, there should be a sudden drop of their signals. The insertion contact force tended to drop off (sensor 3 followed by others) after three minutes approximately because the digit was not moving and hence not penetrating further into the phantom. These steady outputs of the three sensors are

modiolus hugging contacts of the digit along the cochlea phantom which shows that the penetration has taken place. From this information shown in Figure 6.3 it was possible to estimate the shape of the digit (modiolus hugging curvature) or have a clue and identify any contact conditions; the digit/phantom interaction states; interaction duration versus time and the overall completion time of the procedure.

This experiment results showed similar outputs in terms of the pattern of the sensor outputs: - that is, peak rises and sequences of the sensors (1, 2, and 3). Sometimes there were a few top contacts while other times there were bottom contacts or both direction contacts. Amplitude of the signals, contacts conditions and locations depend on the interaction of the digit and phantom. Due to interaction differences, the responses will vary in terms of the magnitude, location and condition of the contacts and that has made difficult to compare these experimental results. This means, each time the digit and the phantom made a contact, result is different from the previous ones because the contact locations, magnitudes and the directions are not same due to new contacts and its magnitude.   Each digit-phantom interaction has its own magnitude, location and direction results but the pattern of results are same. This experiment has shown strain of 0.0324 (32.4 mm strain) which is caused by a contact force of 17.496 N (equation 4.6)

Experiment 6.2: Digit insertion with stylet (manually withdrawn)

Some insertion techniques require that the electrode is set in a straight shape outside the cochlea. The tip of the electrode and stylet can then be positioned at the beginning of the first turn before the stylet is withdrawn as the electrode is advanced restoring a curved shape and

minimising undesired contact with the sensitive cochlea. It was expected in this insertion technique that the minimum digit and cochlear phantom interaction may be achieved by detecting any contact between walls of the cochlea using information gathered from the digit.

Aim: the aim of this experiment was to investigate digit and phantom interaction feedback during insertion of the electrode whilst the stylet was withdrawn.

Method: Initially the stylet was withdrawn from the digit without insertion into the phantom to compare with insertion results. Then, the digit was maintained in a straightened position using the stylet and then inserted into the phantom. The stylet was withdrawn slowly stage by stage to control the shape of the digit so as to hug the modulus of the phantom. As the digit was advanced further into the cochlea phantom, the stylet was slowly withdrawn further, and the digit allowed to relax to its stress-free state unless there was a digit/phantom interaction.

Results: Figure 6.4 shows the response of the digit's sensors as the stylet was withdrawn and the digit was inserted into the phantom and sectioned of Figure 6.4 is shown in Figure 6.5 The comparison between the two illustrates the interaction between the digit and the phantom during insertion.
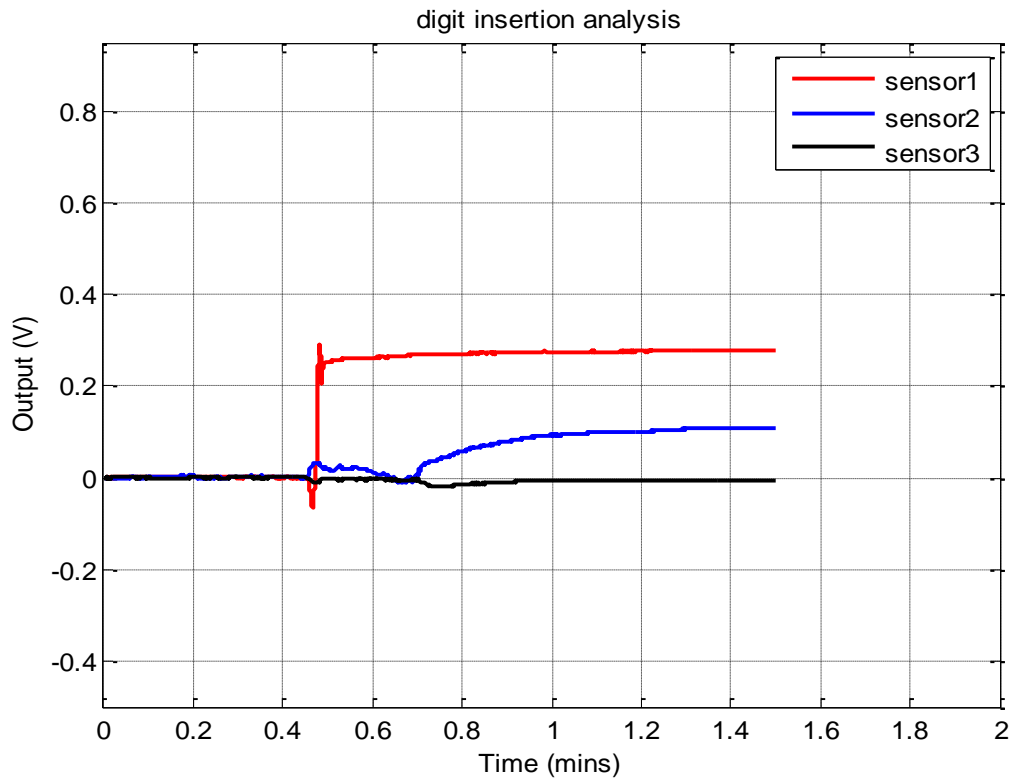
Figure 6.4: Digit and phantom contact response during the insertion with stylet withdrawn

(A) idle state: No contact
(B) - (D) digit/phantom interaction states
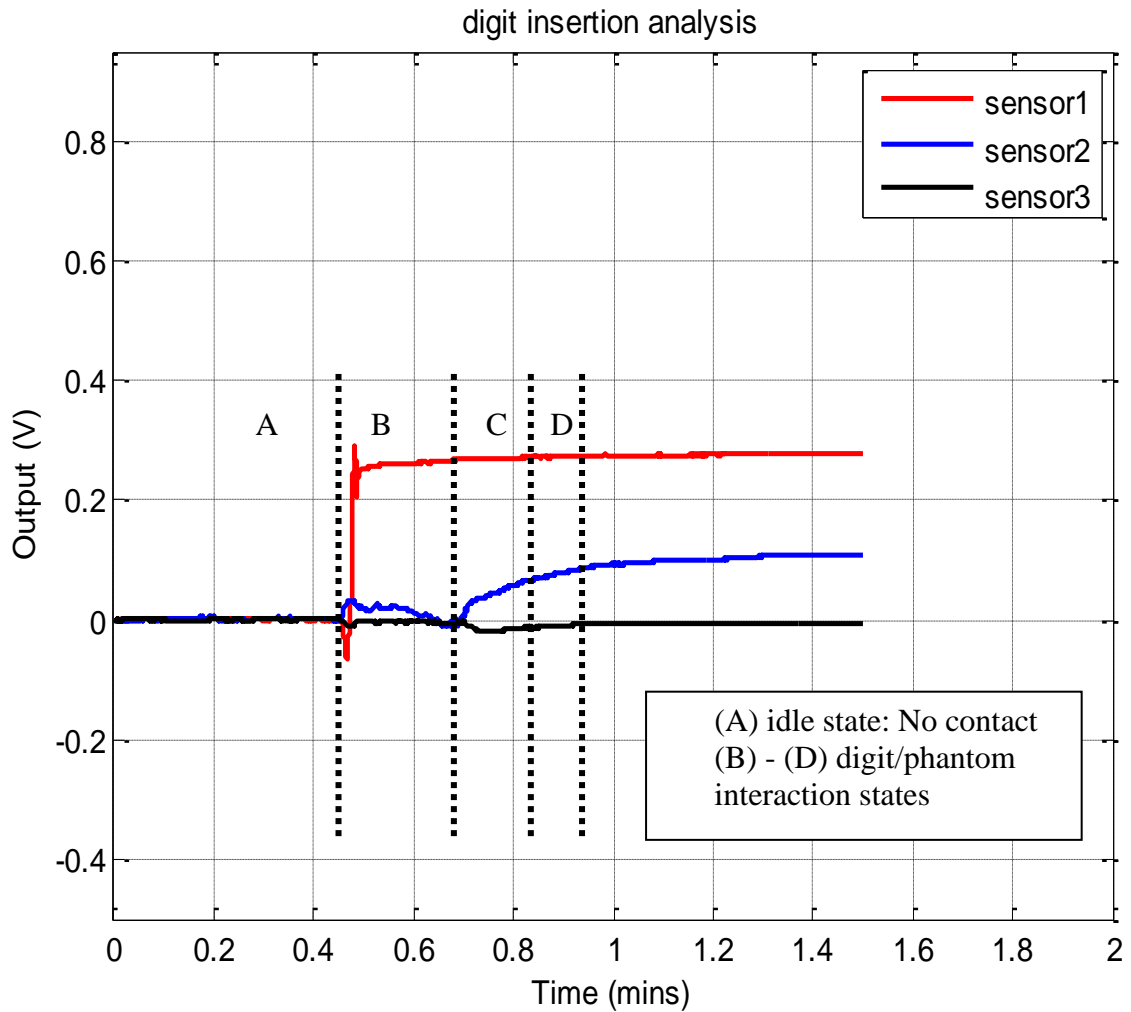
Figure 6.5: Tool/tissue interaction states during the Digit insertion

This experiment showed digit/phantom interaction similar to experiment 6.1 and these interactions could be summarized as follows:

Section A: there was neither any contact nor any bending of the flexible digit; it may be considered to be in an "idle" state, where the digit was advancing into the cochlea without making any contact with the cochlea phantom. This section also showed when the digit was not moving.

Section B: First curvature of the digit is showed by sensor 1. Response signal of sensor 1 (section B) of Figure 6.6 is similar with response signal of sensor 1 in Figure 6.4 (without insertion response). This similarity indicates that sensor 1 (tip of the digit) did not make significant contact except sliding or hugging the modulus of the digit. Also this section showed top contact which showed by positive signal of sensor 2. Similarly, there was no contact between the phantom and location of sensor 3 which is far from the cochlea in this experiment.
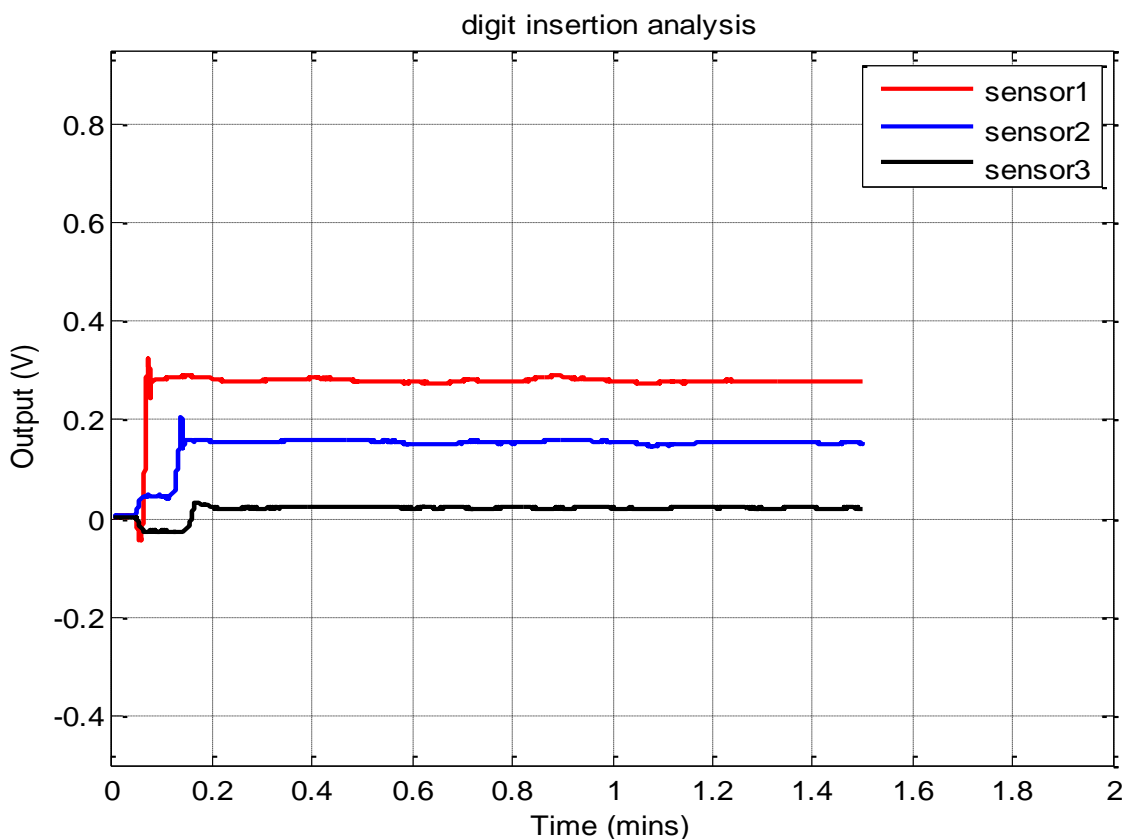
Figure 6.6: Digit response during stylet withdrawal without phantom insertion.

Section C: 2nd curvature of the digit has started as shown by the rising value of sensor 2. Also there is digit contact with the under side of the phantom (negative signal of the sensor 3).

Section D: here the 3rd stage of curvature of the digit has started and is shown by rising signal of the sensor 3. Finally, the flexible digit has conformed to the shape of its unstressed curvature state where there was not any further digit/phantom interaction, it matches the modiolus of the scala tympani and penetration has taken place. The magnitude/strength of the three signal responses can be used to identify the digit's curvature trajectory and location based on the distance of the stylet along the length of the digit before insertion and on the sensors' locations. As shown in experiment 6.2 in addition to phantom and digit contacts, the shape of the digit can also be deduced from these strain readings shown in Figure 6.6. When the stylet passes by the location of the sensor, signal spikes occur. Combining the strain signal spikes with knowledge of sensor locations and how far the robot has moved indicates how far the digit has penetrated the phantom and gives the relative position of the contact locations. Similarly, the shape of the digit can be deduced from the strain data (1st curvature, 2nd curvature and 3rd curvature) yielded by the sensors. This experiment has strain of 14.4 mm strain (7.78 N). The magnitude of the contact between the digit and phantom of this experiment was less than the previous experiment (Exp 6.1). The motion of the robot which was not smooth during the stylet removal and this created higher magnitude where when the removal was manual, the disturbances were less.

There are different digit/phantom interaction states in this experiment. The bending of the digit was controlled by withdrawing the stylet smoothly according to the depth of penetration of the cochlea phantom. The pattern of the signals (signal spikes) had indication of the curvature shape

of the digit. The signal's curvature also has clue of the insertion length of the digit into the cochlea phantom. The curvature signal tells when the bending has passed certain length depending on the location of the sensor. For instance, the first bending of this experiment occurred at 0.12 L = 30 mm. The location of the sensors has a great impact on the response and analysis of the digit and phantom interaction. Slight changes of the sensor locations could change the response signals pattern. A similar digit but with different sensor locations shown in Figure 6.7 was considered and its response to digit/phantom interactions during the digit insertion was shown in Figure 6.8
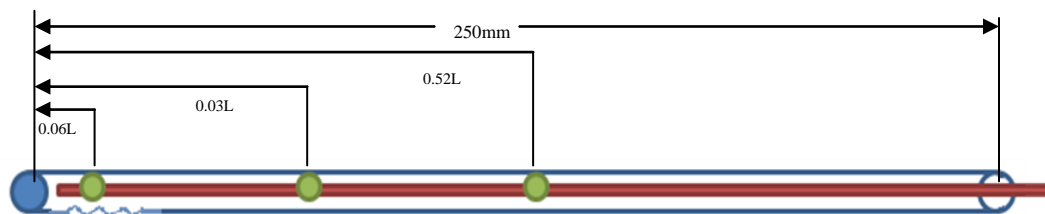
Figure 6.7: Curvature stages of the digit and relative stylet position

A higher spikes of sensor 2 in Figure 6.8 and 9 (sectioned signals of Figure 6.8) shows sensitivity location of sensor 2. Position of the first curve's centre and the location of the sensor 2 coincide with each other and maximum displacement of the sensor happens in this position.
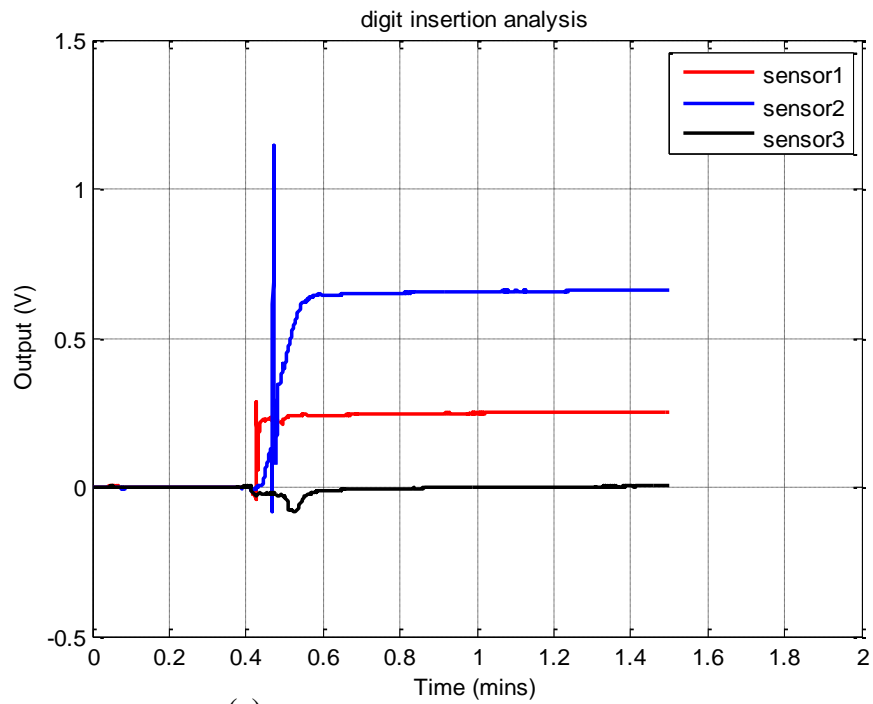
(a)
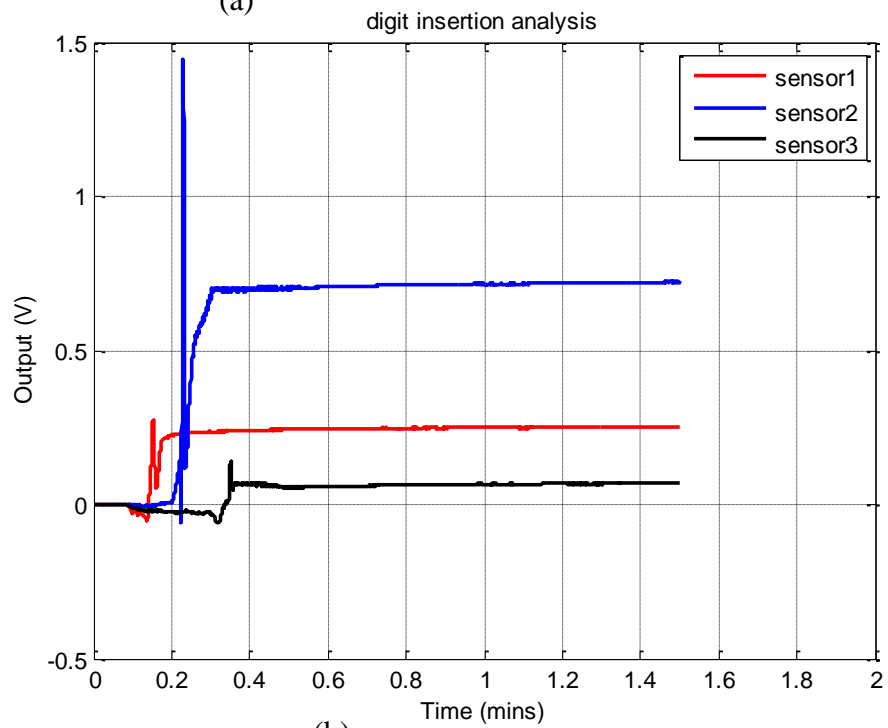
(b)

Figure 6.8: Digit insertions responses. a) free stylet withdrawal (no insertion) response, b) digit insertion with stylet response

Compared to previous experiments, all other signals remain approximately the same in magnitude that the studies are otherwise identical.

In this case, sensor 1 was very close to the tip and has less effect on the curvature of the digit but has more effect on penetration and obstacle effects.
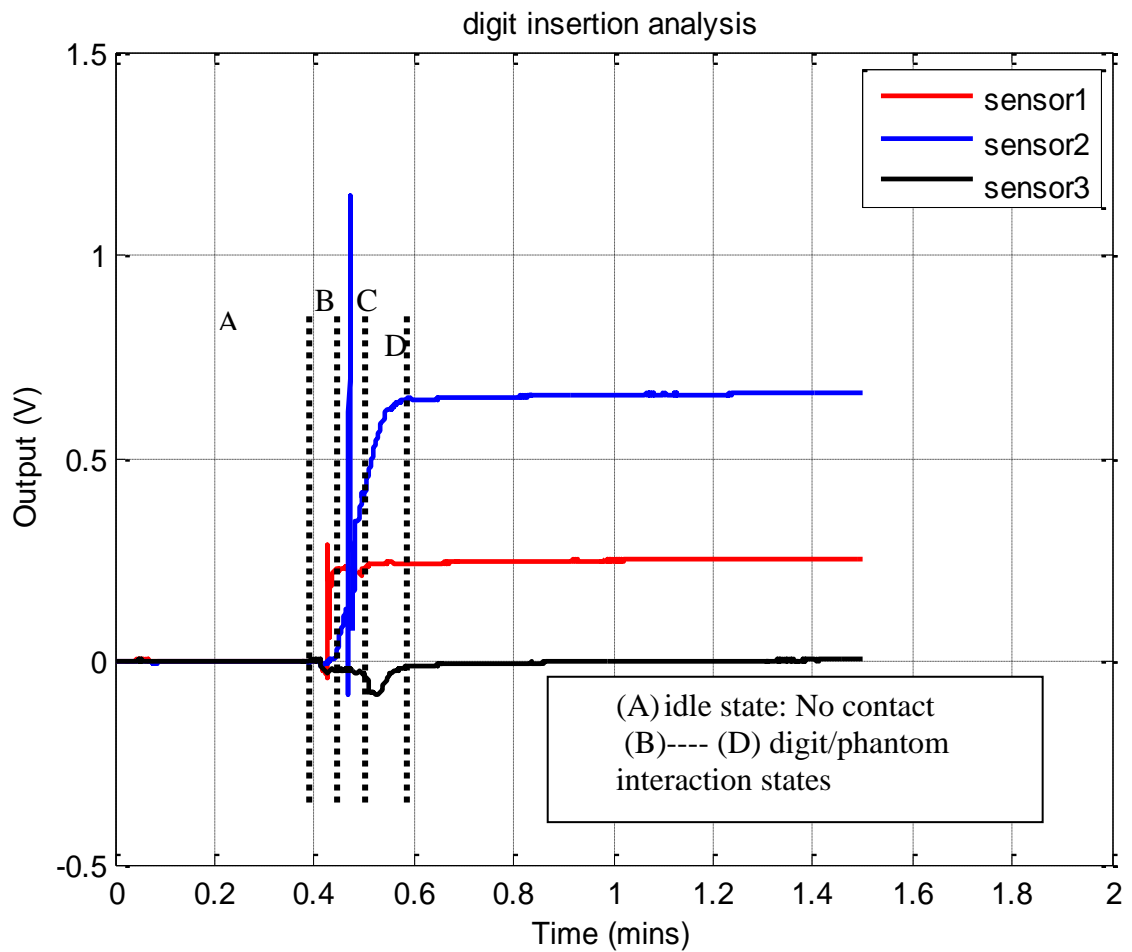
Figure 6.9: Digit/phantom interaction states during the Digit insertion with sensor locations

Another experiment was performed with disturbance (contacts) and the aim of this experiment was to verify the digit's performance during the tool/tissue contacts. While the digit was moving forward, brief `tapping' contacts were made intentionally. The result was shown in Figure 6.10.
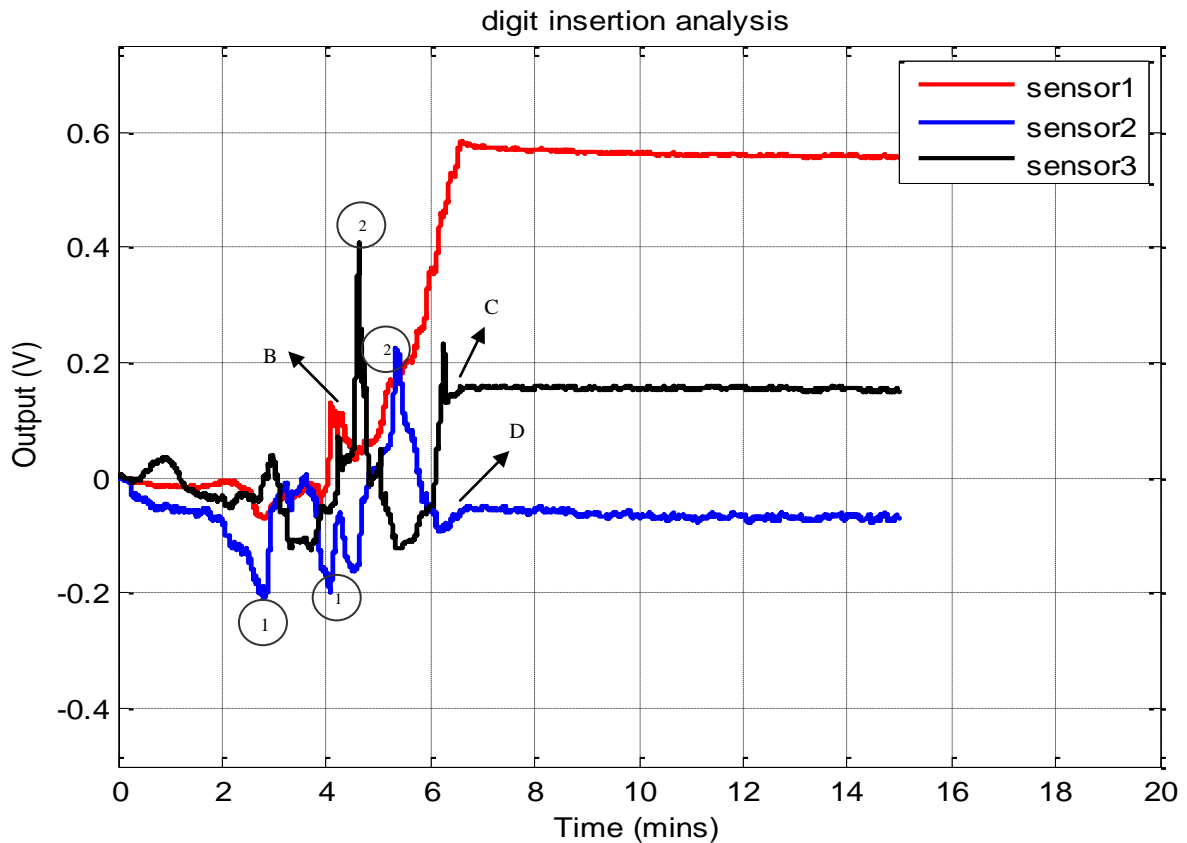
Figure 6.10: Digit insertion with disturbances analysis

Figure 6.10 shows more interaction of the digit and the phantom. Bottom tap contacts of the digit are shown by (1) where top tap contacts are shown by (2). Similar to previous experiments a sharp increase followed by a little decrease, a '*sawtooth*' shape signal, shows the digit's curve stages and these signals are marked as B, C and D. The curve trajectory of the digit takes place

during the stylet withdrawn. Finally, the digit rests in its free-state where there are no further contacts except hugging the modiolus of the scala tympani contacts.

Experiment 6.3: Stylet Insertion with Motion Driver

Aim: to investigate interaction between the digit and the cochlea phantom through the action of the linear motion driver. Intracochlear trauma caused by electrode insertion could be minimised by controlling the flexure of the digit through a non-manual mechanisms.

Method: In this experiment, the steerable digit was inserted into the cochlea phantom where a linear motion driver was used to actuate the withdrawal of the stylet instead of manual withdrawal.
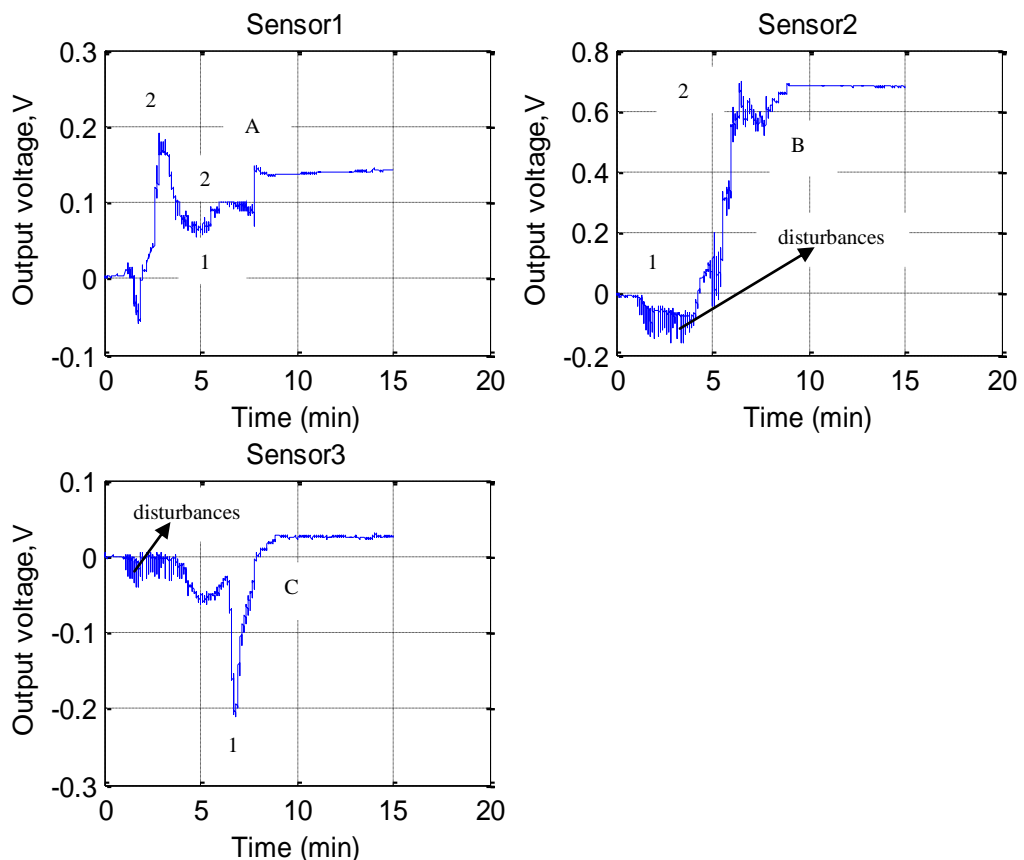
Figure 6.11: Response of the flexible digit due to driver stylet off action

Results: the results obtained from the tactile sensors of the digit are plotted in Figure 6.11.

In this experiment, as in previous studies there are contacts with the bottom of the digit (1) as well as with the top (2). There are a lot of disturbances compared to previous experiments. At the beginning, there was a motion disturbance caused by the movement of the linear actuator. These disturbances occur as a result of a mismatch between the resolutions of the linear actuator which was not as smooth as that of the robot. The controller was making irregular movements due to its less resolution. Motion controller which has high resolution could eliminate these disturbances but this has not been implemented due to economic limitations.

The results show that before the pre-curve of the digit starts, there was an inner wall contact (negative signal of the sensor 1) between the digit and the phantom. Then the digit slides on the inner wall and continues to hug the modiolus of the scala tympani with later and inner wall contacts. There are deep inner contacts indicated by sensor 3 (1) before the digit slides further along the scala tympani. Finally, the digit rests on the final shape of the cochlea where there was not any further digit/phantom interaction.

Besides the motion disturbances and deep contacts, the overall pattern of the graph was similar to previous results (Figure 6.4 and 6.6). As the other results, step A, B and C show stages of the curvature stages of the digit as well as digit and phantom contacts.

CONCLUSIONS

This flexible digit has provided tactile feedback information about interaction between the digit and the cochlea phantom such as contact direction and its magnitude, information about the digit shape, time and position of the contact, relative displacement of the digit (depth insertion).

It was seen that manual stylet insertion had the smallest disturbance compared to the other two experiments. Manual stylet withdrawn has shown small contact force and easy insertion due to few disturbances. The small magnitude of contact forces indicates less insertion force, where less disturbances shows easy insertion and easy lumen mapping due to lack of obstacles. The stylet linear actuator withdrawal procedure has shown a higher magnitude of contact due to the poor selection of linear motor step size. Smaller step size (high resolution) with smooth stationary platen could improve this performance.

One common problem encountered during these studies was repeatability of the above experiments. There are a number of experimental variables and sources of variation that might impact the repeatability and validity of digit/phantom contact interaction data, and this can limit the data's biological relevance and applicability.

All the experiments have shown that the responses produced by the digit have displayed information about what was happening in this digit-phantom interaction, relative position of the digit and the shape of the digit which may be retrieved from these results. Also, time spent while performing each tool/tissue interaction and overall completion time. Similarly, how far

the digit was advanced with the time can be obtained from these peak signals of A, B and C by knowing when the stylet passed the position of the relative sensor location as explained in chapter 5. Also, the robot can give feedback of how far the robot has moved forward which indicates the advancement of the digit into the cochlea. Surface contacts with interference identification needs further algorithm that can filter interferences.

These can be guidelines to assist in the improvement of the surgical technique and to minimise trauma caused by excessive force application. Furthermore, this digit can be used for other similar applications like surgical and diagnostic tools, which involve interaction of surgical tools with soft biological tissue in surgery.

7   Chapter 7 CONCLUSIONS AND FUTURE WORK

In this chapter, the research goals, objectives, and key results are summarized. Also, recommendations for future work on the flexible tactile digit are provided.

7.1   CONCLUSIONS

The purpose of this research was the design and development of a flexible tactile digit to aid palpation and navigation of lumen for clinical applications. More specifically, the design of a steerable tactile digit that can provide tool/tissue interaction feedback to reduce damage to tissues and delicate structures within the cochlea during electrode insertion during the current cochlear implant surgery techniques. It is reported in the literature [33, 67, 71, 74] that trauma and damage during insertion of electrode arrays of the cochlear implantation is related to lack of tactile or haptic feedback of the interactions between cochlear implant electrode and the cochlea during the insertion process. Towards the development of the steerable tactile digit to prevent damaging cochlear membranes through excessive forces requires contact/force sensing capabilities. this research has presented: 1) the design of a distributive tactile digit with digit-phantom contact measurements, 2) the development of a steerable tactile digit for cochlear electrode insertion of tactile information feedback, 3) preliminary experiments evaluating the steerable digit with tactile feedback capability through digit contact characterisation, and 4)

experimental studies evaluating the role of digit/cochlear phantom interaction status feedback in cochlear implant surgery.

A flexible tactile digit has been designed to enhance the sense of touch, which could be used during the surgical tool/tissue interaction, diagnosis or path navigation procedures. The rationale that underlies this study is that the ability to know or understand what is happening inside the lumen or the hidden tissue information from tool/tissue interaction which may help the surgeon to realise the full potential of cochlear implant surgery and other clinical applications such as diagnosis and navigation procedures. The risk of damaging the basilar membrane during insertion of an electrode array into the human cochlear is expected to be significantly reduced through facilitating contact and force feedback to the surgeon about what is happening during the procedure.

The successful prototype trials have shown great promise and the projected outcomes have the potential to make important advancements in minimally invasive surgery. The tests demonstrated that even devices of a relatively simple design have the potential to improve cochlear implant surgery and other lumen mapping applications by providing tactile feedback information which reflects contact condition and magnitude. Equipped with such information the surgeon could reduce the exerted force on the scala tympani during the electrode implantation and consequently minimise the tissue damage and potential damage to the delicate structures within the cochlear caused by current electrode insertion of the cochlear implant.

The digit was also demonstrated to be capable of enhancing tactile sensation for surface texture and irregularities.

The flexible digit has shown the ability to identify different touch characteristics including:

- Contact versus Non Contact.

- Multiple contacts.

- Direction of the contact load.

- Shape of the contact.

- Tip penetration and depth insertion of the digit.

- Relative texture.

- Obstacles.

This additional information could allow the surgeon to plan and place electrode arrays safely and appropriately in the cochlea or in a cavity. Also, the additional information could allow the surgeon to have better understanding of depth insertion and location of the digit as well as overall pictures of what is happening inside the cochlea. Tactile information provided by the digit could be applied to many other palpation and navigation procedures which do not have tactile feedback instruments to enhance their ability.

The main contributions of this study are:

1. The primary contribution of this study is the development of a steerable tactile digit with distributive sense of touch feedback capabilities for minimally invasive surgeries, specifically cochlear electrode insertion procedures. The digit provided tactile feedback that can be used to assist the surgery for cochlear implant electrode insertion procedures for less trauma and damage to sensitive tissue.

2. This tactile feedback approach has shown the feasibility of getting interaction between the digit and the phantom cochlear. The digit can collect signals related to object properties and the provided interaction feedback can enhance the surgeon's tactile capability.

3. Incorporating haptic feedback will enhance the safety, performance and acceptance of surgical technology.

4. The digit provides information about digit-phantom interaction analogy of tool-tissue interaction.

5. The digit can be applied to other lumen mapping and navigation procedures such as endoscope and catheters. The digit can perform lumen mapping through tactile feedback information.

The author foresee future studies carried out using steerable tactile digit enabling enhanced models of cochlear electrode insertion and eventually improved cochlear electrode array placement, minimizing trauma to the cochlea.

7.2 FURTHER WORK

This project is still at an early stage, however, an encouraging start and many improvements are possible building on the basic principle described here.

Far more fundamental to this work is the development of the tactile sensing technology such as the interpretation software/hardware. Evaluation of other sensing technologies (fibre bragg gratings to reduce complexity and facilitate miniaturisation) is another further development of this digit.

This digit has demonstrated basic digit phantom contact information and the next logical thing is to evaluate that this can be do more robustly through an algorithm to present the data more simply to the user. And then that the activities within this project can be replicated by tactile feedback alone (or at least the contact conditions and magnitudes can be discerned electronically and agree with physical reality).

Tactile sensing of this application is quite demanding not only in terms of hardware but also of software. The extraction of information from tactile sensors may require the implementation of complicated algorithms. The hardware and software available, even at an experimental level, are still not adequate for some already defined needs. Software must also be developed in order to analyse the information gathered by the sensors in a more easy and dynamic way. Current this research mainly used Matlab (Solid works V 2010, Dassault Systèmes SolidWorks Corp, Massachusetts, USA) for data analysis and extraction. The display method was basic graphic style. Dynamic analysis and quicker time for data extraction and analysis is needed to present actual tool/tissue interaction. That is, the tactile information of the embedded system must be

introduced to the surgeon with real time. A software interface is needed to develop to automate the calibration process and to provide a visual display of the array against a shape of the cochlea as an aid to surgeons during the insertion process in real time.

The next step is to evaluate smaller sensing technologies (fibre bragg optical gratings and the microcoils) and their miniaturisation resulting in the development of a smaller and more readily/reliably manufacturable solution. Future work to optimise the design through custom sensors or the incorporation of tactile sensors through nanotechnology manufacturing to current electrode array insertion procedures could further improve the tool. The strain gauge sensors required for this application have special requirements. One of them has to do with size. Smaller sensors would give what is going on tool/tissue interaction in smaller access regions. Generally speaking, the surface where sensing means are to be installed should be small, ranging from 0.11 m^2 to 1 mm^2 or even less. This will allow incorporation of sensors within the digit and this can reduce its current bigger size (10mm) to the existing cochlear electrode size (1.3mm). Other potential sensors for this application include optic sensors. Micro and nano-technologies are particularly attractive to tactile sensing implementation because they can produce not only high density arrays of sensors but also devices incorporating both the sensors, the required conditioning electronic circuits and even the hardware for signal acquisition, digital signal processing and transmission. That embedded system will minimize the cost and will make easy the miniaturization.

Generally the tactile sensor is required to have size miniaturization. The approach outlined in this study could be extended by miniaturisation of the digit and its integration with the existing MIS tools to include more realistic surgical procedures. Then it would be ready to be tested with animal tissues. Miniaturization process may need different tactile sensor rather than strain gauge and optic sensors. The sensor elements with a very small size of $80{\times}80{\times}80$ $\mathbf{\mu}m^3$ [103] are shown in literature which is made superelastic carbon microcoils. Similarly during the miniaturisation, the silicon or the substrate must have good thermal conduction and must be uniformly bonded to the gauges in order to dissipate heat and reduce temperature gradients between the gauges. Finally, miniaturisation and other technology used in the further work should underpin the cost effective of the tool. In that way, the digit will it be cheap, will it help minimise trauma, will it provide a better solution to the cochlear implantation and other similar application areas.

REFERENCES

1.   N. Brett, X. Ma, B. Tam, M.V. Griffiths and D.J. Holding (2003). A flexible digit with tactile feedback for invasive clinical applications. Proc. 10th IEEE Conf. on Mechatronics and Machine Vision in Practice, Perth, Western Australia, December 2003.

2.   Paolo Dario, Maria Chiarra Carrozza, Maurilio Marcacci(2000). A novel mechatronic tool for computer-assisted arthroscopy. IEEE transaction on information technology in biomedicine. 4(1), p. 15-29

3.   Howe Robert D, William J. Peine, Dimitrios A. Kontarinis, and Jae S. Son (1995). Remote palpation technology, IEEE Engineering in Medicine and biology, May/June 14(3), p.318-323

4.   Frank Tendik, S. Shankar Sastry, Ronald S. Fearing, and Michael Cohn(1998). Applications of Mechatronics in minimally invasive surgery, IEEE/ASME transactions on mechatronics, 3(1), p.34-42

5.   S. Shimachi, Y. Fujiwara and Y. Hakozaki (2004). New sensing method of force acting on instrument for laparoscopic robot surgery, Computer Assisted Radiology and Surgery. Proceedings of the 18th International Congress and Exhibition International Congress Series, 1268, p.775-780

6.   Stephen J. Rebscher Hetherington A, Bonham B, Wardrop P, Whinney D, Leake PA(2008). Consideration for design of future cochlear implant electrode arrays: electrode array stiffness, size, and depth of insertion, Journal of Rehabilitation Research & Development(JRRD),45(4) p.731-748

7.   Endoscopy, available at: http://www.oralchelation.com/faq/answers75d.htm   (accessed 25th September 2010)

8.   Kazuto Takashima, Kiyoshi Yoshinaka, Tomoki Okazaki and Ken Ikeuchi (2005). An endoscopic tactile sensor for low invasive surgery, sensors and actuators A 119(2), p. 372-383

9.   Gul N. Khan, Duncan F. Gillies(1996). vision based navigation system for an endoscope, Image and Vision computing 14(10), p.763-772

10.   Available at: http://www.racgp.org.au/familyhealth/Painful_knee_general accessed 26th September 2010

11.   Emily Monahan, Kenji Shimada(2006). Computer-aided navigation for arthroscopic hip surgery using encoder linkages for position tracking, The International Journal of Medical Robotics and Computer Assisted Surgery, 2, p.271–278.

12.   available at: http://www.urologyspecialistskc.com/pdfs_9-09/Lap%20Pt%20Info%20for%20print%208.09.pdf accessed 26th September 2010

13.   Dmitry Oleynikova, Mark Rentschler, Adnan Hadzialic, Jason Dumpert, Stephen Platt and Shane Farritor (2004). In vivo camera robots provide improved vision for laparoscopic surgery, International Congress Series, 1268,p. 787– 792

14.   available at: http://kidshealth.org/parent/general/eyes/cochlear.html (accessed 1st August 2009)

15.   Joseph B. Roberson, Jr, MD. (2005). Cochlear implant surgery: Minimally invasive technique, Operative Techniques in Otolaryngology, 16, p.74-77

16.   P.N. Brett, X. Ma, G. Tritto (2004). The potential of robotic technology applied to meet requirements for tools to support microsurgery and cellular surgery (Abstract), Journal of cellular   and   molecular   biology,   50(3),   p.275-280.   Available from:http://www.ncbi.nlm.nih.gov/sites/entrez

17. Caroline G.L. Cao & Paul Milgram (2000). disorientation in minimal access surgery: a case study, proceeding of the IEA 2000/HFES 2000 congress, Santa Monica, CA, p.169-172

18.   Daniel Glozman and Moshe Shoham (2004). Flexible needle steering and optimal trajectory planning for percutaneous therapies., 7th International conference on medical image computing and computer assisted intervention(MICCAI 2004), p.137-144

19. R. Sedaghati, J. Dargahi, and H. Singh(2005). Design and modeling of an endoscopic piezoelectric tactile sensor, International Journal of Solids and Structures 42, p.5872-5886

20. www.educationaldimensions.com/eLearn/endoscope/anatomy.php accessed 3rd September 2009

21. Ana Luisa Trejos, Jagadeesan Jayender, Melissa T. Perri, Michael D. Naish, Rajni V. Patel, and Richard A. Malthaner (2008). Experimental evaluation of robot-assisted tactile sensing for minimally invasive surgery, International Conference on Biomedical Robotics and Biomechatronics, BioRob 2008. 2nd IEEE RAS & EMBS

22. Y hagga M Mizushima, T Matsunaga and M Esashi (2005), Medical and welfare applications of shape memory alloy microcoil actuators, smart matter structure 14(5), p. 266-272.

23. Gregory Tholey, BS, Jaydev P. Desai, PhD, and Andres E. Castellanos, MD (2005). Force Feedback Plays a Significant Role in Minimally Invasive Surgery: Results and Analysis, Annals of surgery, 241(1), p 102-109

24. G. Chena, M.T. Pham, T. Redarce (2009), Sensor-based guidance control of a continuum robot for a semi-autonomous colonoscopy, Robotics and Autonomous systems 57(6-7), p.712-722

25. Javad Dargahi, Siamak Najarian, Bin Liu(2007). Sensitivity analysis of a novel tactile probe for measurement of tissue softness with applications in biomedical robotics, Journal of Materials Processing Technology 183(2-3), p.176–182

26. Yoshinobu Murayama Christos E. Constantinou and Sadao Omata (2005). Development of tactile mapping system for stiffness characterization of tissue slice using novel tactile sensing technology, Sensors and Actuators A, 120(2), p.543-549

27. Raymond P. Onders, Dimarco AF, Ignagni AR, Aiyar H, Mortimer JT(2004). Mapping the phrenic nerve motor point: The key to a successful laparoscopic diaphragm pacing system in the first human series, Surgery,136(4), p.819-826 .

28. Nicholas wettels, Veronica J. Santos , Roland S. Johansson and Gerald E. Loeb (2008). Biomimetic Tactile Array, Advanced Robotics, 22(7), p. 829-849

29. Kha H. N, B.K. Chen, G.M. Clark, R. Jones (2004). Stiffness properties for nucleus standard straight and contour electrode arrays, Medical Engineering & Physics 26 (8), p. 677-685

30. http://aappolicy.aappublications.org/cgi/content/full/pediatrics;126/2/381/F1 accessed 27th Octber 2010

31. Lawrence T. Cohen, Saunders E, Clark GM (2001). Psychophysics of a prototype perimodiolar cochlear implant electrode array, Hearing research, 155 (1-2), p. 63-81

32. J. wang, M, Bhatti, P.T, Arcand, B.Y, Beach, K, Friedrich, C.R, Wise, K.D (2005). A cochlear electrode array with built-in position sensing, International conference on Micro Electro Mechanical systems (MEMS), 18th. 30 Jan.-3 Feb. 2005. (2005). IEEE Xplore

33. Kensall D. Wise, Pamela T. Bhatti, Jianbai Wang,and Craig R. Friedrich (2008). high-density cochlear implants with position sensing and control, Hearing Research, 242 p.22-30

34. Peter S. Roland, Wolfgang Gstottner, Oliver Adunka (2005). Method for hearing Preservation in cochlear implant surgery, Operative Technology in Otolaryngology 16, p.93-100

35. N Donnelly, A Bibas, D Jiang, D-E Bamiou, C Santulli, G Jeronimidis and A Fitzgerald (2009). Effect of cochlear implant electrode insertion on middle-ear function as measured by intra-operative laser Doppler vibrometry, The journal of laryngolgy and otology, 123, p.723-729

36. David Schramm (2004). Revision cochlear implant surgery utilizing the advanced bionics HiRes 90K implant, international congress series 1273, p.133-136

37. J. H. M. Frinjns, J.J. Briaire, A. Zarowski, B.M. Verbist and J. Kuzma.(2004). Concept and initial testing of a new, bassaly perimodiolar electrode design, international congress series 1273 p.105-108

38. B. K. Chen, Clark GM, Jones R.(2003). Evaluation of trajectories and contact pressure for the straight nucleus cochlear implant electrode array—a two-dimensional application of finite elements analysis, medical engineering & physics, 25(2), p.141-147

39. Adunka Oliver, Jan Kiefer and Chapel Hill (2006). Impact of electrode insertion depth on intracochlear trauma, Otolaryngology-Head and Neck surgery 135, p.374-382

40. http://www.medel.at/italian/electric-acoustic-stimulation.php Accessed 27 october 2010

41. Adunka Oliver, Jan Kiefer, Marc H. Unkelbach Thomas Lehnert (2004). Wolfgang Gstoettner, Development and evaluation of an improved cochlear implant electrode design for electric acoustic stimulation, Laryngoscope,114(7), p.1237-41

42. Gani M, Valentini G , Sigrist A, Kós MI Boéx C(2007). Implications of deep electrode insertion on cochlear implant fitting. J Assoc Res Otolaryngol, 8(1), p.69-83.

43. Blake S. Wilson, Michael F. Dorman(2008). Cochlear Implants: A remarkable past and a brilliant future, Hearing Research 242, p.3-21

44. Andress Hussong, Thomas S. Rau, Tobias Ortmaier, Bodo Heinmann, Thomas Lenarz, Omid Majdani(2010). An automated insertion tool for cochlear implants: another step towards atraumatic cochlear implant surgery, International Journal CARS, 5, p.163-171

45. John K. Niparko (2009). Cochlear implants: principles and practices, 2nd ed. Philadelphia, Lippincott Williams and Wilkins

46. Fan-Gang Zeng, Arthur N. Popper, Richard R. Fay (2004). Cochlear Implants: Auditory prostheses and Electric Hearing, New York, Spring

47. Maryanna Tate Maltby (2002). Principles of Hearing Aid Audiology, 2nd ed. London, Wiley

48. Noiseoff, http://www.noiseoff.org/level.1.php accessed 10th October 2010

49. Graeme Clark (2003). Cochlear Implants: Fundamentals and applications, New York, Springer-Verlag,

50. Brian C. J. Moore (2007), Cochlear Hearing Loss: Physiological, Psychological and technical issues, Jon Willey and Sons, 2007, 2nd.

51. Information about hearing, communication and understanding, http://www.ncbi.nlm.nih.gov/bookshelf/br.fcgi?book=curriculum&part=A513, accessed 11th October 2010

52. National hearing service, http://www.rnid.org.uk/ accessed 7th May 2009

53. Royal academy of engineering, http://www.raeng.org.uk/societygov/policy/current_issues/biomedical_engineering/events.htm, accessed 1st August 2009

54. Barry McCormick, Sue Archbold (2003), Cochlear implants for young children, Whurr Publishers, London, 2003

55. Blake S. Wilson, Michael F. Dorman (2008), Cochlear Implants: A remarkable past and a brilliant future. Hearing research 242 (2008) 3-21

56. Arthur N. Popper, Richard R. Fay(2003), cochlear implants: auditory prostheses and electric hearing, Springer, New York, 2nd edition, 2003

57. Annelle V. Hodges, Thomas J. Balkany(2002), cochlear implants for sensorineural hearing loss, Hospital Physician, October 2002

58. http://www.medel.com/english/10_About_Hearing_Implants/About_Hearing_Implants.php accessed 25 May 2009

59. http://blog.asldeafined.com/page/2/ accessed 10th October 2010

60. Rex S. Haberman (2004), Middle ear and mastoid surgery, Thieme, New York, 2004,

61. Philipos C. Loizou (1999), Introduction to Cochlear Implants, IEEE Engineering in Medicine and Biology January/February , 32-42

62. http://www.healthsystem.virginia.edu/internet/otolaryngology/patient_cochlear.cfm accessed 1st August 2009

63. Uwe Baumann, Andrea Nobbe(2006), The cochlear implant electrode-pitch function, Hearing Research 213 (2006) 34-42

64. J. Thomas Roland (2005), Cochlear implant electrode insertion, Operative Techniques in Otolaryngology 16, 86-92

65. Mathieu Gani , Gregory Valentini, Alain Sigrist, Maria-Izabel Kós, and Colette Boëx (2007), Implications of Deep Electrode Insertion on Cochlear Implant Fitting, Journal of Association for Research in Otolaryngology 8(1), 69-83

66. Adunka Oliver, Jan Kiefer, Marc H. Unkelbach Thomas Lehnert, Wolfgang Gstoettner(2004), Development and evaluation of an improved cochlear implant electrode design for electric acoustic stimulation, Laryngoscope 2004 Jul;114(7):1237-41

67. http://www.medel.com/data/downloads/EAS/21707.pdf accessed 22 October 2010

68. Wardop P, Whinney D, Rebscher SJ, Roland JT Jr, Luxford W, Leake PA.(2005), A temporal bone study of insertion trauma and intracochlear position of cochlear implant electrodes: Comparison of Nucleus banded and Nucleus contour TM electrodes, Hearing research, 203 (1-2), p. 54-67

69. Wardop P, Whinney D, Rebscher SJ, Roland JT Jr, Luxford W, Leake PA.(2005), A temporal bone study of insertion trauma and intracochlear position of cochlear implant electrodes.I: Comparison of Spiral clarionTM and Hifocus IITM electrodes, Hearing research, 203 (1-2), p. 68-79

70. Kha H. N, B.K. Chen, G.M. Clark, R. Jones (2004), Stiffness properties for neclues standard straight and contour electrode arrays, Medical Engineering & Physics. 26(8) , p.677-685

71. Oliver Adunka, Harrold C. Pillsbury, Jan Kiefer(2006), Combining, perimodiolar electrode placement and traumatic insertion properties in cochlear implantation- fact or fantasy, Acta Oto-laryngologica, , p.1-8

72. Fang-Gang Zeng, N. Popper, Richard R.Fay (2004), Cochlear implants: auditory prostheses and electric hearing, Spring Verlang, New York, 2004

73. Catherine A. Todd, Fazel Naghdy, and Martin J. Svehla(2007), Force Application During Cochlear Implant Insertion: An Analysis for Improvement of Surgeon Technique, IEEE transactions on biomedical engineering, VOL. 54, NO. 7, JULY 2007

74. Zhang, J., Wei W., Roland J., Manolidis S., Simaan N(2008), Path Planning and Workspace Determination for robot-assisted Insertion of Steerable Electrode Arrays for cochlear implant Surgery, MICCAI'2008, the 11th International Conference on Medical Image Computing and Computer Assisted Intervention , pp. 692-700, 2008

75. Madhukar Vable(2012), Mechanics of Materials, Oxford University press, 2nd edition, August 2012

76. M.E.H.Eltaib, J.R.Hewit (2003), Tactile sensing technology for minimal access surgery-a review, Mechatronics 13 (2003):p.1163-1177

77. M. H. Lee, H. R. Nicholls(1999), Tactile sensing for mechatronics-state of the art survey, Mechatronics, 9(1), October 1999:p.1-31

78. Howe, R.D (1994), Tactile Sensing and Control of Robotic Manipulation, in Journal of Advanced Robotics, v.8, n.3, 1994:p. 245-261.

79. Maria Vatshaug Ottermo, Øyvind Stavdahl, Tor A. Johansen(2004), Palpation Instrument for Augmented Minimally Invasive Surgery, Intelligent Robots and Systems, 2004. (IROS 2004). Proceedings. 2004 IEEE/RSJ International Conference on, 28 Sept.-2 Oct. 2004, vol.4, pp: 3960 - 3964

80. Hsin-Yun Yao and Vincent Hayward, A Tactile Enhancement Instrument for Minimally Invasive Surgery, Computer Aided Surgery, 10(4), pp. 233-239.

81. Siciliano, Bruno, Khatib, Oussama, Cutkosky, Mark R, Howe, Robert D, Provancher, William R(2008), Springer Handbook of Robotics: Force and Tactile Sensors, 2008, Springer Berlin Heidelberg

82. John G, Webster (1988), Tactile sensors for robotics and medicine, John Willey & Sons,inc,1988

83. Clarence W. De Silva(2004), Mechatronics:An Integrated Approach, CRC Press, New York, 2004

84. P. N. Brett and R. S. W. Stone(1997), " A technique for measuring contact force distribution in minimally invasive surgical procedures,"in Proc. IMechE part H4, Vol.211, 1997, pp.309-316

85. Ph.D. dissertation, Attila Kis(2006), Tactile Sensing and Analogic Algorithms, Péter Pázmány Catholic University, 2006

86. Howe, Robert D(1993), Tactile sensing and control of robotic manipulation, Advanced Robotics, Volume 8, Number 3, 1993 , pp. 245-261(17)

87. PhD Thesis, P.Tongpadungrod(2002), "Characteristics of distributive tactile sensing systems," Aston University, UK, 2002

88. http://www.medicaltactile.com/clinician/visualmappingsystem.htm?RD=1 accessed   15 February 2008

89. R. S. W. Stone and Peter N. Brett(1995), A flexible pneumatic actuator for gripping soft irregular shaped objects, IEE Colloquium on 'Innovative Actuators for Mechatronic Systems, UK, London, 1995/170, p.13

90. Ma, X., Brett, P.N(2002), The performance of a 1-D distributive tactile sensing for detecting the position, intensity, and width of a contacting load, IEEE Trans. Instrumentation and Measurement, 51(2), p.331-336

91. P. Tongpadungrod , T.D.L. Rhys, P.N. Brett(2003), An approach to optimise the critical sensor locations in one-dimensional novel distributive tactile surface to maximise performance, Sensors and Actuators A, 105 p.47–54

92. Howard R. Nicholls (1992). Advanced Tactile Sensig For Robotics, London, World Scientific

93. R. E. Ellis, S. Ganeshan, S. J. Lederman(1994), A tactile sensor based on thin plate deformation, Robotica, 12, p.343-351

94. P. N. Brett, Z. Li(2000), A tactile sensing surface for artificial neural network based automatic recognition of the contact force position, in Proc. IMechE part 214(part 1), p.207-214

95. PhD Thesis, Tactile Sensing with Fibre Bragg Gratings and Neural Networks, Barbara M. Cowie, Aston University, 2008

96. Ma, X. Brett PN, Wright MT, Griffiths MV.(2004). Flexible digit with tactile feedback for invasive clinical applications Proc Inst Mech En[H] Engineering medicine, 218(3), p:151-157

97. Iskandar Petra David J. Holding, Keith J. Blow, Betty Tam, Xianghong Ma, Peter N. Brett (2004), The design of a flexible digit towards wirelsess tactile tissue feedback, International conference on Control, Automation, Robotics and Bision, China, 6-9th December 2004, (2004)

98. P. N. Brett, X. Ma, D. J. Holding, M. T. Elliott and I. Petra(2007), "Real-time tracking of a moving contacting load using the distributive tactile sensing method", 14th International Conference on Mechatronics and Machine Vision in Practice, 2007, M2VIP 2007.

99. Patrick Sears and Pierre Dupont(2006), A steerable Needle Technology Using Curved Concentric Tubes, Proceedings of the 2006 IEEE/RSJ, International Conference on Intelligent Robotics and systems, Beijing, China, October 9-15, 2006, (2006)

100. Shepherd RK, Clark GM, Pyman BC.Webb(1985) RL "Banded intracochlear electrode array: evaluation of insertion trauma in human temporal bones", Ann Otol Rhinol Laryngol. 1985 Jan-Feb;94(1 Pt 1), p.55-9

101. Oliver Adunka, Marc H. Unkelbach, Martin G. Mack, Andreas Radeloff, Wolfgang Gstoettner,Predicting Basal Cochlear Length for Electric-Acoustic Stimulation, Arch Otolaryngol Head Neck Surg. 2005;131:488-492

102. Kyowa http://www.kyowa-ei.co.jp/english/products/gages/pdf/bridge.pdf, accessed October 2007

103. Bernard Escude, Chris James, Olivier Deguine, Nadine Cochard, Elias Eter and Bernard Fraysse, The Size of the Cochlea and Predictions of Insertion Depth Angles for Cochlear Implant Electrodes, Audiol Neurotol 2006;11(suppl 1):27–33

104. Chang Chih-Hao et al(2006) "Describing isotropic and anisotropic out-of-plane deformations in thin cubic materials by use of Zernike polynomials" applied optics 2006 Jan 20;45(3):432-7